
Lecture Notes (CS327A)

Advanced Robotic Manipulation

Oussama Khatib

Stanford University

Spring 2005

Contents

- 1 Spatial Descriptions** **1**
 - 1.1 Rigid Body Configuration 1
 - 1.2 Manipulator Kinematics 8
 - 1.3 Manipulator Geometric Model 13

- 2 Manipulator Kinematics** **21**
 - 2.1 Kinematic Model 21
 - 2.1.1 Basic Jacobian 22
 - 2.1.2 Jacobian Matrix 25
 - 2.1.3 Position Representations 26
 - 2.1.4 Rotation Representations 27
 - 2.2 Inverse Kinematic Model 29
 - 2.2.1 Reduction to the Basic Kinematic Model 30
 - 2.2.2 Position Representations 31
 - 2.2.3 Rotation Representations 32
 - 2.2.4 Inverse of the Basic Kinematic Model 33

3	Joint Space Framework	37
3.1	Joint Space Control	37
3.1.1	Motion Coordination	38
3.1.2	Redundant Manipulators	40
3.1.3	PID Control Schemes	41
3.2	Joint Space Dynamic Model	42
3.2.1	Kinetic Energy	42
3.2.2	Potential Energy	46
3.3	Joint Space Dynamic Control	51
4	Operational Space Framework	53
4.1	Basic Concepts	53
4.2	Effector Equations of Motion	56
4.3	End-Effector Motion Control	62
4.3.1	Passive Systems	62
4.3.2	Dynamic Decoupling	63
4.3.3	Goal Position	64
4.3.4	Trajectory Tracking	65
4.4	Active Force Control	67
4.4.1	Generalized Selection Matrices	67
4.4.2	Basic Dynamic Model	71
4.4.3	A Mass-Spring System	73
4.4.4	Unified Motion and Force Control	74
4.4.5	Implementation	74

5	Redundancy and Singularities	81
5.1	Redundant Manipulators Dynamics	82
5.1.1	Equations of Motion	84
5.1.2	Torque/Force Relationship	85
5.1.3	Stability Analysis	86
5.1.4	Dynamic Consistency: An Example	88
5.2	Singular Configurations	90
5.2.1	Control Strategy	90
5.2.2	Types of Singularities	92
5.2.3	Example: The PUMA 560	93
6	Inertial Properties	97
6.1	Inertial Properties and Task Redundancy	98
6.2	Effective Mass/Inertia	101
6.3	Structure of Λ_0^{-1}	102
6.4	Belted Ellipsoid	103
7	Macro-/Mini-Manipulators	107
7.1	Kinematics of Macro/Mini Structures	108
7.2	Dynamics of Macro/Mini Structures	110
7.3	Dextrous Dynamic Coordination	117
8	Multi-Effector/Object System	119
8.1	Augmented Object Model	119
8.2	Redundancy in Multi-Arm Systems	126
8.3	Augmented Object in a Redundant System	127
8.4	Dynamic Consistency in Multi-Arm Systems	129

Chapter 1

Spatial Descriptions

1.1 Rigid Body Configuration

A manipulator is a mechanical system formed by the connection of a set of rigid bodies, *links*, through *joints*. Joints provide each pair of connected links with some freedom of relative motion. The description of the spatial location of a rigid body is therefore the basis for the spatial description of a manipulator.

The *configuration* of a rigid body is a description of its position and orientation. The position of a rigid body is determined by a description of the position of an arbitrary point attached to the rigid body. The orientation of a rigid body is determined by the description of its rotations about this point.

Position of a Point

Let us consider a point \mathcal{P} of an Euclidean affine space E , where an arbitrary point \mathcal{O} has been selected as the origin. The position of \mathcal{P} is

given by the vector $\mathbf{p} = \vec{\mathcal{O}\mathcal{P}}$. With respect to \mathcal{O} , the positions of points: $\mathcal{P}_1, \mathcal{P}_2, \dots, \mathcal{P}_n$ are described by the vectors: $\mathbf{p}_1 = \vec{\mathcal{O}\mathcal{P}_1}, \mathbf{p}_2 = \vec{\mathcal{O}\mathcal{P}_2}, \dots, \mathbf{p}_n = \vec{\mathcal{O}\mathcal{P}_n}$.

For points of the 3-dimensional space, positions are described by vectors $\mathbf{p} \in R^3$. Let $\{\mathbf{x}, \mathbf{y}, \mathbf{z}\}$ be an orthonormal basis of R^3 . The components of a vector \mathbf{p} with respect to this basis are identical to the coordinates of \mathcal{P} given with respect to the coordinate frame $\mathcal{R}(\mathcal{O}, \mathbf{x}, \mathbf{y}, \mathbf{z})$.

Taking the components of the vector \mathbf{p} with respect to another orthonormal basis $\{\mathbf{x}', \mathbf{y}', \mathbf{z}'\}$ correspond to a representation of \mathcal{P} in a coordinate frame having the same origin, \mathcal{O} , and using the unit vectors $\mathbf{x}', \mathbf{y}', \mathbf{z}'$, i.e. $\mathcal{R}'(\mathcal{O}, \mathbf{x}', \mathbf{y}', \mathbf{z}')$, as shown in Figure 2.1. The relationship between these two representations is given by the base transformation or the coordinate transformation between the two frames of same origin.

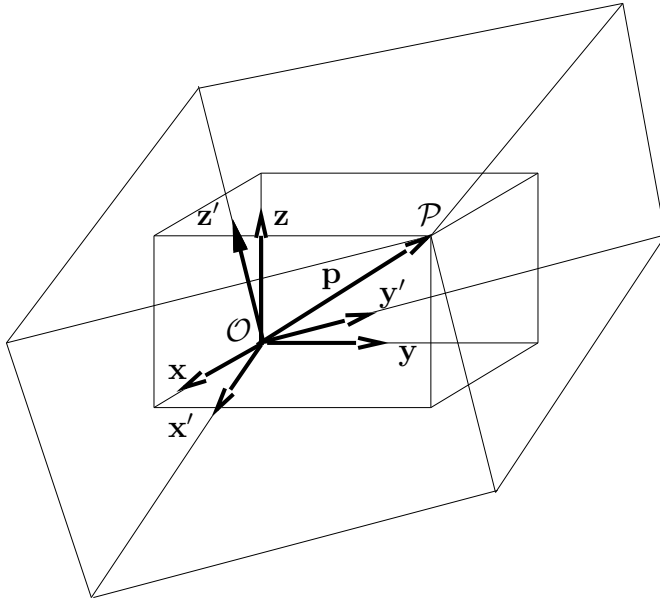


Figure 1.1: Position of a Point

With respect to a different origin, \mathcal{O}' , the vector describing the position

of point \mathcal{P} is $\mathbf{p}' = \mathcal{O}'\vec{\mathcal{P}}$. Although \mathbf{p}' and \mathbf{p} describe the position of the same point, these two vectors are different.

Rotation Transformation

Rotation transformations are transformations that operate on the unit vectors of coordinate frames, while conserving the frame origins. These transformations are equivalent to transformations between orthonormal bases. A rotation transformation is defined by the relationships between the unit vectors of two coordinate frames. The rotation transformation between $\mathcal{R}(\mathcal{O}, \mathbf{x}, \mathbf{y}, \mathbf{z})$ and $\mathcal{R}'(\mathcal{O}, \mathbf{x}', \mathbf{y}', \mathbf{z}')$, of identical origin \mathcal{O} (see Figure 2.2), is described by a 3×3 orthonormal rotation matrix S . The columns of S are the components of the three unit vectors \mathbf{x}' , \mathbf{y}' , and \mathbf{z}' expressed in the coordinate frame R .

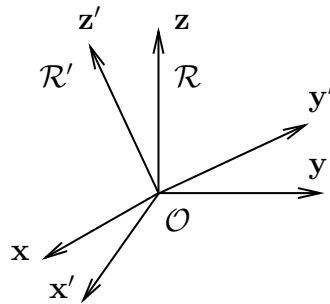


Figure 1.2: Rotation Transformation.

$$S = (\mathbf{x}'_{(\mathcal{R})} \quad \mathbf{y}'_{(\mathcal{R})} \quad \mathbf{z}'_{(\mathcal{R})}). \quad (1.1)$$

Since S is an orthonormal matrix, its inverse is equal to its transpose,

$$S^{-1} = S^T. \quad (1.2)$$

The rows of S define, therefore, the components of the three unit vectors \mathbf{x} , \mathbf{y} , and \mathbf{z} expressed with respect to the coordinate frame \mathcal{R}' ,

$$S = \begin{pmatrix} \mathbf{x}_{(\mathcal{R}')^T} \\ \mathbf{y}_{(\mathcal{R}')^T} \\ \mathbf{z}_{(\mathcal{R}')^T} \end{pmatrix}. \quad (1.3)$$

Compound Rotations

The rotation matrix associated with a transformation resulting from a set of consecutive rotation transformations is given by the product of the corresponding rotation matrices.

Rigid Body Orientation

The orientation of a rigid body with respect to some reference frame \mathcal{R} is described by the rotation transformation between \mathcal{R} and a coordinate frame \mathcal{R}' attached to the rigid body.

Translational Transformation

Translational transformations define the relationships between origins of coordinate frames. The translational transformation of a coordinate frame $\mathcal{R}(\mathcal{O}, \mathbf{x}, \mathbf{y}, \mathbf{z})$ into $\mathcal{R}'(\mathcal{O}', \mathbf{x}, \mathbf{y}, \mathbf{z})$ (see Figure 2.3), is described by a 3×1 column matrix \mathbf{d} . \mathbf{d} defines the coordinates of the origin \mathcal{O}' of \mathcal{R}' in the coordinate frame \mathcal{R} .

Coordinate Transformation

Coordinate transformations define the relationships between coordinate frames. A coordinate frame $\mathcal{R}(\mathcal{O}, \mathbf{x}, \mathbf{y}, \mathbf{z})$ can be transformed into any arbitrary coordinate frame $\mathcal{R}'(\mathcal{O}', \mathbf{x}', \mathbf{y}', \mathbf{z}')$ by a rotation transformation and a translation transformation, as shown in Figure 2.4. If $\mathbf{p}' = (x' \ y' \ z')^T$ is the column matrix representing the coordinates in \mathcal{R}'

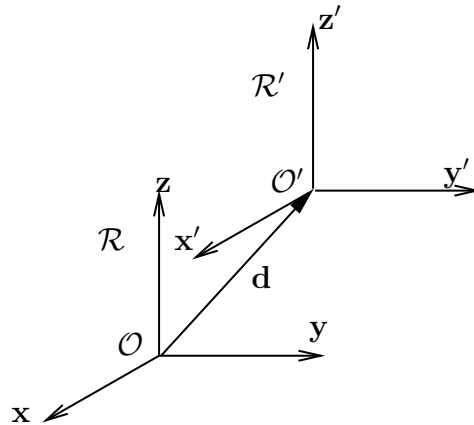


Figure 1.3: Rotation Transformation.

of some point \mathcal{P} , then the coordinates $\mathbf{p} = (x \ y \ z)^T$ in \mathcal{R} of the point \mathcal{P} are given by the relationship

$$\mathbf{p} = S\mathbf{p}' + \mathbf{d}. \quad (1.4)$$

Homogeneous Transformation

The *homogeneous transformation* provides a compact matrix representation of coordinate transformation. A coordinate transformation between \mathcal{R} and \mathcal{R}' that involves a rotation transformation S and a translation transformation \mathbf{d} is represented by the 4×4 matrix,

$$T = \begin{pmatrix} S & \mathbf{d} \\ 0 & 1 \end{pmatrix}. \quad (1.5)$$

Unlike S , the matrix T is not orthonormal. Its inverse is given by

$$T^{-1} = \begin{pmatrix} S^T & -S^T \mathbf{d} \\ 0 & 1 \end{pmatrix}. \quad (1.6)$$

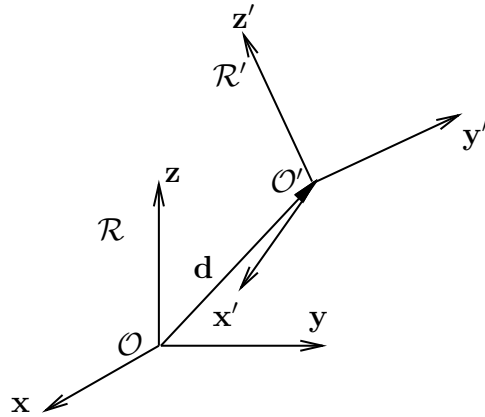


Figure 1.4: Coordinate Transformation.

With homogeneous transformations, the relationship (1.4) becomes,

$$\begin{pmatrix} \mathbf{p} \\ 1 \end{pmatrix} = T \begin{pmatrix} \mathbf{p}' \\ 1 \end{pmatrix}. \quad (1.7)$$

Compound Transformations

In consecutive transformations, the matrices associated with homogeneous transformations operate similarly to rotation matrices. The matrix associated with a transformation resulting from a set of consecutive transformations is given by the product of the corresponding homogeneous transformation matrices.

Rigid Body Position and Orientation

The position and orientation of a rigid body with respect to a coordinate frame $\mathcal{R}(\mathcal{O}, \mathbf{x}, \mathbf{y}, \mathbf{z})$ is defined by the coordinate transformation between

\mathcal{R} and an arbitrary coordinate frame $\mathcal{R}'(\mathcal{O}', \mathbf{x}', \mathbf{y}', \mathbf{z}')$ fixed with respect to the rigid body, as shown in Figure 2.5. The position of the rigid body is described by the translational components of this transformation, while the orientation of the rigid body is described by the rotational components.

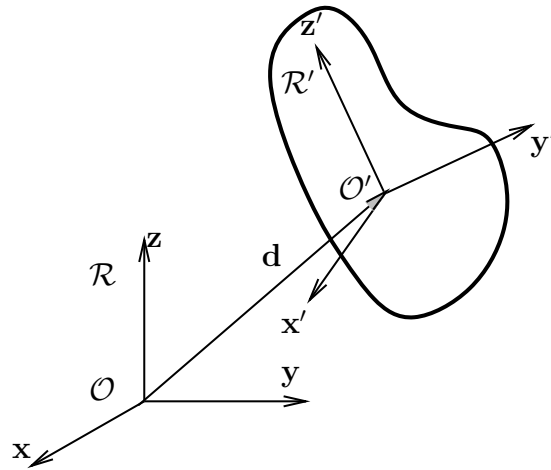


Figure 1.5: Rigid Body Position and Orientation.

1.2 Manipulator Kinematics

A manipulator is treated as a holonomic system with a structure of an open kinematic chain of $n+1$ rigid bodies, i.e., links, articulated through n revolute and/or prismatic joints having *one degree of freedom*.

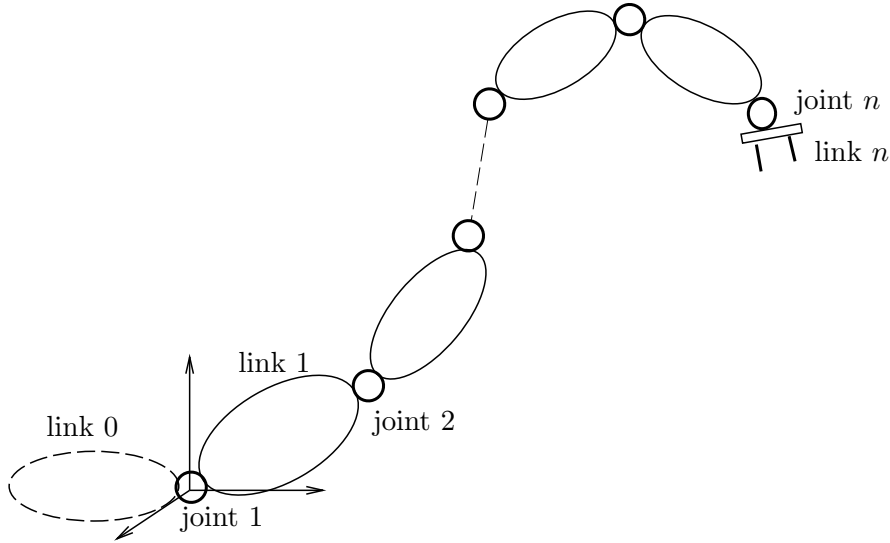


Figure 1.6: An Open Kinematic Chain.

The kinematic relationship between a pair of adjacent links in the chain is described by the coordinate transformation between two coordinate frames attached to the two links. Links are numbered from 0, the *base*, to n , the *end-effector*, while joints are numbered from 1 to n (see Figure 2.6).

A coordinate frame $\mathcal{R}_i(\mathcal{O}_i, \mathbf{x}_i, \mathbf{y}_i, \mathbf{z}_i)$ is attached to link i . The position and orientation of the link i with respect to link $i-1$ is described by the transformation between a coordinate frame $\mathcal{R}_{i-1}(\mathcal{O}_{i-1}, \mathbf{x}_{i-1}, \mathbf{y}_{i-1}, \mathbf{z}_{i-1})$ attached to the link $i-1$ and \mathcal{R}_i .

The \mathbf{z} -axis, \mathbf{z}_i , of a coordinate frame \mathcal{R}_i are selected along the axis of joint i .

Parameters of Denavit-Hartenberg

The kinematic relationship between a pair of adjacent links $i - 1$ and i connected through a one-degree-of-freedom joint i can be completely determined by a set of four parameters $(\alpha_i, a_i, \theta_i, \rho_i)$, called parameters of *Denavit-Hartenberg*. These parameters define the homogeneous transformation between the two coordinate frames attached to the two links. With the convention shown in Figure 2.7, the Denavit-Hartenberg parameters are defined as

α_i : the angle between the \mathbf{z} -axes of \mathcal{R}_i and \mathcal{R}_{i+1} , measured¹ about \mathbf{x}_i ;

a_i : the length of the common normal to the \mathbf{z} -axes of \mathcal{R}_i and \mathcal{R}_{i+1} , measured along \mathbf{x}_i ;

θ_i : the angle between the \mathbf{x} -axes of \mathcal{R}_{i-1} and \mathcal{R}_i measured about \mathbf{z}_i .

ρ_i : the distance between the \mathbf{x} -axes of \mathcal{R}_{i-1} and \mathcal{R}_i measured along \mathbf{z}_i .

$$T_{(i-1)i} = \begin{pmatrix} \cos \theta_i & -\sin \theta_i & 0 & a_{(i-1)} \\ \sin \theta_i \cos \alpha_{(i-1)} & \cos \theta_i \cos \alpha_{(i-1)} & -\sin \alpha_{(i-1)} & -\rho_i \sin \alpha_{(i-1)} \\ \sin \theta_i \sin \alpha_{(i-1)} & \cos \theta_i \sin \alpha_{(i-1)} & \cos \alpha_{(i-1)} & \rho_i \cos \alpha_{(i-1)} \\ 0 & 0 & 0 & 1 \end{pmatrix}. \quad (1.8)$$

Generalized Coordinates

Configuration Parameters of a Mechanism: Any set of parameters that allow to completely specify, in a frame of reference \mathcal{R}_0 , the positions and orientations of all links of the mechanism, i.e. its configuration.

¹in the right-hand sense

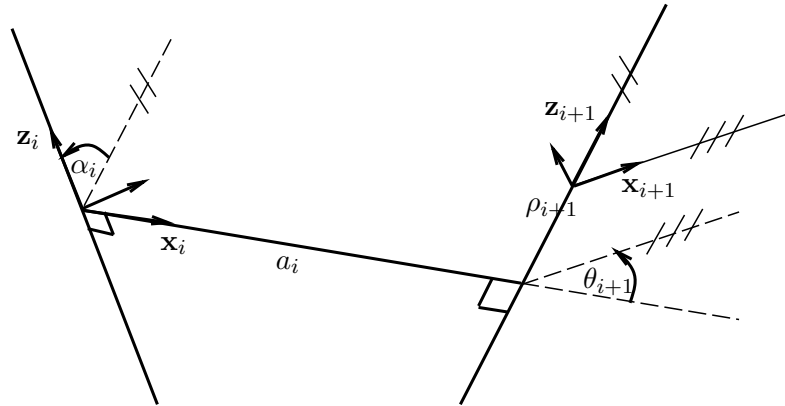


Figure 1.7: Denavit-Hartenberg Parameters

Generalized Coordinates: A set of independent configuration parameters forms a system of *generalized coordinates* for the mechanism. The number of these independent parameters is defined as the number of *degrees of freedom*.

Joint Coordinates: With revolute and/or prismatic joints, a chain of $n + 1$ articulated links possess n degree-of-freedom, and a set $\{q_1, q_2, \dots, q_n\}$ of n *joint coordinates* can be selected as a generalized coordinate system for the manipulator. Let us define the binary parameter

$$\epsilon_i = \begin{cases} 0 & \text{for a revolute joint } \theta_i; \\ 1 & \text{for a prismatic joint } \rho_i. \end{cases} \quad (1.9)$$

The i^{th} generalized coordinate can then be written as

$$q_i = \bar{\epsilon}_i \theta_i + \epsilon_i \rho_i; \quad (1.10)$$

with

$$\bar{\epsilon}_i = 1 - \epsilon_i. \quad (1.11)$$

The configuration of the manipulator can then be described by the vector \mathbf{q} of components q_1, q_2, \dots, q_n in the manipulator *joint space*.

Operational Coordinates

The end-effector configuration is described by the relationships between the reference frame \mathcal{R}_0 and a coordinate frame attached to the end-effector. Although the coordinate frame \mathcal{R}_n could be used for establishing these relationships, it is often more convenient to select a different coordinate frame whose origin is not located at the axis of joint n .

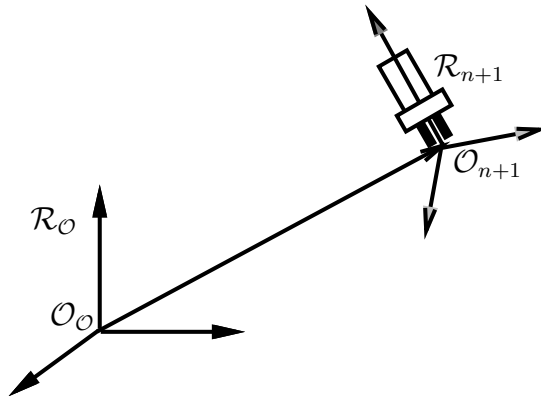


Figure 1.8: End-Effector Position and Orientation

Let $\mathcal{O}_{(n+1)}$ be the selected origin for the additional frame. The configuration of the end-effector can be defined by the relationships between \mathcal{R}_0 and the coordinate frame $\mathcal{R}_{(n+1)}$, as illustrated in Figure 2.8.

End-Effector Configuration Parameters: Any set of parameters that allow to completely specify, in a frame of reference \mathcal{R}_0 , the positions and orientations of the end-effector, i.e. the configuration of the end-effector.

Various sets of parameters, x_1, x_2, \dots, x_m can be used for the description of the end-effector configuration. The number m of parameters varies from one representation to another.

Task Configuration Parameters: A task that involves the position and/or the orientation of the end-effector can be specified by a subset m_κ of the m end-effector configuration parameters. These m_κ parameters are called the *task configuration parameters*

Operational Coordinates: An *operational coordinate system* is a set x_1, x_2, \dots, x_{m_0} of m_0 *independent* end-effector configuration parameters.

The configuration of the end-effector can then be described by the vector \mathbf{x} of components x_1, x_2, \dots, x_{m_0} in *operational space*.

End-Effector Degrees of Freedom: The number m_0 , which is independent of the selected set of end-effector configuration parameters, represents a characteristic which is intrinsic to the mechanical structure of the manipulator and its end-effector. m_0 can be viewed as the number of *degrees of freedom of the end-effector*.

Redundancy and Task Redundancy

A manipulator is said to be *redundant* when the number of its degrees of freedom is greater than the number of its end-effector degrees of freedom. A given configuration of the end-effector of a redundant manipulator can be obtained with an infinite number of different configurations of the redundant mechanism, two such configurations are shown in Figure 2.9. $n - m_0$ represents the number of *degrees of redundancy of a manipulator*.

Redundancy can also be defined with respect to a task κ . Let $m_{\kappa(0)}$ be the number of independent parameters required to specify the configuration of the task. $n - m_{\kappa(0)}$ is defined as the number of *degrees of redundancy of the manipulator with respect to the task κ* .

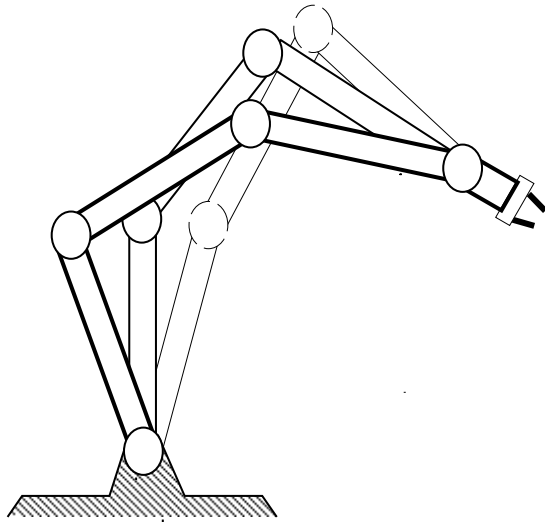


Figure 1.9: A Redundant Manipulator

1.3 Manipulator Geometric Model

The *manipulator geometric model* is the system of m equations describing the end-effector configuration parameters as a function of the manipulator joint coordinates.

At a given configuration \mathbf{q} of the manipulator, the end-effector position and orientation are determined by the matrix $T_{0(n+1)}(\mathbf{q})$ defining the homogeneous transformation between the coordinate frames \mathcal{R}_0 and $\mathcal{R}_{(n+1)}$. These are the coordinate frames associated with the manipulator's fixed base and its end-effector, respectively.

$$T_{0(n+1)}(\mathbf{q}) = T_{01}(q_1)T_{12}(q_2) \dots T_{(n-1)n}(q_n)T_{n(n+1)}; \quad (1.12)$$

where $T_{n(n+1)}$ is a constant matrix. The homogeneous transformation

matrix $T_{0(n+1)}(\mathbf{q})$ is

$$T_{0(n+1)}(\mathbf{q}) = \begin{pmatrix} S_{0(n+1)}(\mathbf{q}) & \mathbf{d}_{0(n+1)}(\mathbf{q}) \\ 0 & 1 \end{pmatrix}. \quad (1.13)$$

$S_{0(n+1)}(\mathbf{q})$ contains the description of the end-effector orientation, while $\mathbf{d}_{0(n+1)}$ determines the end-effector position. Let \mathbf{x} be the $m \times 1$ column matrix of end-effector configuration parameters, and \mathbf{q} the $n \times 1$ column matrix of joint coordinates. The manipulator geometric model associated with the end-effector configuration parameters \mathbf{x} can be obtained from (1.13) and written in the form

$$\mathbf{x} = \mathbf{G}(\mathbf{q}). \quad (1.14)$$

\mathbf{G} is the $m \times 1$ column matrix of m functions G_1, G_2, \dots, G_m . Let \mathbf{x}_p be the column matrix of coordinates defining the position of $\mathcal{O}_{(n+1)}$ in \mathcal{R}_0 , and \mathbf{x}_r the column matrix of coordinates defining the orientation of $\mathcal{R}_{(n+1)}$ in \mathcal{R}_0 . The end-effector configuration can then be represented as

$$\mathbf{x}(\mathbf{q}) = \begin{pmatrix} \mathbf{x}_p(\mathbf{q}) \\ \mathbf{x}_r(\mathbf{q}) \end{pmatrix}. \quad (1.15)$$

Position Representations

The end-effector position, $\mathbf{x}_p(\mathbf{q})$, is obtained from $\mathbf{d}_{0(n+1)}(\mathbf{q})$ which defines the coordinates of the point $\mathcal{O}_{(n+1)}$ in the frame of reference \mathcal{R}_0 . Among the various possible selections of position coordinates (see Figure 2.10) are,

Cartesian coordinates: $\mathbf{x}_p^T = (x \ y \ z)^T$;

cylindrical coordinates: $\mathbf{x}_p^T = (\rho \ \theta \ z)^T$;

spherical coordinates: $\mathbf{x}_p^T = (r \ \theta \ \phi)^T$.

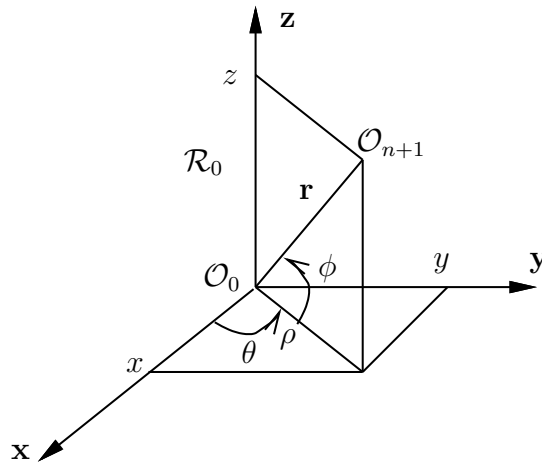


Figure 1.10: Position Representations

Orientation Representations

At a given configuration \mathbf{q} of the manipulator the end-effector orientation can be uniquely determined by the transformation matrix $S_{0(n+1)}(\mathbf{q})$ describing the orientation of the coordinate frame $\mathcal{R}_{(n+1)}$ with respect to the frame of reference \mathcal{R}_0 .

Several different representations can be used to describe the orientation of the end-effector. One of the most straightforward representations of the end-effector orientation is based on the direct use of the elements of $S_{0(n+1)}(\mathbf{q})$.

Direction Cosines

The end-effector rotation matrix $S_{0(n+1)}(\mathbf{q})$ can be written as

$$S_{0(n+1)}(\mathbf{q}) = (\mathbf{s}_1(\mathbf{q}) \quad \mathbf{s}_2(\mathbf{q}) \quad \mathbf{s}_3(\mathbf{q})). \quad (1.16)$$

The direction cosines representation of the end-effector orientation is given by the 9×1 column matrix

$$\mathbf{x}_r(\mathbf{q}) = \begin{pmatrix} \mathbf{s}_1(\mathbf{q}) \\ \mathbf{s}_2(\mathbf{q}) \\ \mathbf{s}_3(\mathbf{q}) \end{pmatrix}. \quad (1.17)$$

This is a redundant representation of the orientation of the end-effector.

Euler Angles

Minimal representations of the orientation can be obtained with angular parameters. A set of three independent angular parameters is sufficient to describe the orientation of a rigid body with respect to a reference frame. Among the various angular representations of rigid body rotation are the Euler angles ψ , θ , and ϕ . The rotation of $\mathcal{R}_{(n+1)}$ with respect to \mathcal{R}_0 can be viewed as the result of three consecutive rotations represented by the matrices:

$$S_\psi = \begin{pmatrix} c\psi & -s\psi & 0 \\ s\psi & c\psi & 0 \\ 0 & 0 & 1 \end{pmatrix}; \quad S_\theta = \begin{pmatrix} 1 & 0 & 0 \\ 0 & c\theta & -s\theta \\ 0 & s\theta & c\theta \end{pmatrix}; \quad S_\phi = \begin{pmatrix} c\phi & -s\phi & 0 \\ s\phi & c\phi & 0 \\ 0 & 0 & 1 \end{pmatrix}.$$

The total rotation of the end-effector is

$$S_{0(n+1)}(\mathbf{q}) = S_\psi S_\theta S_\phi; \quad (1.18)$$

which yields

$$S_{0(n+1)}(\mathbf{q}) = \begin{pmatrix} c\psi c\phi - s\psi c\theta s\phi & -c\psi s\phi - s\psi c\theta c\phi & s\psi s\theta \\ s\psi c\phi + c\psi c\theta s\phi & -s\psi s\phi + c\psi c\theta c\phi & -c\psi s\theta \\ s\theta s\phi & s\theta c\phi & c\theta \end{pmatrix}; \quad (1.19)$$

where s and c represent the sin and cos functions respectively. The Euler angles representation of the orientation is

$$\mathbf{x}_r(\mathbf{q}) = \begin{pmatrix} \psi(\mathbf{q}) \\ \theta(\mathbf{q}) \\ \phi(\mathbf{q}) \end{pmatrix}. \quad (1.20)$$

With s_{ij} denoting the elements of the rotation matrix $S_{0(n+1)}(\mathbf{q})$, and the assumption $s_{33} \neq \pm 1$, the components of $\mathbf{x}_r(\mathbf{q})$ can be obtained from (1.19) as,

$$\begin{aligned}\psi(\mathbf{q}) &= \operatorname{sgn}(s_{13}) \arccos(-s_{23}/\sqrt{1-s_{33}^2}); \\ \theta(\mathbf{q}) &= \arccos(s_{33}); \\ \phi(\mathbf{q}) &= \operatorname{sgn}(s_{31}) \arccos(-s_{32}/\sqrt{1-s_{33}^2}).\end{aligned}\tag{1.21}$$

As for all minimal representations of the orientation, the Euler angles representation can be singular. The singularity of this representation arises at $s_{33} = \pm 1$ or when $(\theta = k\pi, k: \text{integer})$. For these configurations, only the difference or the sum of the angles ψ and ϕ is defined.

Euler Parameters

Rotations *Rotations in the three dimensional space can be defined as the product of two plane symmetries operating on the points of this space.*

Let us consider the two symmetries about the planes \mathcal{U} and \mathcal{V} . Let \mathbf{u} and \mathbf{v} be two unit vectors normal to these planes. Let \mathbf{w} be a unit vector along the line of intersection of the two planes such that \mathbf{u} , \mathbf{v} , and \mathbf{w} is a right-handed frame.

The transformation resulting from the consecutive application of symmetries with respect to planes \mathcal{U} and \mathcal{V} is equivalent to a rotation about \mathbf{w} by an angle θ which is twice the angle between the vectors \mathbf{u} and \mathbf{v} , as shown in Figure 2.12.

This rotation is defined by

$$\begin{aligned}\mathbf{u} \cdot \mathbf{v} &= \cos \theta/2; \\ \mathbf{u} \times \mathbf{v} &= \mathbf{w} \sin \theta/2.\end{aligned}\tag{1.22}$$

Let w_1 , w_2 , and w_3 be the components of the unit vector \mathbf{w} in a frame of reference \mathcal{R} . The rotation by θ about \mathbf{w} is defined by the set of four

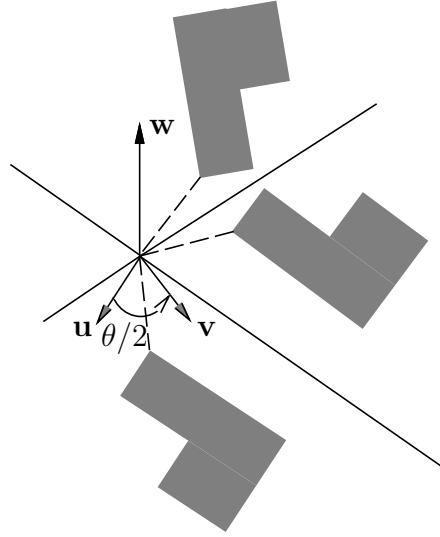


Figure 1.11: Rotations as Two-Plane-Symmetries

parameters

$$\begin{aligned}
 \lambda_0 &= \cos \theta/2; \\
 \lambda_1 &= w_1 \sin \theta/2; \\
 \lambda_2 &= w_2 \sin \theta/2; \\
 \lambda_3 &= w_3 \sin \theta/2.
 \end{aligned} \tag{1.23}$$

λ_0 , λ_1 , λ_2 , and λ_3 are the Euler parameters (Olinde-Rodrigues Parameters). These parameters satisfy the normality condition

$$\lambda_0^2 + \lambda_1^2 + \lambda_2^2 + \lambda_3^2 = 1. \tag{1.24}$$

A rotation between two coordinate frames $\mathcal{R}(\mathcal{O}, \mathbf{x}, \mathbf{y}, \mathbf{z})$ and $\mathcal{R}'(\mathcal{O}, \mathbf{x}', \mathbf{y}', \mathbf{z}')$ can be described by a rotation of an angle θ about a vector \mathbf{w} passing through the origin \mathcal{O} . The 3×3 orthonormal rotation matrix $S_{0(n+1)}(\mathbf{q})$ associated with this rotation transformation is

$$S_{0(n+1)}(\mathbf{q}) = \begin{pmatrix} 2(\lambda_0^2 + \lambda_1^2) - 1 & 2(\lambda_1\lambda_2 - \lambda_0\lambda_3) & 2(\lambda_1\lambda_3 + \lambda_0\lambda_2) \\ 2(\lambda_1\lambda_2 + \lambda_0\lambda_3) & 2(\lambda_0^2 + \lambda_2^2) - 1 & 2(\lambda_2\lambda_3 - \lambda_0\lambda_1) \\ 2(\lambda_1\lambda_3 - \lambda_0\lambda_2) & 2(\lambda_2\lambda_3 + \lambda_0\lambda_1) & 2(\lambda_0^2 + \lambda_3^2) - 1 \end{pmatrix}. \tag{1.25}$$

Solving Euler Parameters from the above equation is complicated by the sign determination problem. This problem results from the fact that equation (1.25) only provides the signs of the products: $(\lambda_0\lambda_1)$, $(\lambda_0\lambda_2)$, $(\lambda_0\lambda_3)$, $(\lambda_1\lambda_2)$, $(\lambda_1\lambda_3)$, $(\lambda_2\lambda_3)$. Assuming that $\theta \in [0, \pi]$, i.e. $\lambda_0 \geq 0$, Euler parameters can be computed as

$$\begin{aligned}\lambda_0 &= \frac{1}{2}\sqrt{s_{11} + s_{22} + s_{33} + 1}; \\ \lambda_1 &= \frac{1}{2}\text{sgn}(s_{32} - s_{23})\sqrt{s_{11} - s_{22} - s_{33} + 1}; \\ \lambda_2 &= \frac{1}{2}\text{sgn}(s_{13} - s_{31})\sqrt{-s_{11} + s_{22} - s_{33} + 1}; \\ \lambda_3 &= \frac{1}{2}\text{sgn}(s_{21} - s_{12})\sqrt{-s_{11} - s_{22} + s_{33} + 1};\end{aligned}\tag{1.26}$$

where sgn is the sign function. Another algorithm for the computation of Euler parameters is based on the following observation:

Lemma 1. *For all rotations, at least one of the Euler parameters has a magnitude larger than 1/2.*

This is a straightforward result from the normality condition (1.24). With Lemma 1, it can be assumed that, between two steps of computation, the sign of the largest Euler parameter is maintained constant. This assumption is valid as long as the computation servo-rate is not slower than half of the rotation rate of change (for a servo-rate of 50Hz, the magnitude of angular velocity must not exceed 100 rad/sec!).

Lemma 1 is the basis for the following algorithm for the evaluation of the Euler parameters. Starting from a known configuration, the values at an instant t_i of $\lambda(t_i)$ are given by the expressions in one of the four columns in Table 2.1 corresponding to the parameter with the largest absolute value at instant $t_{(i-1)}$,

with

$$\begin{aligned}\Delta_0 &= 2\text{sgn}\left(\lambda_0(t_{(i-1)})\right)\sqrt{s_{11} + s_{22} + s_{33} + 1}; \\ \Delta_1 &= 2\text{sgn}\left(\lambda_1(t_{(i-1)})\right)\sqrt{s_{11} - s_{22} - s_{33} + 1}; \\ \Delta_2 &= 2\text{sgn}\left(\lambda_2(t_{(i-1)})\right)\sqrt{-s_{11} + s_{22} - s_{33} + 1}; \\ \Delta_3 &= 2\text{sgn}\left(\lambda_3(t_{(i-1)})\right)\sqrt{-s_{11} - s_{22} + s_{33} + 1}.\end{aligned}\tag{1.27}$$

Table 1.1: Euler Parameters Determination

	$ \lambda_0(t_{(i-1)}) $	$ \lambda_1(t_{(i-1)}) $	$ \lambda_2(t_{(i-1)}) $	$ \lambda_3(t_{(i-1)}) $
$\lambda_0(t_i)$	$\Delta_0/4$	$(s_{32} - s_{23})/\Delta_1$	$(s_{13} - s_{31})/\Delta_2$	$(s_{21} - s_{12})/\Delta_3$
$\lambda_1(t_i)$	$(s_{32} - s_{23})/\Delta_0$	$\Delta_1/4$	$(s_{21} + s_{12})/\Delta_2$	$(s_{13} + s_{31})/\Delta_3$
$\lambda_2(t_i)$	$(s_{13} - s_{31})/\Delta_0$	$(s_{21} + s_{12})/\Delta_1$	$\Delta_2/4$	$(s_{32} + s_{23})/\Delta_3$
$\lambda_3(t_i)$	$(s_{21} - s_{12})/\Delta_0$	$(s_{13} + s_{31})/\Delta_1$	$(s_{32} + s_{23})/\Delta_2$	$\Delta_3/4$

Euler Angles and Euler Parameters

The relationships between Euler angles and Euler parameters are

$$\begin{aligned}
\lambda_0 &= \cos(\theta/2) \cdot \cos((\psi + \phi)/2); \\
\lambda_1 &= \sin(\theta/2) \cdot \cos((\psi - \phi)/2); \\
\lambda_2 &= \sin(\theta/2) \cdot \sin((\psi - \phi)/2); \\
\lambda_3 &= \cos(\theta/2) \cdot \sin((\psi + \phi)/2).
\end{aligned} \tag{1.28}$$

We have seen that the Euler angles representation is singular when $(\theta = k\pi)$. For these configurations, only the sum (when k is even) or the difference (when k is odd) of the angles ψ and ϕ is defined. However, relations (1.28) only use the sum and the difference of these angles, and the singularity of the representation is therefore eliminated with Euler parameters.

Chapter 2

Manipulator Kinematics

2.1 Kinematic Model

The *kinematic model* of a manipulator is the system of m equations which describes the time-derivatives of end-effector configuration parameters as a function of the manipulator joint velocities. This model results from the differentiation of the manipulator geometric model, $\mathbf{x} = \mathbf{G}(\mathbf{q})$. At a given configuration \mathbf{q} , the time derivatives of the end-effector configuration parameters, $\dot{\mathbf{x}}$, can be expressed as linear functions of the joint velocities, $\dot{\mathbf{q}}$. The kinematic model is

$$\dot{\mathbf{x}} = J(\mathbf{q}) \dot{\mathbf{q}}; \quad (2.1)$$

where $J(\mathbf{q})$ is the $m \times n$ *Jacobian matrix* whose elements are

$$J_{ij}(\mathbf{q}) = \frac{\partial}{\partial q_j} G_i(\mathbf{q}). \quad (2.2)$$

The Jacobian matrix can be interpreted as the matrix relating the differential $d\mathbf{q}$ of joint coordinates to the differential $d\mathbf{x}$ of end-effector

configuration parameters. The manipulator kinematic relationships can be then defined by the *manipulator differential model*

$$d\mathbf{x} = J(\mathbf{q}) d\mathbf{q}; \quad (2.3)$$

A third interpretation of the Jacobian matrix is obtained by replacing the differentials $d\mathbf{q}$ and $d\mathbf{x}$ by the elementary displacements of joint coordinates and end-effector configuration parameters. The resulting relationship is called the *manipulator variational model*

$$\delta\mathbf{x} = J(\mathbf{q}) \delta\mathbf{q}. \quad (2.4)$$

2.1.1 Basic Jacobian

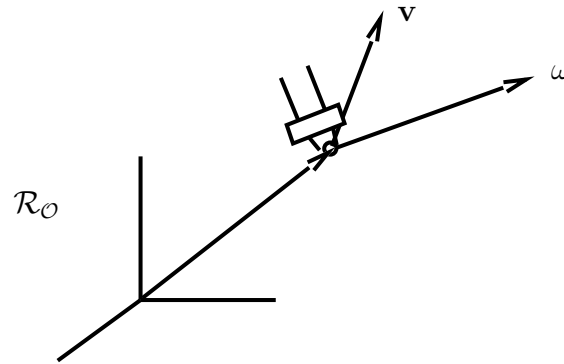


Figure 2.1: End-Effector Velocities

Different representations of the end-effector position and orientation result in different kinematic models (and different Jacobian matrices). However, the kinematic properties of a manipulator are expected to be independent of the type of representation used for the description of the end-effector configuration. These properties are described by a basic kinematic model that is defined independently from the selected end-effector representation. This model relies on the end-effector linear and angular velocities.

Let \mathbf{v} and ω be the vectors of the linear and instantaneous angular velocities at the operational point (\mathbf{x}_p), as illustrated in Figure 3.1. The basic kinematic model describes these velocities in terms of the generalized joint velocities $\dot{\mathbf{q}}$.

The velocity of a link i with respect to link $i-1$ depends on the type of joint i . For a prismatic joint, the velocity is described by a linear velocity vector \mathbf{v}_i . For a revolute joint, the velocity is described by an angular velocity vector ω_i . These vectors are related to \dot{q}_i by

$$\begin{aligned}\mathbf{v}_i &= \epsilon_i \mathbf{z}_i \dot{q}_i; \\ \omega_i &= \bar{\epsilon}_i \mathbf{z}_i \dot{q}_i.\end{aligned}\tag{2.5}$$

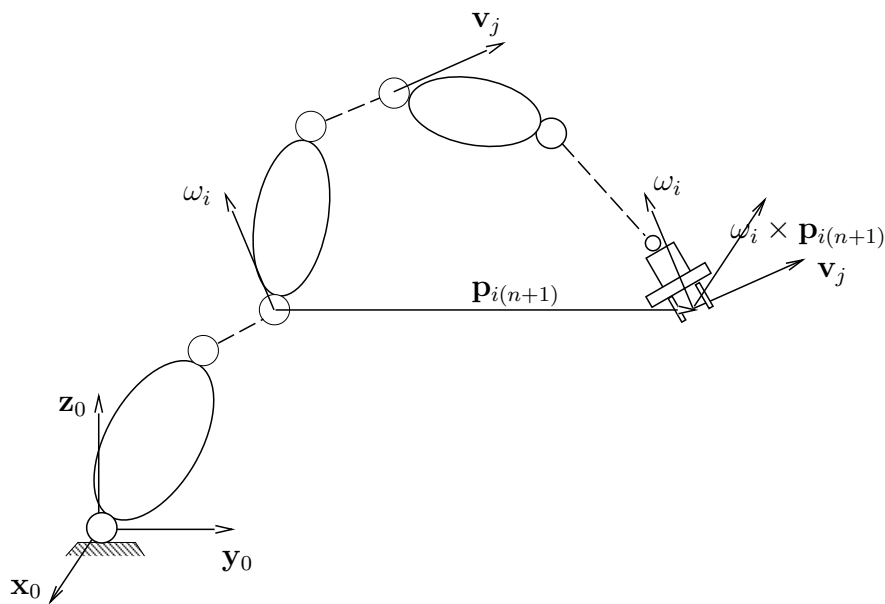


Figure 2.2: Contribution of joint velocities to end-effector velocities

The contribution of a joint to the end-effector velocities depends on the type of that joint (see Figure 3.2). A prismatic joint contributes, \mathbf{v}_i , to the end-effector linear velocity. A revolute joint contributes, ω_i to the end-effector angular velocity and $(\omega_i \times \mathbf{p}_{i(n+1)})$ to its linear velocity.

The vector $\mathbf{p}_{i(n+1)}$ is the vector connecting the origins of frames \mathcal{R}_i and $\mathcal{R}_{(n+1)}$. This yields

$$\mathbf{v} = \sum_{i=1}^n (\epsilon_i \mathbf{z}_i + \bar{\epsilon}_i \mathbf{z}_i \times \mathbf{p}_{i(n+1)}) \dot{q}_i; \quad (2.6)$$

$$\omega_n = \sum_{i=1}^n \bar{\epsilon}_i \mathbf{z}_i \dot{q}_i. \quad (2.7)$$

The basic kinematic model is

$$\vartheta \triangleq \begin{bmatrix} \mathbf{v} \\ \omega \end{bmatrix} = J_O(\mathbf{q}) \dot{\mathbf{q}}. \quad (2.8)$$

In this model, the matrix $J_O(\mathbf{q})$, termed *the basic Jacobian*, is defined independently of the particular set of parameters used to describe the end-effector configuration. The general expression of the basic Jacobian matrix is

$$J_O(\mathbf{q}) = \begin{pmatrix} (\epsilon_1 \mathbf{z}_1 + \bar{\epsilon}_1 \mathbf{z}_1 \times \mathbf{p}_{1(n+1)}) & \cdots & (\epsilon_n \mathbf{z}_n + \bar{\epsilon}_n \mathbf{z}_n \times \mathbf{p}_{n(n+1)}) \\ \bar{\epsilon}_1 \mathbf{z}_1 & \cdots & \bar{\epsilon}_n \mathbf{z}_n \end{pmatrix}. \quad (2.9)$$

The above form provides a vector representation of the Jacobian matrix. The expression of this matrix in a given frame is obtained by evaluating all vectors in that frame. The expressions of equations (2.6 and 2.7) in the coordinate frame \mathcal{R}_0 are

$$\mathbf{v} = \sum_{i=1}^n S_{0i} (\epsilon_i \mathbf{z}_i + \bar{\epsilon}_i \hat{\mathbf{z}}_i \mathbf{p}_{i(n+1)(\mathcal{R}_i)}) \dot{q}_i; \quad (2.10)$$

$$\omega = \sum_{i=1}^n S_{0i} \bar{\epsilon}_i \mathbf{z}_i \dot{q}_i; \quad (2.11)$$

where $\hat{\mathbf{z}}_i$ represents the 3×3 operator of cross product by \mathbf{z}_i and expressed in \mathcal{R}_i . This is

$$\mathbf{z} \triangleq \begin{pmatrix} z_1 \\ z_2 \\ z_3 \end{pmatrix} = \mathbf{z}_i = \begin{pmatrix} 0 \\ 0 \\ 1 \end{pmatrix}; \quad (2.12)$$

and

$$\hat{\mathbf{z}} \triangleq \begin{pmatrix} 0 & -z_3 & z_2 \\ z_3 & 0 & -z_1 \\ -z_2 & z_1 & 0 \end{pmatrix} = \hat{\mathbf{z}}_i = \begin{pmatrix} 0 & -1 & 0 \\ 1 & 0 & 0 \\ 0 & 0 & 0 \end{pmatrix}. \quad (2.13)$$

In frame \mathcal{R}_0 , the $m_0 \times n$ basic Jacobian matrix is given by

$$J_0(\mathbf{q}) = \begin{pmatrix} S_{01}(\epsilon_1 \mathbf{z} + \bar{\epsilon}_1 \hat{\mathbf{z}} \mathbf{p}_{1(n+1)(\mathcal{R}_1)}) & \cdots & S_{0n}(\epsilon_n \mathbf{z} + \bar{\epsilon}_n \hat{\mathbf{z}} \mathbf{p}_{n(n+1)(\mathcal{R}_n)}) \\ \bar{\epsilon}_1 S_{01} \mathbf{z} & \cdots & \bar{\epsilon}_n S_{0n} \mathbf{z} \end{pmatrix}. \quad (2.14)$$

Let $\delta \mathbf{x}_0$ be the m_0 -column matrix formed by the elementary displacement $\delta \mathbf{p}$ and the elementary rotation $\delta \Phi$. The basic variational model is defined as

$$\delta \mathbf{x}_0 \triangleq \begin{pmatrix} \delta \mathbf{p} \\ \delta \Phi \end{pmatrix} = J_0(\mathbf{q}) \delta \mathbf{q}. \quad (2.15)$$

The basic Jacobian matrix, which is defined independently of the selected representation, characterizes the *mobility* of the end-effector at a given configuration.

End-Effector Mobility *The mobility of the end-effector at a configuration \mathbf{q} is defined as the rank of the matrix $J_0(\mathbf{q})$.*

For some configurations, called singular configurations, the end-effector mobility locally decreases. A *singular configuration* is a configuration \mathbf{q} at which the end-effector locally loses the ability to move along or rotate about some direction of the Cartesian space with any specified velocity.

2.1.2 Jacobian Matrix

The Jacobian matrix associated with a given representation, \mathbf{x} , of the end-effector configuration can be obtained from the basic Jacobian matrix $J_0(\mathbf{q})$ by

$$J(\mathbf{q}) = E(\mathbf{x}) J_0(\mathbf{q}); \quad (2.16)$$

The matrix $E(\mathbf{x})$ is only dependent of the type of coordinates selected to represent the position and orientation of the effector. $E(\mathbf{x})$ is an $m \times m_0$ of the form

$$E(\mathbf{x}) = \begin{pmatrix} E_p(\mathbf{x}_p) & 0 \\ 0 & E_r(\mathbf{x}_r) \end{pmatrix}. \quad (2.17)$$

2.1.3 Position Representations

Cartesian Coordinates

The matrix $E_p(\mathbf{x})$ associated with $\mathbf{x}_p = (x \ y \ z)^T$ is identity matrix of order 3.

Cylindrical Coordinates

The matrix $E_p(\mathbf{x})$ associated with $\mathbf{x}_p = (\rho \ \theta \ z)^T$ can be obtained from the differentiation of the relationships expressing the identity

$$(x \ y \ z)^T = (\rho \cos \theta \ \rho \sin \theta \ z)^T;$$

with respect to ρ , θ , and z . This is

$$E_p(\mathbf{x}) = \begin{pmatrix} \cos \theta & \sin \theta & 0 \\ -\sin \theta / \rho & \cos \theta / \rho & 0 \\ 0 & 0 & 1 \end{pmatrix}. \quad (2.18)$$

Spherical Coordinates

The matrix $E_p(\mathbf{x})$ associated with $\mathbf{x}_p = (\rho \ \theta \ \phi)^T$ can be obtained from the differentiation of the relationships expressing the identity

$$(x \ y \ z)^T = (\rho \cos \theta \sin \phi \ \rho \sin \theta \sin \phi \ \rho \cos \phi)^T;$$

with respect to ρ , θ , and ϕ . This is

$$E_p(\mathbf{x}) = \begin{pmatrix} \cos \theta \sin \phi & \sin \theta \sin \phi & \cos \phi \\ -\sin \theta / (\rho \sin \phi) & \cos \theta / (\rho \sin \phi) & 0 \\ \cos \theta \cos \phi / \rho & \sin \theta \cos \phi / \rho & -\sin \phi / \rho \end{pmatrix}. \quad (2.19)$$

2.1.4 Rotation Representations

Direction Cosines

With the direction cosines representation, the end-effector orientation is described by the 9×1 column matrix

$$\mathbf{x}_r = (\mathbf{s}_1^T \ \mathbf{s}_2^T \ \mathbf{s}_3^T)^T;$$

where \mathbf{s}_1 , \mathbf{s}_2 , and \mathbf{s}_3 are the components, in \mathcal{R}_0 , of the three unit vectors $\mathbf{x}_{(n+1)}$, $\mathbf{y}_{(n+1)}$, and $\mathbf{z}_{(n+1)}$, associated with the coordinate frame $\mathcal{R}_{(n+1)}$.

Given the end-effector instantaneous angular velocity vector, ω , the time derivatives of the three unit vectors $\mathbf{x}_{(n+1)}$, $\mathbf{y}_{(n+1)}$, and $\mathbf{z}_{(n+1)}$, are

$$\frac{d\mathbf{x}_{(n+1)}}{dt} = \omega \times \mathbf{x}_{(n+1)}; \quad (2.20)$$

$$\frac{d\mathbf{y}_{(n+1)}}{dt} = \omega \times \mathbf{y}_{(n+1)}; \quad (2.21)$$

$$\frac{d\mathbf{z}_{(n+1)}}{dt} = \omega \times \mathbf{z}_{(n+1)}. \quad (2.22)$$

The components, in \mathcal{R}_0 , of the time derivatives of $\mathbf{x}_{(n+1)}$, $\mathbf{y}_{(n+1)}$, and $\mathbf{z}_{(n+1)}$, are

$$\dot{\mathbf{s}}_1 = -\widehat{\mathbf{s}}_1 \omega; \quad (2.23)$$

$$\dot{\mathbf{s}}_2 = -\widehat{\mathbf{s}}_2 \omega; \quad (2.24)$$

$$\dot{\mathbf{s}}_3 = -\widehat{\mathbf{s}}_3 \omega. \quad (2.25)$$

The matrix $E_r(\mathbf{x})$ associated with $\mathbf{x}_r = (\mathbf{s}_1^T \ \mathbf{s}_2^T \ \mathbf{s}_3^T)^T$ is the 9×3 matrix

$$E_r(\mathbf{x}) = \begin{pmatrix} -\widehat{\mathbf{s}}_1 \\ -\widehat{\mathbf{s}}_2 \\ -\widehat{\mathbf{s}}_3 \end{pmatrix}. \quad (2.26)$$

Euler Angles

The matrix $E_r(\mathbf{x})$ associated with $\mathbf{x}_r = (\psi \ \theta \ \phi)^T$ is

$$E_r(\mathbf{x}) = \begin{pmatrix} -\sin \psi \cos \theta / \sin \theta & \cos \psi \cos \theta / \sin \theta & 1 \\ \cos \psi & \sin \psi & 0 \\ \sin \psi / \sin \theta & -\cos \psi / \sin \theta & 0 \end{pmatrix}. \quad (2.27)$$

Euler Parameters

The relationship between the angular velocity vector ω and the time derivative $\dot{\lambda}$ of Euler parameters $\lambda = (\lambda_0 \lambda_1 \lambda_2 \lambda_3)^T$ is

$$\dot{\lambda} = \frac{1}{2}\check{\lambda}\omega; \quad (2.28)$$

where

$$\check{\lambda} = \begin{pmatrix} -\lambda_1 & -\lambda_2 & -\lambda_3 \\ \lambda_0 & \lambda_3 & -\lambda_2 \\ -\lambda_3 & \lambda_0 & \lambda_1 \\ \lambda_2 & -\lambda_1 & \lambda_0 \end{pmatrix}. \quad (2.29)$$

The matrix $E_r(\mathbf{x})$ associated with Euler parameters is

$$E_r(\mathbf{x}) = \frac{1}{2}\check{\lambda} = \frac{1}{2} \begin{pmatrix} -\lambda_1 & -\lambda_2 & -\lambda_3 \\ \lambda_0 & \lambda_3 & -\lambda_2 \\ -\lambda_3 & \lambda_0 & \lambda_1 \\ \lambda_2 & -\lambda_1 & \lambda_0 \end{pmatrix}. \quad (2.30)$$

2.2 Inverse Kinematic Model

Given a set of velocities or elementary displacements at the manipulator joints, the Jacobian matrix provides a basic tool to uniquely determine the velocities or elementary displacements at the end-effector. Often, however, we are concerned with finding the inverse of the above relationship: the end-effector motion is specified and the problem is to find the corresponding velocities or elementary displacements at the joints.

Given the $m \times n$ matrix $J(\mathbf{q})$ and the m elementary displacements $\delta \mathbf{x}$, the problem is to solve the system of m equations with the n unknowns, $\delta \mathbf{q}$, for all configuration \mathbf{q} ,

$$\delta \mathbf{x} = J(\mathbf{q}) \delta \mathbf{q}. \quad (2.31)$$

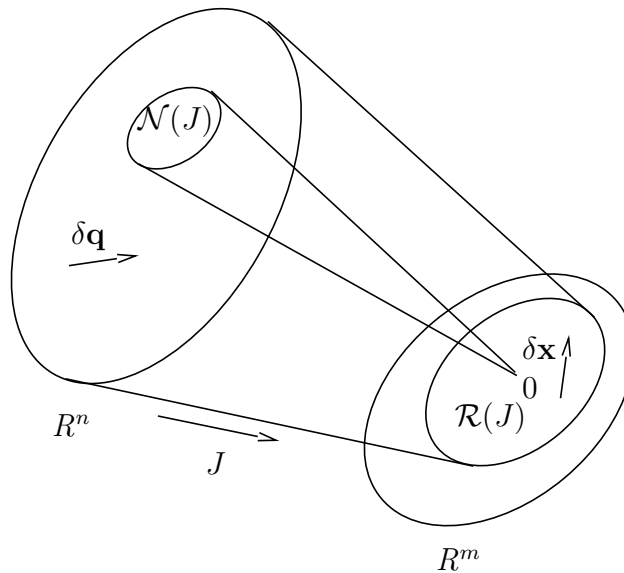


Figure 2.3: The Mapping Associated with the Jacobian Matrix

The matrix $J(\mathbf{q})$ operates between the two vector spaces R^n and R^m , as illustrated in Figure 3.3. A vector $\delta \mathbf{q} \in R^n$ is mapped by J into a vector $\delta \mathbf{x} \in \mathcal{R}(J)$. $\mathcal{R}(J)$ is the range space or the column space of J .

The null space of J , $\mathcal{N}(J)$, is the subspace of R^n such that all vectors $\delta\mathbf{q} \in \mathcal{R}(J)$ verify

$$J(\mathbf{q}) \delta\mathbf{q} = 0. \quad (2.32)$$

Let J_1, J_2, \dots, J_n be the columns of the Jacobian matrix, i.e.

$$J = (J_1 \ J_2 \ \dots \ J_n).$$

The system of equations 2.31 can be written as

$$\delta\mathbf{x} = J_1 \delta\mathbf{q}_1 + J_2 \delta\mathbf{q}_2 + \dots + J_n \delta\mathbf{q}_n. \quad (2.33)$$

In this form $\delta\mathbf{x}$ is expressed as a linear combination of the columns of the Jacobian matrix.

Definition - Theorem 1 The system (2.31) is said to be *consistent* and possesses at least one solution if and only if,

$$\text{rank } J = \text{rank } (J|\delta\mathbf{x}); \quad (2.34)$$

where $(J|\delta\mathbf{x})$ is the $m \times (n+1)$ matrix obtained by augmenting J with the column matrix $\delta\mathbf{x}$.

Theorem 1 states the necessary and sufficient condition for the existence of at least one solution for the system (2.31). This condition requires the vector $\delta\mathbf{x}$ to be in the subspace spanned by the columns of J .

Since the Jacobian is a configuration dependent matrix, the existence of a solution will depend on the manipulator configuration. The Jacobian matrix also depends on the type of representation used to describe the position and orientation of the end-effector.

2.2.1 Reduction to the Basic Kinematic Model

Using the basic Jacobian matrix $J_0(\mathbf{q})$, we are going first to reduce the dimension, m , of the initial problem of equation (2.31) to m_0 ($m_0 \leq m$).

We have seen that a Jacobian matrix $J(\mathbf{q})$ associated with a representation \mathbf{x} of the end-effector configuration is expressed as the product of matrices $E(\mathbf{x})J_0(\mathbf{q})$. The system (2.31) becomes

$$\delta\mathbf{x} = E(\mathbf{x}) \delta\mathbf{x}_0; \quad (2.35)$$

$$\delta\mathbf{x}_0 = J_0(\mathbf{q}) \delta\mathbf{q}. \quad (2.36)$$

$E(\mathbf{x})$ is an $m \times m_0$ matrix with $m \geq m_0$.

Left Inverse The system (2.35) possesses a unique solution $\delta\mathbf{x}_0$ for every $\delta\mathbf{x}$, if and only if, $\text{rank } E = m_0$, i.e. the columns of E are linearly independent. In this case there exists an $m_0 \times m$ *left inverse*, E^+ , such that $E^+E = I_{m_0}$, the identity matrix of order m_0 .

$$\delta\mathbf{x}_0 = E^+(\mathbf{x}) \delta\mathbf{x}. \quad (2.37)$$

The case $\text{rank } E < m_0$ corresponds to configurations where the representation is singular. The formula for a left inverse of E , is

$$E^+ = (E^T E)^{-1} E^T. \quad (2.38)$$

Using equation (2.17), left inverses of $E(\mathbf{x})$ can be written in the form

$$E^+(\mathbf{x}) = \begin{pmatrix} E_p^+(\mathbf{x}_p) & 0 \\ 0 & E_r^+(\mathbf{x}_r) \end{pmatrix}. \quad (2.39)$$

For $m = m_0$, E^+ is simply the inverse matrix E^{-1} .

2.2.2 Position Representations

Cartesian Coordinates

The matrix $E_p^+(\mathbf{x}_p)$ is simply the inverse of the matrix $E_p(\mathbf{x}_p)$ associated with $x_p = (x \ y \ z)^T$. This is the identity matrix of order 3.

Cylindrical Coordinates

The inverse of the matrix $E_p(\mathbf{x}_p)$ associated with $\mathbf{x}_p = (\rho \theta z)^T$ is

$$E_p^{-1}(\mathbf{x}_p) = \begin{pmatrix} \cos \theta & -\rho \sin \theta & 0 \\ -\sin \theta & \rho \cos \theta & 0 \\ 0 & 0 & 1 \end{pmatrix}. \quad (2.40)$$

Spherical Coordinates

The inverse of $E_p(\mathbf{x}_p)$ associated with $\mathbf{x}_p = (\rho \theta \phi)^T$ is

$$E_p^{-1}(\mathbf{x}_p) = \begin{pmatrix} \cos \theta \sin \phi & \rho \sin \theta \sin \phi & \rho \cos \theta \cos \phi \\ -\sin \theta \sin \phi & \rho \cos \theta \sin \phi & \rho \sin \theta \cos \phi \\ \cos \phi & 0 & -\rho \sin \phi \end{pmatrix}. \quad (2.41)$$

2.2.3 Rotation Representations

Direction Cosines

The matrix $E_r(\mathbf{x}_r)$ associated with the direction cosines representation $\mathbf{x}_r = (\hat{\mathbf{s}}_1^T \hat{\mathbf{s}}_2^T \hat{\mathbf{s}}_3^T)^T$ is the 9×3 matrix

$$E_r(\mathbf{x}) = \begin{pmatrix} -\hat{\mathbf{s}}_1 \\ -\hat{\mathbf{s}}_2 \\ -\hat{\mathbf{s}}_3 \end{pmatrix};$$

of rank 3. To find a left inverse of E , one could use $(E_r^T E_r)^{-1} E_r^T$. Observing

$$E_r^T(\mathbf{x}_r) E_r(\mathbf{x}_r) = (\hat{\mathbf{s}}_1^T \hat{\mathbf{s}}_1 + \hat{\mathbf{s}}_2^T \hat{\mathbf{s}}_2 + \hat{\mathbf{s}}_3^T \hat{\mathbf{s}}_3) = 2 I_3;$$

yields

$$E_r^+(\mathbf{x}_r) = \frac{1}{2} E_r^T(\mathbf{x}_r) = \frac{1}{2} (-\hat{\mathbf{s}}_1^T \quad -\hat{\mathbf{s}}_2^T \quad -\hat{\mathbf{s}}_3^T). \quad (2.42)$$

Euler Angles

The inverse of $E_r(\mathbf{x}_r)$ associated with $\mathbf{x}_r = (\psi \ \theta \ \phi)^T$ is

$$E_r^{-1}(\mathbf{x}_r) = \begin{pmatrix} 0 & \cos \psi & \sin \psi \sin \theta \\ 0 & \sin \psi & -\cos \psi \sin \theta \\ 1 & 0 & \cos \theta \end{pmatrix}. \quad (2.43)$$

Euler Parameters

The matrix $E_r(\mathbf{x}_r)$ associated with the Euler parameters representation is a 4×3 matrix of rank 3. A left inverse $E_r^+(\mathbf{x}_r)$ can be obtained by $[E_r^T(\mathbf{x}_r)E_r(\mathbf{x}_r)]^{-1}E_r^T(\mathbf{x}_r)$. Observing

$$\check{\lambda}^T \check{\lambda} = I_3; \quad (2.44)$$

yields

$$E_r^+(\mathbf{x}_r) = 4E_r^T = 2 \begin{pmatrix} -\lambda_1 & \lambda_0 & -\lambda_3 & \lambda_2 \\ -\lambda_2 & \lambda_3 & \lambda_0 & -\lambda_1 \\ -\lambda_3 & -\lambda_2 & \lambda_1 & \lambda_0 \end{pmatrix}. \quad (2.45)$$

2.2.4 Inverse of the Basic Kinematic Model

The initial problem is now reduced to the problem of solving the basic kinematic model (2.36)

$$\delta \mathbf{x}_0 = J_0(\mathbf{q}) \delta \mathbf{q}.$$

This is a system of m_0 equations with n unknowns, where $m_0 \leq n$.

Right Inverse The system (2.36) possesses at least one solution $\delta \mathbf{q}$ for every $\delta \mathbf{x}_0$, if and only if, $\text{rank } J_0 = m_0$, i.e. the columns of J_0 span R^{m_0} . In this case there exists an $n \times m_0$ *right inverse*, J_0^+ , such that $J_0 J_0^+ = I_{m_0}$, the identity matrix of order m_0 . A right (left) inverse is a special case of a generalized inverse.

General Solution Let $J_0^\#(\mathbf{q})$ be a generalized inverse of the basic Jacobian matrix. The general solution of the system (2.36) is

$$\delta \mathbf{q} = J_0^\#(\mathbf{q}) \delta \mathbf{x}_0 + [I_n - J_0^\#(\mathbf{q}) J_0(\mathbf{q})] \delta \mathbf{q}_0; \quad (2.46)$$

where I_n is the identity matrix of order n , and the elementary joint displacement $\delta \mathbf{q}_0$ is arbitrary.

The $n \times n$ matrix $[I_n - J_0^\#(\mathbf{q}) J_0(\mathbf{q})]$ operates on vectors $\delta \mathbf{q}_0 \in R^n$ to produce vectors $\delta \mathbf{q}_n \in \mathcal{N}(J)$

$$\delta \mathbf{q}_n = [I_n - J_0^\#(\mathbf{q}) J_0(\mathbf{q})] \delta \mathbf{q}_0.$$

The mapping by J_0 of these vectors is the zero-vector of R^{m_0} ,

$$J_0 \delta \mathbf{q}_n = [J_0 - J_0 J_0^\#(\mathbf{q}) J_0(\mathbf{q})] \delta \mathbf{q}_0 = 0.$$

Example 4 Let us consider the problem of solving the kinematic model of the three-degree-of-freedom manipulator shown in Figure 3.4. This manipulator is redundant with respect to the task of positioning its end-effector. The Jacobian matrix associated with this task is

$$J(\mathbf{q}) = \begin{pmatrix} -l_1 s_1 - l_2 s_{12} - l_3 s_{123} & -l_2 s_{12} - l_3 s_{123} & -l_3 s_{123} \\ l_1 c_1 + l_2 c_{12} + l_3 c_{123} & l_2 c_{12} + l_3 c_{123} & l_3 c_{123} \end{pmatrix}.$$

For simplicity, we will assume that the configuration of the manipulator lies in the subspace defined by $\{q_1 = q_2 = 0\}$ and that $l_1 = l_2 = l_3 = 1$. In this subspace, the Jacobian is

$$J = \begin{pmatrix} -s_3 & -s_3 & -s_3 \\ 2 + c_3 & 1 + c_3 & c_3 \end{pmatrix}.$$

This 2×3 matrix is of rank 2. The pseudo-inverse, J^+ is the 3×2 matrix $J^T (J J^T)^{-1}$. The matrix $(J J^T)$ is

$$J J^T = \begin{pmatrix} 3s_3 & -3(1 + c_3)s_3 \\ -3(1 + c_3)s_3 & 3c_3 + 6c_3 + 5 \end{pmatrix};$$

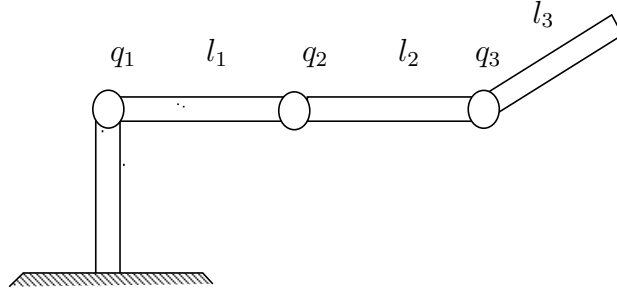


Figure 2.4: A Three-Degree-Of-Freedom Manipulator

and

$$(JJ^T)^{-1} = \frac{1}{6s3} \begin{pmatrix} 3cc3 + 6c3 + 5 & 3(1 + c3)s3 \\ 3(1 + c3)s3 & 3ss3 \end{pmatrix};$$

which yields

$$J^+ = \frac{1}{6s3} \begin{pmatrix} (1 + 3c3) & 3s3 \\ -2 & 0 \\ -(5 + 3c3) & -3s3 \end{pmatrix}.$$

The general solution in this subspace is

$$\delta \mathbf{q} = J^+ \delta \mathbf{x} + [I_3 - J^+ J] \delta \mathbf{q}_0;$$

where the 3×3 matrix $[I_3 - J^+ J]$ associated with the null space is

$$[I_3 - J^+ J] = \begin{pmatrix} 1 & -2 & 1 \\ -2 & 4 & -2 \\ 1 & -2 & 1 \end{pmatrix}.$$

This matrix is of rank 1.

Chapter 3

Joint Space Framework

Robot control has been traditionally viewed from the perspective of a manipulator's joint motions, and significant effort has been devoted to the development of *joint space* dynamic models and control methodologies. However, the limitations of joint space control techniques, especially in constrained motion tasks, have motivated alternative approaches for dealing with task-level dynamics and control. The discussion here focuses on the joint space framework.

3.1 Joint Space Control

By its very nature, joint space control calls for transformations whereby joint space descriptions are obtained from the robot task specifications. Typically, a joint space control system is organized following the general structure shown in Figure 3.1. At the highest level, tasks are specified in terms of end-effector or manipulated object's motion, compliances, and contact forces and moments. Tasks are then transformed at the intermediate level into descriptions in terms of joint positions, veloci-

ties, accelerations, compliances, and joint torques. This provides the needed input to the control level, which acts at the robot joints.

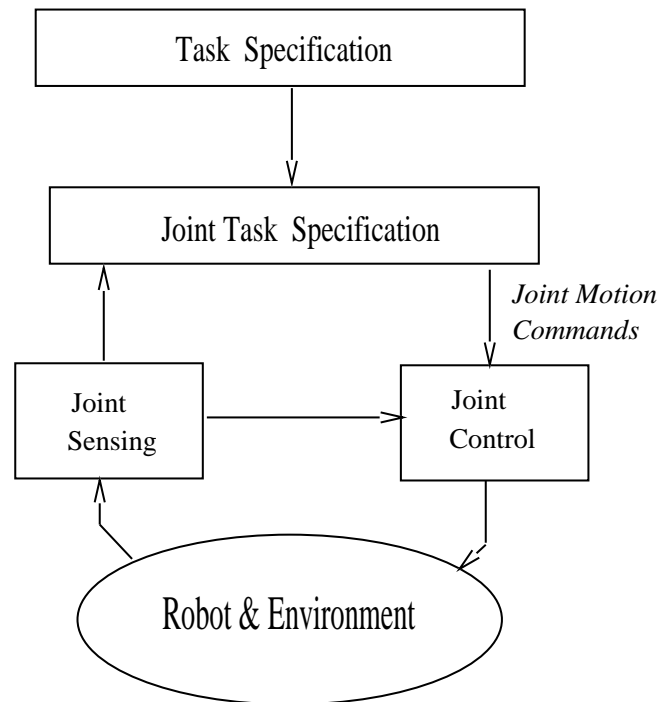


Figure 3.1: Joint Space Control Structure

3.1.1 Motion Coordination

An important kinematic issue associated with motion control of robot mechanisms, is the *inverse kinematic problem* or more generally the task transformation problem. This problem is raised by the discrepancy between the space where robot tasks are specified and the space in which the control is taking place.

Tasks are specified with respect to the robot's end-effector or manipulated object, while motions are typically controlled through the action

of servo-controllers that effect the positions and velocities of the robot's joints. Finding the set of joint trajectories, inputs to the joint servo-controllers, that would produce the specified task is the central issue in the task transformation problem.

Obviously, the need for solutions of the inverse kinematic problem is not limited to the motion control problem. The inverse kinematic is needed in workspace analysis, design, simulations, and planning of robot motions. By its computational complexity, however, the inverse kinematic problem becomes more critical in real-time control implementations. This is, for instance, the case of tasks when the robot is called to accommodate motion that cannot be completely pre-planned or to make corrections generated by external sensory devices.

The computation complexity of the inverse kinematic problem has led to solutions based on the inverse of the linearized kinematic model. This model expresses the relationship between the vector $\delta\mathbf{q}$ associated with the variations of joint positions and the vector $\delta\mathbf{x}$ associated with the corresponding variations of the positions and orientations of the end-effector,

$$\delta\mathbf{x} = J(\mathbf{q})\delta\mathbf{q}; \quad (3.1)$$

where $J(\mathbf{q})$ is the Jacobian matrix. For an n -degree-of-freedom manipulator with an end-effector operating in an m -dimensional space, $J(\mathbf{q})$ is an $m \times n$ matrix.

Using the linearized kinematic model (3.1), Whitney (1972) proposed the *resolved motion-rate control* approach for the coordination of manipulator joint motions. The resolved motion-rate control uses the inverse of the linear relationship of equation (3.1). For a non-redundant manipulator for which a non-redundant representation of the position and orientation of the end-effector is used, i.e. $n = m = m_0$, the solution is simply

$$\delta\mathbf{q} = J^{-1}(\mathbf{q})\delta\mathbf{x}. \quad (3.2)$$

For a given trajectory of the end-effector, motion control is achieved by continuously controlling the manipulator from the current position \mathbf{q} to the position $\mathbf{q} + \delta\mathbf{q}$.

3.1.2 Redundant Manipulators

Motion redundancy is an important characteristic for extending robot applications to complex tasks and workspaces. Manipulators with six degrees of freedom can generally realize an arbitrary position and orientation of the end-effector. However, this cannot be achieved if certain joint movements are precluded by obstacles. The workspace of a six-degree-of-freedom arm has to be carefully structured and motions carefully planned to satisfy obstacle constraints. By appropriate addition of motion redundancy, the dexterity of a manipulator can be greatly improved.

The joint space task transformation problem is exacerbated for mechanisms with redundancy or at kinematic singularities. The typical approach involves the use of pseudo- or generalized inverses to solve an under-constrained or degenerate system of linear equations, while optimizing some given criterion.

The position and orientation of the end-effector of a redundant mechanism can be obtained with an infinite number of postures of its links. Generalized inverses and pseudo-inverses (Whitney 1972, Liegeois 1977, Fournier 1980, Hanafusa et al. 1981) have been used to solve the kinematic equation (3.1). Using a generalized inverse $J^\#(\mathbf{q})$ of the Jacobian matrix, the general solution of the system (3.1) is

$$\delta\mathbf{q} = J^\#(\mathbf{q})\delta\mathbf{x} + [I - J^\#(\mathbf{q})J(\mathbf{q})]\delta\mathbf{q}_0; \quad (3.3)$$

where I is the identity matrix of appropriate dimensions and $\delta\mathbf{q}_0$ denotes an arbitrary vector. The matrix $[I - J^\#(\mathbf{q})J(\mathbf{q})]$ defines the null space associated with $J^\#(\mathbf{q})$, and vectors of the form $[I - J^\#(\mathbf{q})J(\mathbf{q})]\delta\mathbf{q}_0$ correspond to zero-variation of the position and orientation of the end-effector. The additional freedom of motion associated with null space is generally used to minimize some criteria, such as the avoidance of joint limits (Liegeois, 1977; Fournier, 1980), obstacles (Hanafusa, Yoshikawa, and Nakamura, 1981; Kircanski and Vukobratovic, 1984; Espiau and Boulic, 1985) and kinematic singularities (Luh and Gu, 1985), the minimization of actuator joint forces (Hollerbach and Suh, 1985), or obtaining isotropic velocity characteristics (Ghosal and Roth, 1987).

3.1.3 PID Control Schemes

Current industrial robots relies almost exclusively on the concept of joint position control. In these robots, PID controllers are used to independently control a manipulator's joints. Since the inertia seen at each joint varies with the robot configuration, the PID gains are selected for some average configuration in the workspace. The dynamic interaction between joints is ignored, and the disturbance rejection of the dynamic forces relies on the use of large gains and high servo rates.

The implementation of PID control is quite simple, and the performance of PID controllers has been sufficient for many industrial tasks. However, the performance of PID controllers decreases when dynamic effects become significant. The undesirable effects increase with the range of motion, speed, and acceleration at which the robot is operating.

3.2 Joint Space Dynamic Model

A manipulator is treated as a holonomic system with a structure of an open kinematic chain of $n + 1$ rigid bodies, i.e. links, connected through n *revolute* and/or *prismatic* joints having *one degree of freedom*.

With revolute and/or prismatic joints, a chain of $n + 1$ links possess n degree-of-freedom. The set $\{q_1, q_2, \dots, q_n\}$ of n *joint coordinates* form a system of generalized coordinates for the manipulator. The configuration of the manipulator is described by the vector \mathbf{q} of components q_1, q_2, \dots, q_n in the manipulator *joint space*.

Using the Lagrangian formalism, the equations of motion in joint space of an n -degree-of-freedom manipulator are

$$\frac{d}{dt} \left(\frac{\partial L}{\partial \dot{\mathbf{q}}} \right) - \frac{\partial L}{\partial \mathbf{q}} = \mathbf{\Gamma}; \quad (3.4)$$

where $\mathbf{\Gamma}$ is the generalized force vector and where $L(\mathbf{q}, \dot{\mathbf{q}})$ is the Lagrangian given by

$$L(\mathbf{q}, \dot{\mathbf{q}}) = T(\mathbf{q}, \dot{\mathbf{q}}) - U(\mathbf{q});$$

where T and U are the total kinetic energy and potential energy of the manipulator, respectively.

3.2.1 Kinetic Energy

The kinetic energy of this holonomic system is a quadratic form of the generalized velocities

$$T(\mathbf{q}, \dot{\mathbf{q}}) = \frac{1}{2} \dot{\mathbf{q}}^T A(\mathbf{q}) \dot{\mathbf{q}}; \quad (3.5)$$

where $A(\mathbf{q})$ designates the $n \times n$ symmetric matrix of the quadratic form, i.e. the kinetic energy matrix. The kinetic energy of the i^{th} link is

$$T_i = \frac{1}{2} (m_i \mathbf{v}_{C_i}^T \mathbf{v}_{C_i} + \omega_i^T I_{C_i} \omega_i); \quad (3.6)$$

where \mathbf{v}_{C_i} and ω_i represent, respectively, the linear velocity vector and the angular velocity vector at the center of mass, C_i of link i . m_i is the mass of link i and I_{C_i} is the i^{th} link's inertia matrix evaluated at the center of mass C_i . The kinetic energy of the manipulator is

$$T = \sum_{i=1}^n T_i.$$

Velocities at Center-of-Mass The manipulator kinematics yields

$$\mathbf{v}_{C_i} = J_{vi} \dot{\mathbf{q}}; \quad (3.7)$$

and

$$\omega_i = J_{\omega i} \dot{\mathbf{q}}. \quad (3.8)$$

Jacobian Matrix J_{vi}

The Jacobian matrix J_{vi} can be directly obtained by differentiating the position vector \mathbf{p}_{C_i} , which locates the center-of-mass of link i with respect to the manipulator base, as shown in Figure 3.2

$$J_{vi}(\mathbf{q}) = \left[\frac{\partial \mathbf{p}_{C_i}}{\partial q_1} \quad \frac{\partial \mathbf{p}_{C_i}}{\partial q_2} \quad \cdots \quad \frac{\partial \mathbf{p}_{C_i}}{\partial q_i} \quad \mathbf{0} \quad \mathbf{0} \quad \cdots \quad \mathbf{0} \right]. \quad (3.9)$$

The matrix $J_{vi}(\mathbf{q})$ can also be obtained from the general form

$$J_{vi}(\mathbf{q}) = [(\epsilon_1 \mathbf{z}_1 + \bar{\epsilon}_1 \mathbf{z}_1 \times \mathbf{p}_{1C_i}) \quad \cdots \quad (\epsilon_i \mathbf{z}_i + \bar{\epsilon}_i \mathbf{z}_i \times \mathbf{p}_{iC_i}) \quad \mathbf{0} \quad \cdots \quad \mathbf{0}]; \quad (3.10)$$

where \mathbf{p}_{jC_i} is the vector connecting joint j to C_i , as shown in Figure 3.3. \mathbf{z}_i is the unit vector along joint axis i .

Jacobian Matrix $J_{\omega i}$

The matrix $J_{\omega i}(\mathbf{q})$ is given by

$$J_{\omega i}(\mathbf{q}) = (\bar{\epsilon}_1 \mathbf{z}_1 \quad \bar{\epsilon}_2 \mathbf{z}_2 \quad \cdots \quad \bar{\epsilon}_i \mathbf{z}_i \quad \mathbf{0} \quad \mathbf{0} \quad \cdots \quad \mathbf{0}). \quad (3.11)$$

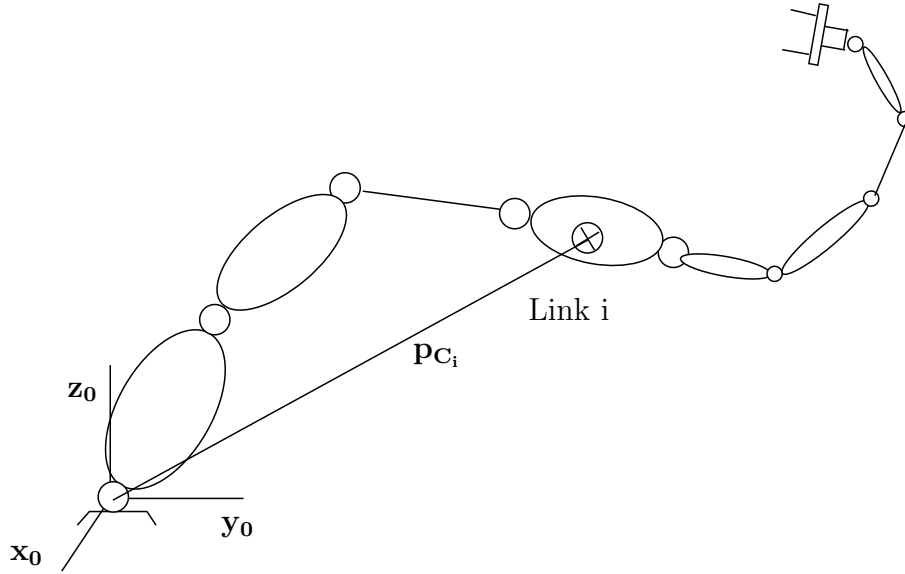


Figure 3.2: Position of Center of Mass

Kinetic Energy Matrix The kinetic energy matrix $A(\mathbf{q})$ of the manipulator is

$$A(\mathbf{q}) = \sum_{i=1}^n (m_i J_{v_i}^T J_{v_i} + J_{\omega_i}^T I_{C_i} J_{\omega_i}). \quad (3.12)$$

The equations of motion (3.4) can be written in the form

$$A(\mathbf{q})\ddot{\mathbf{q}} + \mathbf{b}(\mathbf{q}, \dot{\mathbf{q}}) + \mathbf{g}(\mathbf{q}) = \mathbf{\Gamma}; \quad (3.13)$$

where $\mathbf{b}(\mathbf{q}, \dot{\mathbf{q}})$ represents the vector of centrifugal and Coriolis forces. This vector is

$$\mathbf{b}(\mathbf{q}, \dot{\mathbf{q}}) = \dot{A}(\mathbf{q})\dot{\mathbf{q}} - \frac{1}{2} \begin{pmatrix} \dot{\mathbf{q}}^T A_{q_1} \dot{\mathbf{q}} \\ \dot{\mathbf{q}}^T A_{q_2} \dot{\mathbf{q}} \\ \vdots \\ \dot{\mathbf{q}}^T A_{q_n} \dot{\mathbf{q}} \end{pmatrix}; \quad (3.14)$$

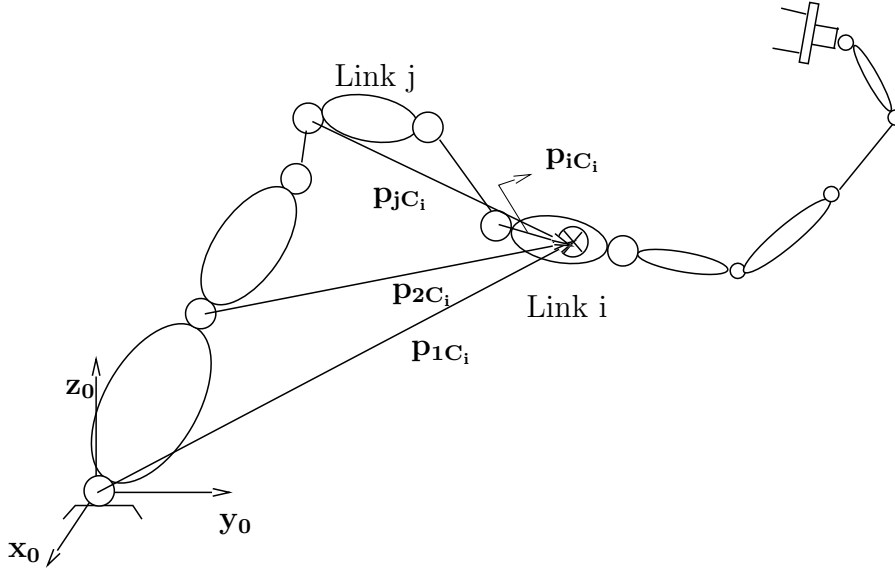


Figure 3.3: Position Vectors: $\mathbf{p}_{1C_i}, \dots, \mathbf{p}_{jC_i}, \dots$, and \mathbf{p}_{iC_i}

where

$$A_{q_i} = \frac{\partial A}{\partial q_i}.$$

Centrifugal and Coriolis Forces Using the Christoffel symbols, the vector $\mathbf{b}(\mathbf{q}, \dot{\mathbf{q}})$ can be obtained from the partial derivatives of $A(\mathbf{q})$ and the generalized velocities, $\dot{\mathbf{q}}$. The Christoffel symbols are

$$b_{i,jk} = \frac{1}{2}(a_{ijk} + a_{ikj} - a_{jki}); \quad (3.15)$$

where a_{ijk} is the partial derivative with respect to q_k of the $\{ij\}$ element of the matrix $A(\mathbf{q})$

$$a_{ijk} = \frac{\partial a_{ij}}{\partial q_k}.$$

Using the Christoffel symbols, the centrifugal and Coriolis force vector can be written as

$$\mathbf{b}(\mathbf{q}, \dot{\mathbf{q}}) = B(\mathbf{q})[\dot{\mathbf{q}}\dot{\mathbf{q}}] + C(\mathbf{q})[\dot{\mathbf{q}}^2]; \quad (3.16)$$

where $B(\mathbf{q})$ is the $n \times n(n-1)/2$ matrix associated with the Coriolis forces given by

$$B(\mathbf{q}) = \begin{pmatrix} 2b_{1,12} & \dots & 2b_{1,1n} & 2b_{1,23} & \dots & 2b_{1,2n} & \dots & 2b_{1,(n-1)n} \\ 2b_{2,12} & \dots & 2b_{2,1n} & 2b_{2,23} & \dots & 2b_{2,2n} & \dots & 2b_{2,(n-1)n} \\ \cdot & \cdot & \cdot & \cdot & \cdot & \cdot & \cdot & \cdot \\ \cdot & \cdot & \cdot & \cdot & \cdot & \cdot & \cdot & \cdot \\ \cdot & \cdot & \cdot & \cdot & \cdot & \cdot & \cdot & \cdot \\ 2b_{n,12} & \dots & 2b_{n,1n} & 2b_{n,23} & \dots & 2b_{n,2n} & \dots & 2b_{n,(n-1)n} \end{pmatrix}; \quad (3.17)$$

and where $C(\mathbf{q})$ is the $n \times n$ matrix associated with the centrifugal forces given by

$$C(\mathbf{q}) = \begin{pmatrix} b_{1,11} & b_{1,22} & \dots & b_{1,nn} \\ b_{2,11} & b_{2,22} & \dots & b_{2,nn} \\ \cdot & \cdot & \cdot & \cdot \\ \cdot & \cdot & \cdot & \cdot \\ \cdot & \cdot & \cdot & \cdot \\ b_{n,11} & b_{n,22} & \dots & b_{n,nn} \end{pmatrix}. \quad (3.18)$$

$[\dot{\mathbf{q}}\dot{\mathbf{q}}]$ and $[\dot{\mathbf{q}}^2]$ are the symbolic notations for the $n(n-1)/2 \times 1$ and $n \times 1$ column matrices:

$$[\dot{\mathbf{q}}^2] = [\dot{q}_1^2 \quad \dot{q}_2^2 \dots \dot{q}_n^2]^T; \quad (3.19)$$

and

$$[\dot{\mathbf{q}}\dot{\mathbf{q}}] = [\dot{q}_1\dot{q}_2 \quad \dot{q}_1\dot{q}_3 \dots \dot{q}_1\dot{q}_n \quad \dot{q}_2\dot{q}_3 \dots \dot{q}_2\dot{q}_n \dots \dot{q}_{n-1}\dot{q}_n]^T. \quad (3.20)$$

3.2.2 Potential Energy

If \mathbf{g}_0 represents the vector of gravity acceleration, as shown in Figure 3.4 the potential energy $U_i(\mathbf{q})$ corresponding to link i is

$$U_i(\mathbf{q}) = m_i(-\mathbf{p}_{C_i})^T \mathbf{g}_0.$$

The manipulator potential energy can be written as

$$U(\mathbf{q}) = -\sum_{i=1}^n m_i \mathbf{p}_{C_i}^T \mathbf{g}_0. \quad (3.21)$$

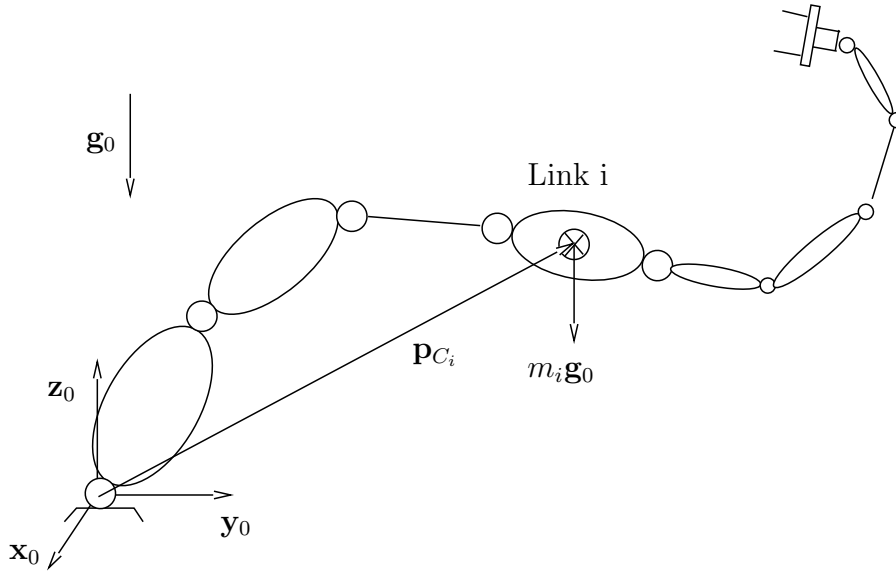


Figure 3.4: Gravity Forces

The vector of gravity forces, $\mathbf{g}(\mathbf{q})$ is given by

$$\mathbf{G}(\mathbf{x}) = \nabla U(\mathbf{q}).$$

The j^{th} component of \mathbf{g} is

$$g_j = \frac{\delta U}{\delta q_i} = - \sum_{i=1}^n \left(\frac{\delta \mathbf{p}_{C_i}}{\delta q_i} \right)^T m_i \mathbf{g}_0.$$

Using the transpose of the Jacobian matrix associated with the vector \mathbf{p}_{C_i} , the vector of gravity forces can be written as

$$\mathbf{g}(\mathbf{q}) = - \sum_{i=1}^n J_{vi}^T (m_i \mathbf{g}_0). \quad (3.22)$$

Example 1

The links of the RP manipulator shown in Figure 3.5 have total mass m_1 and m_2 . The center of mass of link 1 is located at a distance l_1 of the

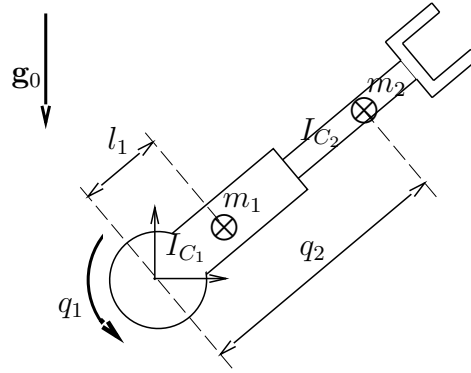


Figure 3.5: An RP Manipulator

joint axis 1, and the center of mass of link 2 is located at the distance q_2 from the joint axis 1. The inertia tensors of these links evaluated at the center of mass with respect to axes parallel to \mathcal{R}_0 are

$$I_{C_1} = \begin{pmatrix} I_{xx1} & 0 & 0 \\ 0 & I_{yy1} & 0 \\ 0 & 0 & I_{zz1} \end{pmatrix}; \quad \text{and} \quad I_{C_2} = \begin{pmatrix} I_{xx2} & 0 & 0 \\ 0 & I_{yy2} & 0 \\ 0 & 0 & I_{zz2} \end{pmatrix}.$$

Matrix A

The kinetic energy matrix A is obtained by applying equation (3.12) to this 2 d.o.f manipulator:

$$A = m_1 J_{v1}^T J_{v1} + J_{\omega 1}^T I_{C_1} J_{\omega 1} + m_2 J_{v2}^T J_{v2} + J_{\omega 2}^T I_{C_2} J_{\omega 2}.$$

J_{v1} and J_{v2} are obtained by direct differentiation of the vectors:

$$\mathbf{p}_{C_1} = \begin{bmatrix} l_1 c_1 \\ l_1 s_1 \\ 0 \end{bmatrix}; \quad \text{and} \quad \mathbf{p}_{C_2} = \begin{bmatrix} q_2 c_1 \\ q_2 s_1 \\ 0 \end{bmatrix}.$$

In \mathcal{R}_0 , these matrices are:

$$J_{v1} = \begin{bmatrix} -l_1 s_1 & 0 \\ l_1 c_1 & 0 \\ 0 & 0 \end{bmatrix}; \quad J_{v2} = \begin{bmatrix} -q_2 s_1 & c_1 \\ q_2 c_1 & s_1 \\ 0 & 0 \end{bmatrix}.$$

This yields

$$m_1(J_{v1}^T J_{v1}) = \begin{bmatrix} m_1 l_1^2 & 0 \\ 0 & 0 \end{bmatrix}; \quad (m_2 J_{v2}^T J_{v2}) = \begin{bmatrix} m_2 q_2^2 & 0 \\ 0 & m_2 \end{bmatrix}.$$

The matrices $J_{\omega 1}$ and $J_{\omega 2}$ are given by

$$J_{\omega 1} = [\bar{\epsilon}_1 \mathbf{z}_1 \quad \mathbf{0}] = \quad \text{and} \quad J_{\omega 2} = [\bar{\epsilon}_1 \mathbf{z}_1 \quad \bar{\epsilon}_2 \mathbf{z}_2].$$

Joint 1 is revolute and joint 2 is prismatic. In \mathcal{R}_0 , these matrices are:

$$J_{\omega 1} = J_{\omega 2} = \begin{bmatrix} 0 & 0 \\ 0 & 0 \\ 1 & 0 \end{bmatrix}.$$

and

$$(J_{\omega 1}^T I_{C_1} J_{\omega 1}) = \begin{bmatrix} I_{zz1} & 0 \\ 0 & 0 \end{bmatrix}; \quad (J_{\omega 2}^T I_{C_2} J_{\omega 2}) = \begin{bmatrix} I_{zz2} & 0 \\ 0 & 0 \end{bmatrix}.$$

Finally, the matrix A is

$$A = \begin{bmatrix} m_1 l_1^2 + I_{zz1} + m_2 q_2^2 + I_{zz2} & 0 \\ 0 & m_2 \end{bmatrix}.$$

Centrifugal and Coriolis Vector \mathbf{b}

The Christoffel Symbols are defined as

$$b_{i,jk} = \frac{1}{2}(a_{ijk} + a_{ikj} - a_{jki}); \quad \text{where} \quad a_{ijk} = \frac{\partial a_{ij}}{\partial q_k}; \quad \text{with} \quad b_{iii} = b_{iji} = 0.$$

For this manipulator, only a_{11} (see matrix A) is configuration dependent – function of q_2 . This implies that only a_{112} is non-zero,

$$a_{112} = 2m_2 q_2.$$

Matrix B

$$B = \begin{bmatrix} 2b_{112} \\ 0 \end{bmatrix} = \begin{bmatrix} 2m_2 q_2 \\ 0 \end{bmatrix}.$$

Matrix C

$$C = \begin{bmatrix} 0 & b_{122} \\ b_{211} & 0 \end{bmatrix} = \begin{bmatrix} 0 & 0 \\ -m_2 q_2 & 0 \end{bmatrix}.$$

Vector b

$$\mathbf{b} = \begin{bmatrix} 2m_2 q_2 \\ 0 \end{bmatrix} [\dot{q}_1 \dot{q}_2] + \begin{bmatrix} 0 & 0 \\ -m_2 q_2 & 0 \end{bmatrix} \begin{bmatrix} \dot{q}_1^2 \\ \dot{q}_2^2 \end{bmatrix}.$$

The Gravity Vector g

$$\mathbf{g} = -[J_{v1}^T m_1 \mathbf{g}_0 + J_{v2}^T m_2 \mathbf{g}_0].$$

In \mathcal{R}_0 , the gravity vector is

$$\mathbf{g} = \begin{bmatrix} -l_1 s_1 & l_1 c_1 & 0 \\ 0 & 0 & 0 \end{bmatrix} \begin{bmatrix} 0 \\ -m_1 g_0 \\ 0 \end{bmatrix} + \begin{bmatrix} -q_2 s_1 & q_2 c_1 & 0 \\ c_1 & s_1 & 0 \end{bmatrix} \begin{bmatrix} 0 \\ -m_2 g_0 \\ 0 \end{bmatrix};$$

and

$$\mathbf{g} = \begin{bmatrix} (m_1 l_1 + m_2 q_2) g_0 c_1 \\ m_2 g_0 s_1 \end{bmatrix}.$$

Equations of Motion

$$\begin{bmatrix} m_1 l_1^2 + I_{zz1} + m_2 q_2^2 + I_{zz2} & 0 \\ 0 & m_2 \end{bmatrix} \begin{bmatrix} \ddot{q}_1 \\ \ddot{q}_2 \end{bmatrix} + \begin{bmatrix} 2m_2 q_2 \\ 0 \end{bmatrix} [\dot{q}_1 \dot{q}_2] + \begin{bmatrix} 0 & 0 \\ -m_2 q_2 & 0 \end{bmatrix} \begin{bmatrix} \dot{q}_1^2 \\ \dot{q}_2^2 \end{bmatrix} + \begin{bmatrix} (m_1 l_1 + m_2 q_2) g_0 c_1 \\ m_2 g_0 s_1 \end{bmatrix} = \begin{bmatrix} \Gamma_1 \\ \Gamma_2 \end{bmatrix}.$$

3.3 Joint Space Dynamic Control

In dynamic control schemes, the manipulator dynamic model is used to compensate for the configuration dependency of the inertias, and for the inertial coupling, centrifugal, Coriolis, and gravity forces. This technique is based on the theory of nonlinear dynamic decoupling (Freund, 1975), or the so called “computed torque method.”

The dynamic decoupling and motion control of a manipulator in joint space is achieved by selecting the control structure

$$\Gamma = \hat{A}(\mathbf{q})\Gamma^* + \hat{\mathbf{b}}(\mathbf{q}, \dot{\mathbf{q}}) + \hat{\mathbf{g}}(\mathbf{q}); \quad (3.23)$$

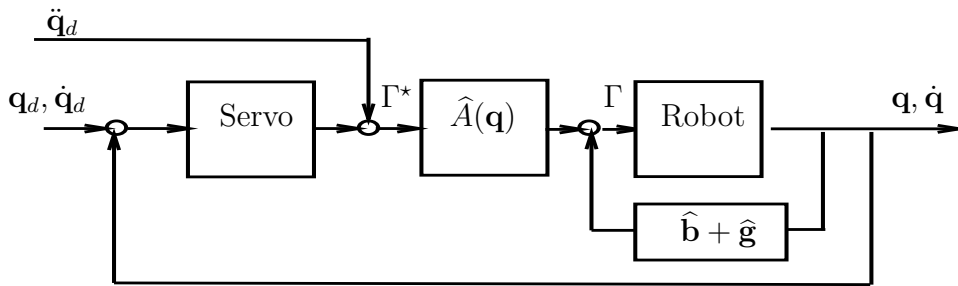


Figure 3.6: Joint Space Dynamic Control

where, $\hat{A}(\mathbf{q})$, $\hat{\mathbf{b}}(\mathbf{q}, \dot{\mathbf{q}})$, and $\hat{\mathbf{g}}(\mathbf{q})$ represent the estimates of $A(\mathbf{q})$, $\mathbf{b}(\mathbf{q}, \dot{\mathbf{q}})$, and $\mathbf{g}(\mathbf{q})$. Γ^* is the input of the decoupled system. At this level, various control structures can be selected, e.g. PID, adaptive control, or robust control.

Chapter 4

Operational Space Framework

Task specification for motion and contact forces, dynamics, and force sensing feedback, are most closely linked to the end-effector's motion. Joint space dynamic models are, obviously, unable to provide a description of the end-effector's dynamic behavior, which is crucial for the analysis and control of the end-effector's motion and applied forces.

4.1 Basic Concepts

The basic idea in the operational space approach (Khatib 1980, Khatib 1987) is to control motions and contact forces through the use of control forces that act directly at the level of the end-effector. These control forces are produced by the application of corresponding torques and forces at the manipulator joints.

For instance, subjecting the end-effector to the gradient of an attractive potential field will result in joint motions that position the effector at

the configuration corresponding to the minimum of this potential field. This type of control can be shown to be stable. However, the dynamic performance of such a control scheme will clearly be limited, given the inertial interactions between the moving links.

High performance control of end-effector motions and contact forces requires the construction of a model describing the dynamic behavior as perceived at the end-effector, or more precisely at the point on the effector where the task is specified. This point is called the *operational point*.

A coordinate system associated with the operational point is used to define a set of *operational coordinates*. A set of operational forces acting on the end-effector is associated with the system of operational coordinates selected to describe the position and orientation of the end-effector. The construction of the end-effector dynamic model is achieved by expressing the relationship between its positions, velocities, accelerations, and the operational forces acting on it.

The operational forces are produced by submitting the manipulator to the corresponding joint forces, using a simple force transformation. The use of the forces generated at the end-effector to control motions leads to a natural integration of active force control. In this framework, simultaneous control of motions and forces is achieved by a unified command vector for controlling both the motions and forces at the operational point.

The operational space robot control system is organized in a hierarchical structure, as shown in Figure 4.1, of three control levels:

- *Task Specification Level*: At this level, tasks are described in terms of motion and contact forces of the manipulated object or tool.
- *Effector Level*: This level is associated with the end-effector dynamic model, the basis for the control of the end-effector motion and contact forces. The output here is the vector of joint forces and torques to be produced by the joint level in order to generate the operational forces and moments associated with the end-effector control vector.

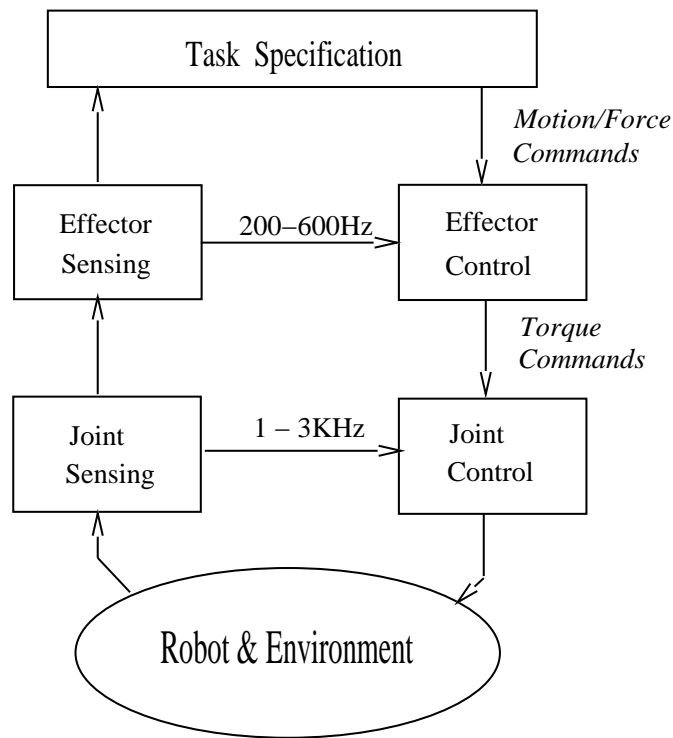


Figure 4.1: Operational Space Control Structure

- *Joint Level:* This level is formed by the set of individual joint torque controllers, allowing each joint to produce its assigned torque component for producing the vector of joint torques corresponding to the end-effector control vector.

4.2 Effector Equations of Motion

When the dynamic response or impact force at some point on the end-effector or manipulated object is of interest, the inertial properties involved are those evaluated at that point, termed the *operational point*. Attaching a coordinate frame to the end-effector at the operational point and using the relationships between this frame and the reference frame attached to the manipulator base provide a description, \mathbf{x} , of the configuration, i.e. position and orientation, of the effector.

First, let us consider the case of non-redundant manipulators, where a set of operational coordinates forms a system of generalized coordinates for the manipulator. The manipulator configuration is represented by the column matrix \mathbf{q} of n joint coordinates, and the end-effector position and orientation are described, in the frame of reference \mathcal{R}_0 , by the $m_0 \times 1$ column matrix \mathbf{x} of independent configuration parameters, i.e., operational coordinates. The number, m_0 , of independent parameters needed to describe the position and orientation of the end-effector determines the number of degrees of freedom the end-effector possesses. With the non-redundancy assumption we have the equality $n = m_0$.

Now let us examine the conditions under which a set of independent end-effector configuration parameters can be used as a generalized coordinate system for a non-redundant manipulator. In the reference frame \mathcal{R}_0 , the system of m_0 equations expressing the components of \mathbf{x} as functions of joint coordinates, i.e., *the geometric model*, is given by

$$\mathbf{x} = \mathbf{G}(\mathbf{q}). \quad (4.1)$$

Let \underline{q}_i and \bar{q}_i be respectively the minimal and maximal bounds of the i^{th} joint coordinate q_i . The manipulator configuration represented by the point \mathbf{q} in joint space is confined to the hyper-parallelepiped defined by the products of the intervals $[\underline{q}_i, \bar{q}_i]$,

$$\mathcal{D}_q = \prod_{i=1}^n [\underline{q}_i, \bar{q}_i]. \quad (4.2)$$

Let \mathcal{D}_x be the domain of the operational space corresponding to the vector-function \mathbf{G} over \mathcal{D}_q . Obviously, for an arbitrary kinematic linkage and arbitrary joint boundaries, \mathbf{G} is not one-to-one. Generally, a

configuration \mathbf{x} of the end-effector could be obtained from several different configurations \mathbf{q}_{c1} , \mathbf{q}_{c2} , etc., of the manipulator. The restriction to a domain where \mathbf{G} is one-to-one is therefore necessary in order to construct, with the operational coordinates, a system of generalized coordinates for the manipulator.

In addition, for some configurations, the end-effector motion is restricted by the linkage constraints and its freedom of motion locally decreases. These are the singular configurations, which can be found by considering the differential characteristics of the geometric model \mathbf{G} . Singular configurations, $\mathbf{q} \in \mathcal{D}_{\mathbf{q}}$, are those where the Jacobian matrix $J(\mathbf{q})$ involved in the variational or kinematic model associated with \mathbf{G} ,

$$\delta \mathbf{x} = J(\mathbf{q})\delta \mathbf{q};$$

is singular.

Let $\tilde{\mathcal{D}}_q$ be a domain obtained from \mathcal{D}_q by excluding the manipulator singular configurations and such that the vector function \mathbf{G} of (4.1) is one-to-one. Let $\tilde{\mathcal{D}}_x$ designate the domain

$$\tilde{\mathcal{D}}_x = \mathbf{G}(\tilde{\mathcal{D}}_q). \quad (4.3)$$

The independent parameters x_1, x_2, \dots, x_{m_0} form a complete set of configuration parameters for a non-redundant manipulator, in the domain $\tilde{\mathcal{D}}_x$ of the operational space and thus constitute a system of generalized coordinates for the manipulator.

The kinetic energy of the holonomic system is a quadratic form of the generalized operational velocities

$$T(\mathbf{x}, \dot{\mathbf{x}}) = \frac{1}{2} \dot{\mathbf{x}}^T \Lambda(\mathbf{x}) \dot{\mathbf{x}}; \quad (4.4)$$

where $\Lambda(\mathbf{x})$ designates the $m_0 \times m_0$ symmetric matrix of the quadratic form, i.e., the kinetic energy matrix. This matrix describes the effector's inertial properties.

Using the Lagrangian formalism, the end-effector equations of motion are

$$\frac{d}{dt} \left(\frac{\partial L}{\partial \dot{\mathbf{x}}} \right) - \frac{\partial L}{\partial \mathbf{x}} = \mathbf{F}; \quad (4.5)$$

where the Lagrangian $L(\mathbf{x}, \dot{\mathbf{x}})$ is

$$L(\mathbf{x}, \dot{\mathbf{x}}) = T(\mathbf{x}, \dot{\mathbf{x}}) - U(\mathbf{x});$$

and $U(\mathbf{x})$ represents the potential energy due to gravity. \mathbf{F} is the operational force vector. Let $\mathbf{p}(\mathbf{x})$ be the vector of gravity forces

$$\mathbf{p}(\mathbf{x}) = \nabla U(\mathbf{x}).$$

The end-effector equations of motion in operational space can be written (Khatib 1980, Khatib 1987) in the form

$$\Lambda(\mathbf{x})\ddot{\mathbf{x}} + \boldsymbol{\mu}(\mathbf{x}, \dot{\mathbf{x}}) + \mathbf{p}(\mathbf{x}) = \mathbf{F}; \quad (4.6)$$

where $\boldsymbol{\mu}(\mathbf{x}, \dot{\mathbf{x}})$ is the vector of centrifugal and Coriolis forces.

Joint Space/Operational Space Relationships

The relationship between the matrices $\Lambda(\mathbf{x})$ and $A(\mathbf{q})$ can be established by stating the identity between the two quadratic forms of kinetic energy:

$$\frac{1}{2}\dot{\mathbf{q}}^T A(\mathbf{q})\dot{\mathbf{q}} = \frac{1}{2}\dot{\mathbf{x}}^T \Lambda(\mathbf{x})\dot{\mathbf{x}}.$$

Using the kinematic model this identity yields

$$A(\mathbf{q}) = J^T(\mathbf{q})\Lambda(\mathbf{x})J(\mathbf{q}). \quad (4.7)$$

The relationship between the centrifugal and Coriolis forces $\mathbf{b}(\mathbf{q}, \dot{\mathbf{q}})$ and $\boldsymbol{\mu}(\mathbf{x}, \dot{\mathbf{x}})$ can be established by the expansion of the expression of $\boldsymbol{\mu}(\mathbf{x}, \dot{\mathbf{x}})$ that results from (4.5),

$$\boldsymbol{\mu}(\mathbf{x}, \dot{\mathbf{x}}) = \dot{\Lambda}(\mathbf{x})\dot{\mathbf{x}} - \nabla T(\mathbf{x}, \dot{\mathbf{x}}).$$

Using the expression of $\Lambda(\mathbf{x})$ in (4.7), $\boldsymbol{\mu}(\mathbf{x}, \dot{\mathbf{x}})$ can be written as

$$\begin{aligned} \dot{\Lambda}(\mathbf{x})\dot{\mathbf{x}} &= J^{-T}(\mathbf{q})\dot{A}(\mathbf{q})\dot{\mathbf{q}} - \Lambda(\mathbf{q})\mathbf{h}(\mathbf{q}, \dot{\mathbf{q}}) + \dot{J}^{-T}(\mathbf{q})A(\mathbf{q})\dot{\mathbf{q}}; \\ \nabla T(\mathbf{x}, \dot{\mathbf{x}}) &= J^{-T}(\mathbf{q})\mathbf{l}(\mathbf{q}, \dot{\mathbf{q}}) + \dot{J}^{-T}(\mathbf{q})A(\mathbf{q})\dot{\mathbf{q}}; \end{aligned}$$

where

$$\mathbf{h}(\mathbf{q}, \dot{\mathbf{q}}) = \dot{J}(\mathbf{q})\dot{\mathbf{q}}. \quad (4.8)$$

and

$$l_i(\mathbf{q}, \dot{\mathbf{q}}) = \frac{1}{2}\dot{\mathbf{q}}^T A_{q_i}(\mathbf{q})\dot{\mathbf{q}}; \quad (i = 1, \dots, n).$$

The subscript q_i indicates the partial derivative with respect to the i^{th} joint coordinate. Observing from the definition of $\mathbf{b}(\mathbf{q}, \dot{\mathbf{q}})$ that,

$$\mathbf{b}(\mathbf{q}, \dot{\mathbf{q}}) = \dot{A}(\mathbf{q})\dot{\mathbf{q}} - \mathbf{l}(\mathbf{q}, \dot{\mathbf{q}});$$

yields,

$$\boldsymbol{\mu}(\mathbf{x}, \dot{\mathbf{x}}) = J^{-T}(\mathbf{q})\mathbf{b}(\mathbf{q}, \dot{\mathbf{q}}) - \Lambda(\mathbf{q})\mathbf{h}(\mathbf{q}, \dot{\mathbf{q}}). \quad (4.9)$$

The relationship between the expressions of gravity forces can be obtained using the identity between the functions expressing the gravity potential energy in the two systems of generalized coordinates and the relationships between the partial derivatives with respect to these coordinates. Using the definition of the Jacobian matrix yields,

$$\mathbf{p}(\mathbf{x}) = J^{-T}(\mathbf{q})\mathbf{g}(\mathbf{q}). \quad (4.10)$$

In the foregoing relations, the components involved in the end-effector equations of motion, i.e., Λ , $\boldsymbol{\mu}$, \mathbf{p} , are expressed in terms of joint coordinates. This solves the ambiguity in defining the configuration of the manipulator corresponding to a configuration of the end-effector in the domain \mathcal{D}_x . With these expressions, the restriction to the domain $\tilde{\mathcal{D}}_x$, where \mathbf{G} is one-to-one, then becomes unnecessary. Indeed, the domain of definition of the end-effector dynamic model of a non-redundant manipulator can be extended to the domain $\overline{\mathcal{D}}_x$ defined by

$$\overline{\mathcal{D}}_x = \mathbf{G}(\overline{\mathcal{D}}_q);$$

where $\overline{\mathcal{D}}_q$ is the domain resulting from \mathcal{D}_q by excluding the kinematic singular configurations.

Finally, the above relationships allow to rewrite the end-effector inertial and gravity forces which appear in the left-hand side of equation (4.6) as

$$J^{-T}(\mathbf{q})[A(\mathbf{q})\ddot{\mathbf{q}} + \mathbf{b}(\mathbf{q}, \dot{\mathbf{q}}) + \mathbf{g}(\mathbf{q})] = \Lambda(\mathbf{x})\ddot{\mathbf{x}} + \boldsymbol{\mu}(\mathbf{x}, \dot{\mathbf{x}}) + \mathbf{p}(\mathbf{x}).$$

Substituting the right-hand sides of equations (3.13) and (4.6) yields

$$\mathbf{\Gamma} = J^T(\mathbf{q})\mathbf{F}. \quad (4.11)$$

This shows the extension to the dynamic case of the force/torque relationship whose derivation from the virtual work principle assumes static equilibrium. This relationship is the basis for the actual control of manipulators in operational space.

The joint space centrifugal and Coriolis force vector $\mathbf{b}(\mathbf{q}, \dot{\mathbf{q}})$ can be written in the form

$$\mathbf{b}(\mathbf{q}, \dot{\mathbf{q}}) = B(\mathbf{q})[\dot{\mathbf{q}}\dot{\mathbf{q}}]; \quad (4.12)$$

where $B(\mathbf{q})$ is the $n \times n(n+1)/2$ matrix given by

$$B(\mathbf{q}) = \begin{pmatrix} b_{1,11} & 2b_{1,12} & \dots & 2b_{1,1n} & b_{1,22} & 2b_{1,23} & \dots & 2b_{1,2n} & \dots & b_{1,nn} \\ b_{2,11} & 2b_{2,12} & \dots & 2b_{2,1n} & b_{2,22} & 2b_{2,23} & \dots & 2b_{2,2n} & \dots & b_{2,nn} \\ \cdot & \cdot & \cdot & \cdot & \cdot & \cdot & \cdot & \cdot & \cdot & \cdot \\ \cdot & \cdot & \cdot & \cdot & \cdot & \cdot & \cdot & \cdot & \cdot & \cdot \\ \cdot & \cdot & \cdot & \cdot & \cdot & \cdot & \cdot & \cdot & \cdot & \cdot \\ b_{n,11} & 2b_{n,12} & \dots & 2b_{n,1n} & b_{n,22} & 2b_{n,23} & \dots & 2b_{n,2n} & \dots & b_{n,nn} \end{pmatrix}; \quad (4.13)$$

and

$$[\dot{\mathbf{q}}\dot{\mathbf{q}}] = [\dot{q}_1^2 \quad \dot{q}_1\dot{q}_2 \quad \dot{q}_1\dot{q}_3 \dots \dot{q}_1\dot{q}_n \quad \dot{q}_2^2 \quad \dot{q}_2\dot{q}_3 \dots \dot{q}_2\dot{q}_n \dots \dot{q}_n^2]^T. \quad (4.14)$$

$b_{i,jk}$ are the Christoffel symbols given as a function of the partial derivatives of the joint space kinetic energy matrix $A(\mathbf{q})$ *w.r.t.* the generalized coordinates \mathbf{q} by

$$b_{i,jk} = \frac{1}{2} \left(\frac{\partial a_{ij}}{\partial q_k} + \frac{\partial a_{ik}}{\partial q_j} - \frac{\partial a_{jk}}{\partial q_i} \right). \quad (4.15)$$

Similarly the vector $\mathbf{h}(\mathbf{q}, \dot{\mathbf{q}})$ can be written as

$$\mathbf{h}(\mathbf{q}, \dot{\mathbf{q}}) = H(\mathbf{q})[\dot{\mathbf{q}}\dot{\mathbf{q}}]. \quad (4.16)$$

The expression of the operational space centrifugal and Coriolis forces becomes

$$\boldsymbol{\mu}(\mathbf{x}, \dot{\mathbf{x}}) = [J^{-T}(\mathbf{q})B(\mathbf{q}) - \Lambda(\mathbf{q})H(\mathbf{q})][\dot{\mathbf{q}}\dot{\mathbf{q}}]. \quad (4.17)$$

In summary the relationships between the components of the joint space dynamic model and those of the operational space dynamic model are

$$\begin{aligned}\Lambda(\mathbf{x}) &= J^{-T}(\mathbf{q})A(\mathbf{q})J^{-1}(\mathbf{q}); \\ \boldsymbol{\mu}(\mathbf{x}, \dot{\mathbf{x}}) &= [J^{-T}(\mathbf{q})B(\mathbf{q}) - \Lambda(\mathbf{q})H(\mathbf{q})][\dot{\mathbf{q}}\dot{\mathbf{q}}]; \\ \mathbf{p}(\mathbf{x}) &= J^{-T}(\mathbf{q})\mathbf{g}(\mathbf{q}).\end{aligned}$$

4.3 End-Effector Motion Control

The generalized joint forces $\mathbf{\Gamma}$ required to produce the operational forces \mathbf{F} are

$$\mathbf{\Gamma} = J^T(\mathbf{q})\mathbf{F}; \quad (4.18)$$

This relationship is the basis for the actual control of manipulators in operational space.

4.3.1 Passive Systems

The most simple design of end-effector motion control is to submit the end-effector to the gradient of an attractive potential field. An attractive potential field to a goal position \mathbf{x}_{goal} is a positive continuous differentiable function, which attains its minimum when $\mathbf{x} = \mathbf{x}_{\text{goal}}$. This is for instance

$$U_{\text{goal}} = \frac{1}{2}k_p(\mathbf{x} - \mathbf{x}_{\text{goal}})^T(\mathbf{x} - \mathbf{x}_{\text{goal}});$$

where k_p is a constant.

In order to compensate for the gravity effects, the control vector must in addition include an estimate of the gravity forces, $\hat{\mathbf{p}} = \nabla_x \hat{U}$. The end-effector equations of motion become

$$\frac{d}{dt}\left(\frac{\partial T}{\partial \dot{\mathbf{x}}}\right) - \frac{\partial(T - U)}{\partial \mathbf{x}} = -\frac{\partial(U_{\text{goal}} - \hat{U})}{\partial \mathbf{x}}.$$

With a perfect gravity compensation ($\hat{U} = U$), the equations can be written as

$$\frac{d}{dt}\left(\frac{\partial T}{\partial \dot{\mathbf{x}}}\right) - \frac{\partial(T - U_{\text{goal}})}{\partial \mathbf{x}} = 0. \quad (4.19)$$

The resulting system is a conservative system with a stable oscillatory motion around the goal position \mathbf{x}_{goal} . Asymptotic stabilization of this system can be achieved by the addition of dissipative forces \mathbf{F}_s . Since

all non-dissipative forces in this control design are conservative, the asymptotic stability condition can be simply stated as

$$\mathbf{F}_s^T \dot{\mathbf{x}} < 0; \quad \text{for } \dot{\mathbf{x}} \neq \mathbf{0}. \quad (4.20)$$

For instance, \mathbf{F}_s could be selected as

$$\mathbf{F}_s = -k_v \dot{\mathbf{x}};$$

and the asymptotic stability condition implies that k_v must be positive. This type of control ignores the dynamic interaction between the moving links in the mechanical system, and its dynamic performance is very limited.

4.3.2 Dynamic Decoupling

The dynamic decoupling and motion control of the manipulator in operational space is achieved by selecting the control structure

$$\mathbf{F} = \hat{\Lambda}(\mathbf{x})\mathbf{F}^* + \hat{\boldsymbol{\mu}}(\mathbf{x}, \dot{\mathbf{x}}) + \hat{\mathbf{p}}(\mathbf{x}); \quad (4.21)$$

where, $\hat{\Lambda}(\mathbf{x})$, $\hat{\boldsymbol{\mu}}(\mathbf{x}, \dot{\mathbf{x}})$, and $\hat{\mathbf{p}}(\mathbf{x})$ represent the estimates of $\Lambda(\mathbf{x})$, $\boldsymbol{\mu}(\mathbf{x}, \dot{\mathbf{x}})$, and $\mathbf{p}(\mathbf{x})$. The system (4.6) under the command (4.21) can be represented by

$$I_{m_0} \ddot{\mathbf{x}} = G(\mathbf{x})\mathbf{F}^* + \boldsymbol{\eta}(\mathbf{x}, \dot{\mathbf{x}}) + \mathbf{d}(t); \quad (4.22)$$

where I_{m_0} is the $m_0 \times m_0$ identity matrix, and

$$G(\mathbf{x}) = \Lambda^{-1}(\mathbf{x})\hat{\Lambda}(\mathbf{x}); \quad (4.23)$$

$$\boldsymbol{\eta}(\mathbf{x}, \dot{\mathbf{x}}) = \Lambda^{-1}(\mathbf{x})[\tilde{\boldsymbol{\mu}}(\mathbf{x}, \dot{\mathbf{x}}) + \tilde{\mathbf{p}}(\mathbf{x})]. \quad (4.24)$$

with

$$\tilde{\boldsymbol{\mu}}(\mathbf{x}, \dot{\mathbf{x}}) = \hat{\boldsymbol{\mu}}(\mathbf{x}, \dot{\mathbf{x}}) - \boldsymbol{\mu}(\mathbf{x}, \dot{\mathbf{x}}); \quad (4.25)$$

$$\tilde{\mathbf{p}}(\mathbf{x}) = \hat{\mathbf{p}}(\mathbf{x}) - \mathbf{p}(\mathbf{x}). \quad (4.26)$$

$\mathbf{d}(t)$ includes unmodeled disturbances. With a perfect nonlinear dynamic decoupling, the end-effector becomes equivalent to a *single unit mass*, I_{m_0} , moving in the m_0 -dimensional space,

$$I_{m_0} \ddot{\mathbf{x}} = \mathbf{F}^*. \quad (4.27)$$

\mathbf{F}^* is the input of the decoupled end-effector. This provides a general framework for the selection of various control structures

The stability and robustness of this type of control structures require good estimates of the manipulator dynamic parameters. The parameters related to the Coriolis and centrifugal forces are particularly critical for the stability of the system. In fact it is better to set $\hat{\boldsymbol{\mu}}(\mathbf{x}, \dot{\mathbf{x}})$ in equation (4.21) to zero rather than to use a poor estimate, which could result in a globally unstable damping in the system.

4.3.3 Goal Position

For tasks that involve large motion to a goal position, where a particular trajectory is not required, a PD controller of the form

$$\mathbf{F}^* = -k_v \dot{\mathbf{x}} - k_p(\mathbf{x} - \mathbf{x}_g); \quad (4.28)$$

where \mathbf{x}_g is the goal position will result in a poor coordination of the end-effector motions along its degrees of freedom. This is primarily due to actuator saturations, bandwidth and velocity limitation. A coordination allowing a straight line motion of the end-effector with an upper speed limit has been found to be a desirable behavior for this type of tasks. By rewriting equation (4.28) as

$$\mathbf{F}^* = -k_v(\dot{\mathbf{x}} - \dot{\mathbf{x}}_d); \quad (4.29)$$

where

$$\dot{\mathbf{x}}_d = \frac{k_p}{k_v}(\mathbf{x}_g - \mathbf{x}); \quad (4.30)$$

\mathbf{F}^* can be interpreted as a pure velocity servo-control with a velocity gain k_v , and a desired velocity vector $\dot{\mathbf{x}}_d$. The desired velocity is a

linear function of the position error. For large motions the initial velocity command will be very large, approaching zero as the desired goal position is reached. The limitation on the end-effector velocity can be obtained by limiting the magnitude of $\dot{\mathbf{x}}_d$ at V_{max} while its direction still points toward the desired goal position. The resulting control is

$$\mathbf{F}^* = -k_v(\dot{\mathbf{x}} - \nu\dot{\mathbf{x}}_d); \quad (4.31)$$

where

$$\nu = \text{sat}\left(\frac{V_{max}}{|\dot{\mathbf{x}}_d|}\right); \quad (4.32)$$

and $\text{sat}(x)$ is the saturation function:

$$\text{sat}(x) = \begin{cases} x & \text{if } |x| \leq 1.0 \\ \text{sgn}(x) & \text{if } |x| > 1.0. \end{cases} \quad (4.33)$$

and $\text{sgn}(x)$ is the sign function.

This allows a straight line motion of the end-effector at a given speed V_{max} . The velocity vector $\dot{\mathbf{x}}$ is now controlled to be pointed towards the goal position while its magnitude is limited to V_{max} . The end-effector will then travel in a straight line with velocity V_{max} except during the acceleration and deceleration segments. This type of command vector is particularly useful when used in conjunction with the gradient of an artificial potential field for collision avoidance.

4.3.4 Trajectory Tracking

For tasks where the desired motion of the end-effector is specified, a linear dynamic behavior can be obtained by selecting

$$\mathbf{F}^* = I_{m_0} \ddot{\mathbf{x}}_d - k_v(\dot{\mathbf{x}} - \dot{\mathbf{x}}_d) - k_p(\mathbf{x} - \mathbf{x}_d); \quad (4.34)$$

where \mathbf{x}_d , $\dot{\mathbf{x}}_d$ and $\ddot{\mathbf{x}}_d$ are the desired position, velocity and acceleration, respectively, of the end-effector. k_p and k_v are the position and velocity gains. The above dynamic decoupling and motion control result in the following end-effector closed loop behavior

$$I_{m_0} \ddot{\mathbf{e}}_x + k_v \dot{\mathbf{e}}_x + k_p \mathbf{e}_x = 0;$$

where

$$\boldsymbol{\epsilon}_x = \mathbf{x} - \mathbf{x}_d.$$

4.4 Active Force Control

High performance control of end-effector motion and contact forces requires the description of how motions along different axes are interacting, and how the apparent or equivalent inertia or mass of the end-effector varies with configurations and directions.

The operational space formulation provides a natural framework to address the problem of motion and force control in an integrated manner, allowing the development of a unified approach for the control of end-effector motions and contact forces.

In constrained motion operations, the end-effector is subjected to a set of geometric constraints which restrict its freedom of motion. However, active forces and moments at these constraints can still be controlled. The number of degrees of freedom for the motion of the constrained end-effector is given by the difference between the number of degrees of freedom of the unconstrained end-effector and the number of the independent equations, that specify the geometric constraints. The description of a fine motion task involves specifications of the forces and moments that must be applied at the geometric constraints, and specifications of the end-effector motion freedom directions.

4.4.1 Generalized Selection Matrices

In the operational space framework, the control of the end-effector motions and contact forces is based on a model which describes the dynamic behavior as perceived at some reference point on (or attached to) the end-effector. It is with respect to this point \mathcal{O} , called the *operational point*, that the end-effector translational and rotational motions, active forces and moments are specified. Forces and moments applied at the operational point are defined by a global reference frame $\mathcal{R}_{\mathcal{O}}(\mathcal{O}, \mathbf{x}_0, \mathbf{y}_0, \mathbf{z}_0)$. This frame always remains parallel to the fixed reference frame, $\mathcal{R}_O(O, \mathbf{x}_0, \mathbf{y}_0, \mathbf{z}_0)$, irrespectively of the orientation of the end-effector. This is illustrated in Figure 4.2, which also shows the end-effector frame $\mathcal{R}(\mathcal{O}, \mathbf{x}, \mathbf{y}, \mathbf{z})$, which translates and rotates with the end-effector.

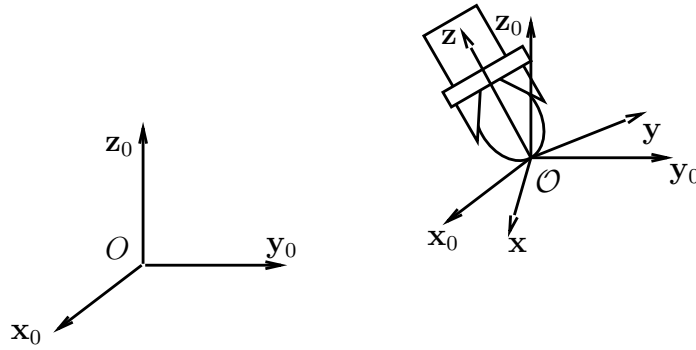


Figure 4.2: Reference Frames

Let us consider the case of the simple one-point contact task, illustrated in Figure 4.3. Let \mathcal{F}_d be the vector of desired forces to be applied by the end-effector at the contact point. The freedom of motion of the constrained end-effector lies in the subspace orthogonal to \mathcal{F}_d . A convenient coordinate frame for the description of such a task is the coordinate frame $\mathcal{R}_{\mathcal{F}}(\mathcal{O}, \mathbf{x}_{\mathcal{F}}, \mathbf{y}_{\mathcal{F}}, \mathbf{z}_{\mathcal{F}})$ obtained from \mathcal{R}_0 by a rotation transformation, $S_{\mathcal{F}}$. For this type of contact, it is convenient to select the axis $\mathbf{z}_{\mathcal{F}}$ along the direction of the desired force \mathcal{F}_d . Clearly, this assignment of axes might not be the most appropriate for other types of contact. For multiple contact tasks, the z axis can be more efficiently selected along one of the axes of freedom of translational motion.

In the coordinate frame $\mathcal{R}_{\mathcal{F}}$, the motion specification matrix can be defined as

$$\Sigma_{\mathcal{F}} = \begin{pmatrix} \sigma_{\mathcal{F}_x} & 0 & 0 \\ 0 & \sigma_{\mathcal{F}_y} & 0 \\ 0 & 0 & \sigma_{\mathcal{F}_z} \end{pmatrix}; \quad (4.35)$$

where $\sigma_{\mathcal{F}_x}$, $\sigma_{\mathcal{F}_y}$, and $\sigma_{\mathcal{F}_z}$ are binary numbers assigned the value 1 when a free motion is specified along the axes $\mathcal{O}\mathbf{x}_{\mathcal{F}}$, $\mathcal{O}\mathbf{y}_{\mathcal{F}}$, and $\mathcal{O}\mathbf{z}_{\mathcal{F}}$ respectively, and zero otherwise. In the case of the task of Figure 4.3, these are (1,1,0).

The directions of force control are described by the force specification

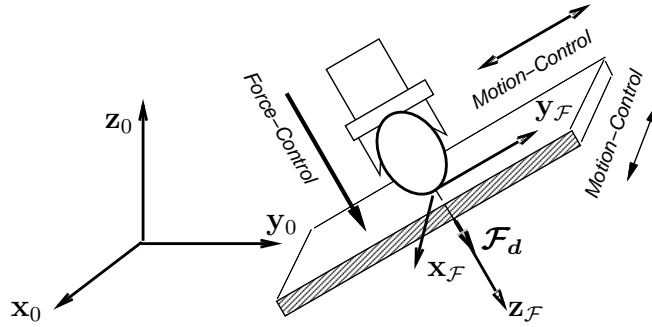


Figure 4.3: A Constrained Motion Task

matrix $\bar{\Sigma}_{\mathcal{F}}$ associated with $\Sigma_{\mathcal{F}}$ and defined by

$$\bar{\Sigma}_{\mathcal{F}} = I_3 - \Sigma_{\mathcal{F}}; \quad (4.36)$$

where I_3 designates the 3×3 identity matrix.

A similar specification matrix can be defined for tasks involving constrained rotations and applied moments. Let \mathbf{M}_d be the vector, in the frame of reference $\mathcal{R}_0(\mathcal{O}, \mathbf{x}_0, \mathbf{y}_0, \mathbf{z}_0)$, of moments that are to be applied by the end-effector, and $\mathcal{R}_{\mathcal{M}}(\mathcal{O}, \mathbf{x}_{\mathcal{M}}, \mathbf{y}_{\mathcal{M}}, \mathbf{z}_{\mathcal{M}})$ is a coordinate frame obtained from $\mathcal{R}_0(\mathcal{O}, \mathbf{x}_0, \mathbf{y}_0, \mathbf{z}_0)$ by a rotation $S_{\mathcal{M}}$. The axis $\mathbf{z}_{\mathcal{M}}$ can be selected along the direction of the moment vector \mathbf{M}_d or one of the axes of freedom of rotation.

To a task specified in terms of end-effector rotations and applied moments in the coordinate frame $\mathcal{R}_{\mathcal{M}}$, are associated the rotation/moment specification matrices $\Sigma_{\mathcal{M}}$ and $\bar{\Sigma}_{\mathcal{M}}$, defined as

$$\Sigma_{\mathcal{M}} = \begin{pmatrix} \sigma_{\mathcal{M}_x} & 0 & 0 \\ 0 & \sigma_{\mathcal{M}_y} & 0 \\ 0 & 0 & \sigma_{\mathcal{M}_z} \end{pmatrix}; \quad (4.37)$$

where $\sigma_{x_{\mathcal{M}}}$, $\sigma_{y_{\mathcal{M}}}$, and $\sigma_{z_{\mathcal{M}}}$ are binary numbers assigned the value 1 when a free rotation is specified about the axes $\mathcal{O}\mathbf{x}_{\mathcal{M}}$, $\mathcal{O}\mathbf{y}_{\mathcal{M}}$, and $\mathcal{O}\mathbf{z}_{\mathcal{M}}$

respectively, and zero otherwise. The directions of moment control are described by the torque specification matrix $\bar{\Sigma}_{\mathcal{M}}$ associated with $\Sigma_{\mathcal{M}}$ and defined by

$$\bar{\Sigma}_{\mathcal{M}} = I_3 - \Sigma_{\mathcal{M}}; \quad (4.38)$$

Tasks involving both position/force and orientation/moment specifications (see Figure 4.4), are described by the *generalized task specification matrices*

$$\Omega = \begin{pmatrix} S_{\mathcal{F}}^T \Sigma_{\mathcal{F}} S_{\mathcal{F}} & 0 \\ 0 & S_{\mathcal{M}}^T \Sigma_{\mathcal{M}} S_{\mathcal{M}} \end{pmatrix}; \quad (4.39)$$

and

$$\bar{\Omega} = \begin{pmatrix} S_{\mathcal{F}}^T \bar{\Sigma}_{\mathcal{F}} S_{\mathcal{F}} & 0 \\ 0 & S_{\mathcal{M}}^T \bar{\Sigma}_{\mathcal{M}} S_{\mathcal{M}} \end{pmatrix}; \quad (4.40)$$

associated with specifications of motion and forces, respectively.

Ω and $\bar{\Omega}$ act on vectors described in the reference frame \mathcal{R}_0 . A command vector, for instance, initially expressed in \mathcal{R}_0 is transformed by the rotation matrix $S_{\mathcal{F}}$ to the task coordinate frame $\mathcal{R}_{\mathcal{F}}$. The motion directions are then selected in this frame by the application of $\Sigma_{\mathcal{F}}$. Finally the resulting vector is transformed back in \mathcal{R}_0 by $S_{\mathcal{F}}^T$.

For tasks specified with respect to the end-effector coordinate frame, the generalized specification matrix can be similarly defined with respect to that coordinate frame.

The rotation matrices $S_{\mathcal{F}}^T$ and $S_{\mathcal{M}}^T$ are different in general, as illustrated in the example of Figure 4.4. However, these two matrices will be often identical in practical cases.

The generalized specification matrix provides a description of the task in the same coordinate frame (reference frame \mathcal{R}_0) where the manipulator geometric, kinematic and dynamic models are specified. This results in a more efficient implementation of the control system for real-time operations. Control systems using specifications based only on the matrices $\Sigma_{\mathcal{F}}$ and $\Sigma_{\mathcal{M}}$ will require costly geometric, kinematic, and dynamic transformations between the reference frame and the task coordinate frames.

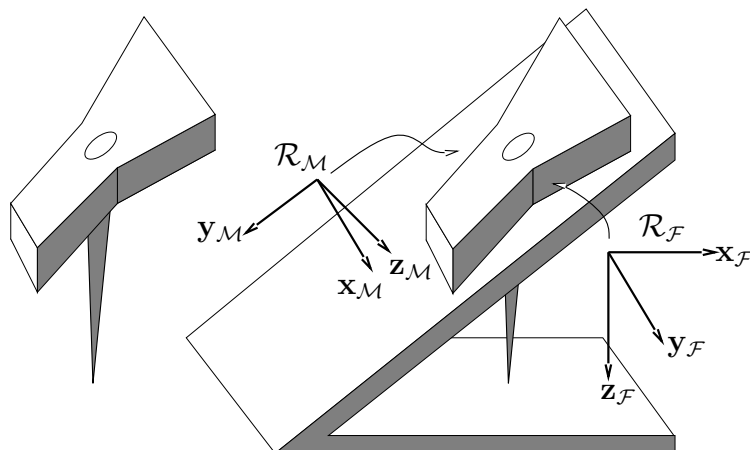


Figure 4.4: Example of Force/Moment Compliant Frames

4.4.2 Basic Dynamic Model

By the nature of coordinates associated with spatial rotations, operational forces acting along rotation coordinates are not homogeneous to moments and vary with the type of representation being used (e.g. Euler angles, direction cosines, Euler parameters). While this characteristic does not raise any difficulty in free motion operations, the homogeneity issue is important in tasks where both motions and active forces are involved. This issue is also a concern in the analysis of inertial properties. These properties are, in fact, expected to be independent of the type of representation used for the description of the end-effector orientation.

The homogeneity issue is addressed by using the relationships between operational velocities and instantaneous angular velocities. The Jacobian matrix $J(\mathbf{q})$ associated with a given selection, \mathbf{x} , of operational coordinates can be expressed as

$$J(\mathbf{q}) = E(\mathbf{x})J_O(\mathbf{q}); \quad (4.41)$$

where $J_O(\mathbf{q})$ is *the basic Jacobian* defined independently of the particular set of parameters used to describe the end-effector configuration,

while $E(\mathbf{x})$ is dependent upon those parameters. $E(\mathbf{x})$ is of the form

$$E(\mathbf{x}) = \begin{pmatrix} E_p(\mathbf{x}_p) & 0 \\ 0 & E_r(\mathbf{x}_r) \end{pmatrix}; \quad (4.42)$$

where $E_p(\mathbf{x}_p)$ depends on the selected position representation, \mathbf{x}_p , while $E_r(\mathbf{x}_r)$ depends on the selected orientation representation, \mathbf{x}_r . For Cartesian coordinates, $E_p(\mathbf{x})$ is the identity matrix of order 3.

The basic Jacobian establishes the relationships between generalized joint velocities $\dot{\mathbf{q}}$ and end-effector linear and angular velocities \mathbf{v} and $\boldsymbol{\omega}$.

$$\boldsymbol{\vartheta} \triangleq \begin{bmatrix} \mathbf{v} \\ \boldsymbol{\omega} \end{bmatrix} = J_O(\mathbf{q})\dot{\mathbf{q}}. \quad (4.43)$$

Using the basic Jacobian matrix, the mass and inertial properties at the end-effector are described by

$$\Lambda_O(\mathbf{x}) = J_O^{-T}(\mathbf{q})A(\mathbf{q})J_O^{-1}(\mathbf{q}). \quad (4.44)$$

The above matrix is related to the kinetic energy matrix associated with a set of operational coordinates, \mathbf{x} , by

$$\Lambda(\mathbf{x}) = E^{-T}(\mathbf{x})\Lambda_O(\mathbf{x})E^{-1}(\mathbf{x}). \quad (4.45)$$

Like angular velocities, moments are defined as instantaneous quantities. A generalized operational force vector \mathbf{F} associated with a set of operational coordinates, \mathbf{x} , is related to forces and moments by

$$\mathbf{F}_0 \triangleq \begin{bmatrix} \mathcal{F} \\ \mathcal{M} \end{bmatrix} = E^T(\mathbf{x}) \mathbf{F}; \quad (4.46)$$

where \mathcal{F} and \mathcal{M} are the vectors of forces and moments. With respect to linear and angular velocities, the end-effector equations of motion can be written as

$$\Lambda_0(\mathbf{x})\dot{\boldsymbol{\vartheta}} + \boldsymbol{\mu}_0(\mathbf{x}, \boldsymbol{\vartheta}) + \mathbf{p}_0(\mathbf{x}) = \mathbf{F}_0; \quad (4.47)$$

where $\Lambda_0(\mathbf{x})$, $\boldsymbol{\mu}_0(\mathbf{x}, \boldsymbol{\vartheta})$, and $\mathbf{p}_0(\mathbf{x})$ are defined similarly to $\Lambda(\mathbf{x})$, $\boldsymbol{\mu}(\mathbf{x}, \dot{\mathbf{x}})$, and $\mathbf{p}(\mathbf{x})$ using $J_0(\mathbf{q})$ instead of $J(\mathbf{q})$. In equation (4.47), the dynamics of the end-effector is described with respect to linear and angular velocities. Therefore, a task transformation of the description of end-effector orientation is needed. Such a transformation involves the inverse of $E(\mathbf{x})$ and its derivatives.

4.4.3 A Mass-Spring System

Let us consider for instance, the problem of controlling the contact forces of a one-degree-of-freedom manipulator acting along the direction \mathbf{z} using a force sensor. The dynamic behavior of this end-effector/sensor system can be modeled as a simple mass, m , and spring, k_s , system, as shown in Figure 4.5.

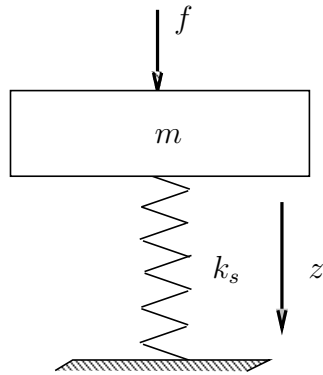


Figure 4.5: A Mass/Spring System

The dynamic model of the end-effector/sensor system is

$$m \ddot{z} + k_s z = f;$$

where f represents the control force along the \mathbf{z} direction. The measurement of contact forces at the sensor is

$$f_s = k_s z.$$

This allows to rewrite the dynamic model of the mass/sensor system as

$$m \frac{1}{k_s} \ddot{f}_s + f_s = f.$$

Based on this model, force control can be achieved by selecting

$$f = f_s - m [k_f (f_s - f_d) + k_{v_f} \dot{f}_s]; \quad (4.48)$$

and the closed loop behavior is given as

$$\ddot{f}_s + k_s k_{v_f} \dot{f}_s + k_s k_f (f_s - f_d) = 0.$$

4.4.4 Unified Motion and Force Control

For a multi-linked manipulator, the end-effector/sensor equations of motion can be written as

$$\Lambda_0(\mathbf{x})\dot{\boldsymbol{\vartheta}} + \boldsymbol{\mu}_0(\mathbf{x}, \boldsymbol{\vartheta}) + \mathbf{p}_0(\mathbf{x}) + \mathbf{F}_{\text{contact}} = \mathbf{F}_0; \quad (4.49)$$

The vector $\mathbf{F}_{\text{contact}}$ represents the contact forces acting at the end effector. The unified approach for end-effector dynamic decoupling, motion and active force control is achieved by selecting the control structure

$$\mathbf{F}_0 = \mathbf{F}_{\text{motion}} + \mathbf{F}_{\text{active-force}}; \quad (4.50)$$

where

$$\mathbf{F}_{\text{motion}} = \widehat{\Lambda}_0(\mathbf{x})\Omega\mathbf{F}_{\text{motion}}^* + \widehat{\boldsymbol{\mu}}_0(\mathbf{x}, \boldsymbol{\vartheta}) + \widehat{\mathbf{p}}_0(\mathbf{x}); \quad (4.51)$$

$$\mathbf{F}_{\text{active-force}} = \widehat{\Lambda}_0(\mathbf{x})\overline{\Omega}\mathbf{F}_{\text{active-force}}^* + \mathbf{F}_{\text{sensor}}; \quad (4.52)$$

and $\widehat{\Lambda}_0(\mathbf{x})$, $\widehat{\boldsymbol{\mu}}_0(\mathbf{x}, \dot{\mathbf{x}})$, and $\widehat{\mathbf{p}}_0(\mathbf{x})$ represent the estimates of $\Lambda_0(\mathbf{x})$, $\boldsymbol{\mu}_0(\mathbf{x}, \dot{\mathbf{x}})$, and $\mathbf{p}_0(\mathbf{x})$. The vectors $\mathbf{F}_{\text{motion}}^*$ and $\mathbf{F}_{\text{active-force}}^*$ represent the inputs to the decoupled system. The generalized joint forces $\boldsymbol{\Gamma}$ required to produce the operational forces \mathbf{F}_0 are

$$\boldsymbol{\Gamma} = J_0^T(\mathbf{q})\mathbf{F}_0. \quad (4.53)$$

With perfect estimates of the dynamic parameters and perfect sensing of contact forces, i.e. $\mathbf{F}_{\text{sensor}} = \mathbf{F}_{\text{contact}}$, the closed loop system is described by the following two decoupled sub-systems:

$$\Omega\dot{\boldsymbol{\vartheta}} = \Omega\mathbf{F}_{\text{motion}}^*; \quad (4.54)$$

$$\overline{\Omega}\dot{\boldsymbol{\vartheta}} = \overline{\Omega}\mathbf{F}_{\text{active-force}}^*. \quad (4.55)$$

The unified motion and force control system is shown in Figure 4.6.

4.4.5 Implementation

To further enhance the efficiency of the real-time implementation, the control system is decomposed into two layers – a low rate dynamic parameter evaluation layer, that updates the dynamic parameters, and a

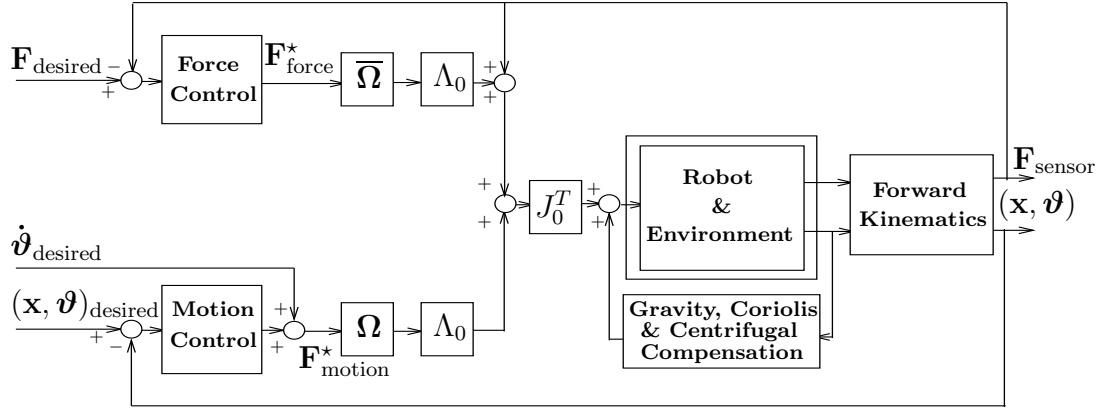


Figure 4.6: Unified Motion and Force Control Structure

high rate servo control layer that computes the command vector using the updated dynamic coefficients. This is achieved by factoring the equations of motion into the product of a matrix with coefficients independent of the velocities, and a vector which contains the velocity terms. The matrix of coefficients is then given as a function of the manipulator's configuration. With this separation of the velocity and configuration dependency of the dynamics, the real-time computation of the equations of motion coefficients can be paced by the rate of configuration changes, which is much lower than that of the mechanism dynamics.

Goal-Position Control

Given a desired position and orientation vector, $\mathbf{x}_d = (\mathbf{x}_{pd}^T \ \mathbf{x}_{rd}^T)^T$, the input of the decoupled end-effector can be selected as

$$\mathcal{F}^* = -k_p(\mathbf{x}_p - \mathbf{x}_{pd}) - k_v\dot{\mathbf{x}}_p;$$

and

$$\mathcal{M}^* = -k_p \delta\Phi - k_v \omega;$$

where $\delta\Phi$ is the *instantaneous angular error* corresponding to the error, $\delta\mathbf{x}_r$ between the actual orientation of the end-effector \mathbf{x}_r and its desired orientation \mathbf{x}_{rd} .

$$\delta\mathbf{x}_r = \mathbf{x}_r - \mathbf{x}_{rd}. \quad (4.56)$$

We have seen that the time derivative of \mathbf{x}_r is related to the corresponding angular velocity vector $\boldsymbol{\omega}$ by

$$\dot{\mathbf{x}}_r = E_r(\mathbf{x}_r) \boldsymbol{\omega}. \quad (4.57)$$

Replacing velocities by elementary rotations yields

$$\delta\mathbf{x}_r = E_r(\mathbf{x}_r) \delta\Phi. \quad (4.58)$$

Using the left inverse of E_r , the *instantaneous angular error* can be written as

$$\delta\Phi = E_r^+(\mathbf{x}_r) \delta\mathbf{x}_r;. \quad (4.59)$$

The closed loop behavior is

$$\ddot{\mathbf{x}}_p + k_v \dot{\mathbf{x}}_p + k_p(\mathbf{x}_p - \mathbf{x}_{pd}) = 0;$$

and

$$\dot{\boldsymbol{\omega}} + k_v \boldsymbol{\omega} + k_p \delta\Phi = 0.$$

Direction Cosines: With the direction cosines representation, the end-effector orientation is described by the 9×1 column matrix

$$\mathbf{x}_r = (\mathbf{s}_1^T \ \mathbf{s}_2^T \ \mathbf{s}_3^T)^T.$$

The desired orientation is given as

$$\mathbf{x}_{rd} = (\mathbf{s}_{1d}^T \ \mathbf{s}_{2d}^T \ \mathbf{s}_{3d}^T)^T.$$

The left inverse in this case is simply given by

$$E_r^+ = \frac{1}{2} E_r^T;$$

where

$$E_r^T(\mathbf{x}_r) = (-\hat{\mathbf{s}}_1^T \quad -\hat{\mathbf{s}}_2^T \quad -\hat{\mathbf{s}}_3^T).$$

This yields

$$\delta\Phi = \frac{1}{2}E_r^T(\mathbf{x}_r)(\mathbf{x}_r - \mathbf{x}_{rd});$$

Since

$$E_r^T(\mathbf{x}_r)\mathbf{x}_r = \hat{\mathbf{s}}_1\mathbf{s}_1 + \hat{\mathbf{s}}_2\mathbf{s}_2 + \hat{\mathbf{s}}_3\mathbf{s}_3 = 0;$$

the angular rotation error is

$$\delta\Phi = -\frac{1}{2}(\hat{\mathbf{s}}_1\mathbf{s}_{1d} + \hat{\mathbf{s}}_2\mathbf{s}_{2d} + \hat{\mathbf{s}}_3\mathbf{s}_{3d}). \quad (4.60)$$

Euler Parameters The end-effector orientation is described by the 4×1 column matrix

$$\mathbf{x}_r = \boldsymbol{\lambda} = (\lambda_0 \quad \lambda_1 \quad \lambda_2 \quad \lambda_3)^T.$$

The desired orientation is

$$\boldsymbol{\lambda}_d = (\lambda_{0d} \quad \lambda_{1d} \quad \lambda_{2d} \quad \lambda_{3d})^T.$$

The orientation error vector is

$$\delta\boldsymbol{\lambda} = \boldsymbol{\lambda} - \boldsymbol{\lambda}_d.$$

The left inverse in this case is

$$E_r^+(\mathbf{x}_r) = 2\overset{\vee}{\boldsymbol{\lambda}}^T;$$

where

$$\overset{\vee}{\boldsymbol{\lambda}}^T = \begin{pmatrix} -\lambda_1 & \lambda_0 & -\lambda_3 & \lambda_2 \\ -\lambda_2 & \lambda_3 & \lambda_0 & -\lambda_1 \\ -\lambda_3 & -\lambda_2 & \lambda_1 & \lambda_0 \end{pmatrix}.$$

Noting that

$$\overset{\vee}{\boldsymbol{\lambda}}^T \boldsymbol{\lambda} = 0;$$

the angular rotation error can be written as

$$\delta\Phi = -2\overset{\vee}{\boldsymbol{\lambda}}^T \boldsymbol{\lambda}_d. \quad (4.61)$$

Trajectory Tracking

In this case, the input of the decoupled end-effector can be selected as

$$\mathcal{F}^* = \ddot{\mathbf{x}}_{pd} - k_p(\mathbf{x}_p - \mathbf{x}_{pd}) - k_v(\dot{\mathbf{x}}_p - \dot{\mathbf{x}}_{pd});$$

and

$$\mathcal{M}^* = \dot{\boldsymbol{\omega}}_d - k_p \boldsymbol{\delta\Phi} - k_v (\boldsymbol{\omega} - \boldsymbol{\omega}_d);$$

where

$$\boldsymbol{\omega}_d = E_r^+(\mathbf{x}_{rd}) \dot{\mathbf{x}}_{rd};$$

and the desired angular acceleration, $\dot{\boldsymbol{\omega}}_d$, is obtained by taking the time-derivative of equation (4.57)

$$\ddot{\mathbf{x}}_{rd} = E_r(\mathbf{x}_{rd}) \dot{\boldsymbol{\omega}}_d + \dot{E}_r(\mathbf{x}_{rd}) \boldsymbol{\omega}_d; \quad (4.62)$$

and using the left inverse E_r^+ yields,

$$\dot{\boldsymbol{\omega}}_d = E_r^+(\mathbf{x}_{rd}) \ddot{\mathbf{x}}_{rd} - E_r^+(\mathbf{x}_{rd}) \dot{E}_r(\mathbf{x}_{rd}) \boldsymbol{\omega}_d.$$

The closed loop behavior is

$$(\ddot{\mathbf{x}}_p - \ddot{\mathbf{x}}_{pd}) + k_v(\dot{\mathbf{x}}_p - \dot{\mathbf{x}}_{pd}) + k_p(\mathbf{x}_p - \mathbf{x}_{pd}) = 0;$$

and

$$(\dot{\boldsymbol{\omega}} - \dot{\boldsymbol{\omega}}_d) + k_v(\boldsymbol{\omega} - \boldsymbol{\omega}_d) + k_p \boldsymbol{\delta\Phi} = 0.$$

Direction Cosines With this representation, the end-effector orientation is described by

$$\mathbf{x}_r = (\mathbf{s}_1^T \ \mathbf{s}_2^T \ \mathbf{s}_3^T)^T;$$

where \mathbf{s}_1 , \mathbf{s}_2 , and \mathbf{s}_3 are the components in the base reference frame of the three unit-vectors $\mathbf{x}_{(n+1)}$, $\mathbf{y}_{(n+1)}$, and $\mathbf{z}_{(n+1)}$, associated with the end-effector frame. The second time derivatives of these three vectors are given by

$$\frac{d^2 \mathbf{x}_{(n+1)}}{dt^2} = -\mathbf{x}_{(n+1)} \times \dot{\boldsymbol{\omega}} + (\mathbf{x}_{(n+1)} \times \boldsymbol{\omega}) \times \boldsymbol{\omega}; \quad (4.63)$$

$$\frac{d^2 \mathbf{y}_{(n+1)}}{dt^2} = -\mathbf{y}_{(n+1)} \times \dot{\boldsymbol{\omega}} + (\mathbf{y}_{(n+1)} \times \boldsymbol{\omega}) \times \boldsymbol{\omega}; \quad (4.64)$$

$$\frac{d^2 \mathbf{z}_{(n+1)}}{dt^2} = -\mathbf{z}_{(n+1)} \times \dot{\boldsymbol{\omega}} + (\mathbf{z}_{(n+1)} \times \boldsymbol{\omega}) \times \boldsymbol{\omega}. \quad (4.65)$$

However for any set of three vectors \mathbf{u} , \mathbf{v} , and \mathbf{w} , we have the property

$$\mathbf{u} \times \mathbf{v} \times \mathbf{w} = (\mathbf{u}^T \mathbf{v}) \mathbf{w} - (\mathbf{v}^T \mathbf{w}) \mathbf{u}.$$

Using the above property yields,

$$\ddot{\mathbf{x}}_r = E(\mathbf{x}_r) \dot{\boldsymbol{\omega}} + R(\mathbf{x}_r, \boldsymbol{\omega}) \boldsymbol{\omega} - (\boldsymbol{\omega}^T \boldsymbol{\omega}) \mathbf{x}_r;$$

where $R(\mathbf{x}_r, \boldsymbol{\omega})$ is the 9×3 matrix

$$R(\mathbf{x}_r, \boldsymbol{\omega}) = \begin{pmatrix} (\mathbf{s}_1^T \boldsymbol{\omega}) I_3 \\ (\mathbf{s}_2^T \boldsymbol{\omega}) I_3 \\ (\mathbf{s}_3^T \boldsymbol{\omega}) I_3 \end{pmatrix}.$$

Using the left inverse of $E(\mathbf{x}_r)$, the angular acceleration is

$$\dot{\boldsymbol{\omega}} = \frac{1}{2} E_r^T [\ddot{\mathbf{x}}_r - R(\mathbf{x}_r, \boldsymbol{\omega}) \boldsymbol{\omega} + (\boldsymbol{\omega}^T \boldsymbol{\omega}) \mathbf{x}_r].$$

Since

$$E_r^T(\mathbf{x}_r) \mathbf{x}_r = 0;$$

the angular acceleration can be written as

$$\dot{\boldsymbol{\omega}} = \frac{1}{2} E_r^T(\mathbf{x}_r) \ddot{\mathbf{x}}_r + \frac{1}{2} R^T(\mathbf{x}_r, \boldsymbol{\omega}) \dot{\mathbf{x}}_r.$$

The desired angular acceleration is

$$\dot{\boldsymbol{\omega}}_d = \frac{1}{2} E_r^T(\mathbf{x}_{rd}) \ddot{\mathbf{x}}_{rd} + \frac{1}{2} R^T(\mathbf{x}_{rd}, \boldsymbol{\omega}_d) \dot{\mathbf{x}}_{rd}.$$

Euler Parameters: In this case, it can be shown that the acceleration associated with Euler parameters are given by (Khatib 1980)

$$\ddot{\boldsymbol{\lambda}} = \frac{1}{4} \overset{\vee}{\boldsymbol{\lambda}} \dot{\boldsymbol{\omega}} - \frac{1}{2} (\boldsymbol{\omega}^T \boldsymbol{\omega}) \boldsymbol{\lambda}. \quad (4.66)$$

Since

$$\overset{\vee}{\boldsymbol{\lambda}} \boldsymbol{\lambda} = 0;$$

The angular acceleration vector can be written as

$$\dot{\boldsymbol{\omega}} = 4 \overset{\vee}{\boldsymbol{\lambda}} \ddot{\boldsymbol{\lambda}}. \quad (4.67)$$

The desired angular acceleration is

$$\dot{\boldsymbol{\omega}}_d = 4 \overset{\vee}{\boldsymbol{\lambda}}_d \ddot{\boldsymbol{\lambda}}_d. \quad (4.68)$$

Chapter 5

Redundancy and Singularities

A manipulator is said to be *redundant* when the number, n , of its degrees of freedom is greater than the number, m , of its end-effector degrees of freedom. In this definition, redundancy is a characteristic of the manipulator. The extent of the manipulator redundancy is given by $(n - m)$, which defines the manipulator degree of redundancy.

In manipulation, there is also *task redundancy*. This type of redundancy is associated with tasks that involve a subset of the parameters needed to describe the configuration of the end effector. This redundancy concerns all types of manipulators. For instance, positioning the end effector of a non-redundant manipulator results in a *redundancy with respect to the task* of controlling the end-effector position.

A manipulator is said to be redundant with respect to a task if the number, m_{Task} , of independent parameters needed to describe the task configuration is smaller than the number n of the manipulator degrees of freedom.

5.1 Redundant Manipulators Dynamics

A set of operational coordinates – describing only the end-effector position and orientation – is obviously insufficient to completely specify the configuration of a redundant manipulator. Therefore, the dynamic behavior of the entire system cannot be described by a dynamic model using operational coordinates. Nevertheless, the dynamic behavior of the end effector itself can still be described, and its equations of motion in operational space can still be established. In fact, the structure of the effector dynamic model has been shown (Khatib 1980, Khatib 1987) to be identical to that obtained in the case of non-redundant manipulators (equation (4.6)). In the redundant case, however, the matrix Λ should be interpreted as a “*pseudo kinetic energy matrix*.” As shown below, this matrix is related to the joint-space kinetic energy matrix by

$$\Lambda^{-1}(\mathbf{q}) = J(\mathbf{q})A^{-1}(\mathbf{q})J^T(\mathbf{q}). \quad (5.1)$$

The above relationship provides a general expression for the matrix Λ that applies to both redundant and non-redundant manipulators. While equation (4.6) provides a description of the whole system dynamics for non-redundant manipulators, the equation associated with a redundant manipulator only describes the dynamic behavior of its end effector. In that case, the equation can be thought of as a “projection” of the system’s dynamics into the operational space. The remainder of the dynamics will affect joint motions in the null space of the redundant system. This analysis is discussed below.

The operational space equations of motion describe the dynamic response of a manipulator to the application of an operational force \mathbf{F} at the end effector. For non-redundant manipulators, the relationship between operational forces, \mathbf{F} , and joint torques, $\mathbf{\Gamma}$, is

$$\mathbf{\Gamma} = J^T(\mathbf{q})\mathbf{F}. \quad (5.2)$$

However, this relationship becomes incomplete for redundant manipulators that are in motion. Analysis of the kinematic aspect of redundancy shows that, at a given configuration, there is an infinity of elementary displacements of the redundant mechanism that could take place

without altering the configuration of the effector. Those displacements correspond to motion in the null space associated with a generalized inverse of the Jacobian matrix.

There is also a null space associated with the transpose of the Jacobian matrix. When the redundant manipulator is not at static equilibrium, there is an infinity of joint torque vectors that could be applied without affecting the resulting forces at the end effector. These are the joint torques acting within the null space of $J^T(\mathbf{q})$. With the addition of null space joint torques, the relationship between end-effector forces and manipulator joint torques takes the following general form

$$\mathbf{\Gamma} = J^T(\mathbf{q})\mathbf{F} + [I - J^T(\mathbf{q})J^{T\#}(\mathbf{q})]\mathbf{\Gamma}_0; \quad (5.3)$$

where $\mathbf{\Gamma}_0$ is an arbitrary generalized joint torque vector, which will be projected in the null space of J^T , and $J^{T\#}$ is a generalized inverse of J^T . Clearly, equation (5.3) is dependent on $J^{T\#}$ and there is an infinity of generalized inverses for J^T , namely, $\{J^{T\#} \mid J^T = J^T J^{T\#} J^T\}$. Below, it is shown that only one of these generalized inverses is consistent with the system dynamics.

We start by applying to the manipulator system (3.13), a joint torque vector in the general form (5.3). To establish the relationship between operational acceleration and operational force, we premultiply equation (3.13) by the matrix $J(\mathbf{q})A^{-1}(\mathbf{q})$, and use the relationship between joint acceleration and operational accelerations ($\ddot{\mathbf{x}} - \dot{J}(\mathbf{q})\dot{\mathbf{q}} = J(\mathbf{q})\ddot{\mathbf{q}}$). The resulting equation can be written as

$$\begin{aligned} \ddot{\mathbf{x}} + (J(\mathbf{q})A^{-1}(\mathbf{q})\mathbf{b}(\mathbf{q}, \dot{\mathbf{q}}) - \dot{J}(\mathbf{q})\dot{\mathbf{q}}) + J(\mathbf{q})A^{-1}(\mathbf{q})\mathbf{g}(\mathbf{q}) = \\ (J(\mathbf{q})A^{-1}(\mathbf{q})J^T(\mathbf{q}))\mathbf{F} + J(\mathbf{q})A^{-1}(\mathbf{q})[I - J^T(\mathbf{q})J^{T\#}(\mathbf{q})]\mathbf{\Gamma}_0. \end{aligned} \quad (5.4)$$

This equation expresses the relationship between $\ddot{\mathbf{x}}$ and \mathbf{F} . the matrix $(J(\mathbf{q})A^{-1}(\mathbf{q})J^T(\mathbf{q}))$, which premultiplies \mathbf{F} , is homogeneous to the inverse of a kinetic energy matrix. This matrix, which exists everywhere outside kinematic singularities, is the *pseudo kinetic energy matrix* of equation (5.1)

$$\Lambda(\mathbf{q}) = (J(\mathbf{q})A^{-1}(\mathbf{q})J^T(\mathbf{q}))^{-1}.$$

Equation (5.4) shows that the acceleration at the operational point is affected by $\mathbf{\Gamma}_0$ unless the term involving $\mathbf{\Gamma}_0$ is zero. That is, in order for joint torques associated with the null space in equation (5.3) not to produce any operational acceleration, it is necessary that

$$J(\mathbf{q})A^{-1}(\mathbf{q}) \left[I - J^T(\mathbf{q})J^{\#T}(\mathbf{q}) \right] \mathbf{\Gamma}_0 = 0. \quad (5.5)$$

A generalized inverse of $J(\mathbf{q})$ satisfying the above constraint is said to be *dynamically consistent* (Khatib 1990).

Theorem 1: (*Dynamic Consistency*)

A generalized inverse that is consistent with the dynamic constraint of equation (5.5), $\bar{J}(\mathbf{q})$, is unique and is given by

$$\bar{J}(\mathbf{q}) = A^{-1}(\mathbf{q})J^T(\mathbf{q})\Lambda(\mathbf{q}). \quad (5.6)$$

The proof is based on a straightforward analysis of equation (5.5). This equation can be rewritten as

$$\left[J(\mathbf{q})A^{-1}(\mathbf{q}) - \left(J(\mathbf{q})A^{-1}(\mathbf{q})J^T(\mathbf{q}) \right) J^{\#T}(\mathbf{q}) \right] \mathbf{\Gamma}_0 = 0;$$

which, using the definition of Λ , yields

$$\Lambda(\mathbf{q})J(\mathbf{q})A^{-1}(\mathbf{q}) = J^{\#T}(\mathbf{q}).$$

Notice that $\bar{J}(\mathbf{q})$ of equation (5.6) is actually the generalized inverse of the Jacobian matrix corresponding to the solution of $\delta\mathbf{x} = J(\mathbf{q})\delta\mathbf{q}$ that minimizes the manipulator's instantaneous kinetic energy.

5.1.1 Equations of Motion

Now, the end-effector equations of motion for a redundant manipulator can be obtained by using the dynamically consistent generalized inverse in equation (5.4) and premultiplying this equation by the matrix $\Lambda(\mathbf{q})$. The resulting equations are of the same form as equation (4.6)

established for non-redundant manipulators. In the case of redundancy, however, the inertial properties vary not only with the end-effector configuration, but also with the manipulator posture.

$$\Lambda(\mathbf{q})\ddot{\mathbf{x}} + \mu(\mathbf{q}, \dot{\mathbf{q}}) + \mathbf{p}(\mathbf{q}) = \mathbf{F}; \quad (5.7)$$

where

$$\mu(\mathbf{q}, \dot{\mathbf{q}}) = \bar{\mathcal{J}}^T(\mathbf{q})\mathbf{b}(\mathbf{q}, \dot{\mathbf{q}}) - \Lambda(\mathbf{q})\dot{J}(\mathbf{q})\dot{\mathbf{q}}; \quad (5.8)$$

$$\mathbf{p}(\mathbf{q}) = \bar{\mathcal{J}}^T(\mathbf{q})\mathbf{g}(\mathbf{q}). \quad (5.9)$$

Equation (5.7) provides a description of the dynamic behavior of the end effector in operational space. This equation is simply the projection of the joint-space equations of motion (3.13), by the dynamically consistent generalized inverse $\bar{\mathcal{J}}^T(\mathbf{q})$,

$$\bar{\mathcal{J}}^T(\mathbf{q}) \{A(\mathbf{q})\ddot{\mathbf{q}} + \mathbf{b}(\mathbf{q}, \dot{\mathbf{q}}) + \mathbf{g}(\mathbf{q}) = \mathbf{\Gamma}\} \implies \Lambda(\mathbf{q})\ddot{\mathbf{x}} + \mu(\mathbf{q}, \dot{\mathbf{q}}) + \mathbf{p}(\mathbf{q}) = \mathbf{F}. \quad (5.10)$$

The above property also applies to non-redundant manipulators, where the matrix $\bar{\mathcal{J}}^T(\mathbf{q})$ reduces to $J^{-T}(\mathbf{q})$.

5.1.2 Torque/Force Relationship

The dynamically consistent relationship between joint torques and operational forces for redundant manipulator systems is

$$\mathbf{\Gamma} = J^T(\mathbf{q})\mathbf{F} + [I - J^T(\mathbf{q})\bar{\mathcal{J}}^T(\mathbf{q})]\mathbf{\Gamma}_0. \quad (5.11)$$

This relationship provides a decomposition of joint torques into two dynamically decoupled control vectors: joint torques corresponding to forces acting at the end effector ($J^T\mathbf{F}$); and joint torques that only affect internal motions, $([I - J^T(\mathbf{q})\bar{\mathcal{J}}^T(\mathbf{q})]\mathbf{\Gamma}_0)$.

Using this decomposition, the end effector can be controlled by operational forces, while internal motions can be independently controlled by joint torques that are guaranteed not to alter the end effector's dynamic

Table 5.1: Position/Force Duality

	Position	Force
(*)	$\delta \mathbf{q} = J^{-1} \delta \mathbf{x}$	$\mathbf{\Gamma} = J^T \mathbf{F}$
(**)	$\delta \mathbf{q} = \bar{J} \delta \mathbf{x} + [I - \bar{J} J] \delta \mathbf{q}_0$	$\mathbf{\Gamma} = J^T \mathbf{F} + [I - J^T \bar{J}^T] \mathbf{\Gamma}_0$

(*) non-redundant manipulators, (**) redundant manipulators

behavior. This relationship is the basis for implementing the dextrous dynamic coordination strategy for macro-/mini-manipulators.

With the relationship (5.11), the force/position duality for non-redundant manipulators can be extended to the case of redundant manipulators as summarized in Table 1.

5.1.3 Stability Analysis

Dynamic decoupling at the end-effector of a redundant manipulator and the control of its motion and contact forces can be accomplished with the very same operational control structure used for the effectors of non-redundant manipulators. However, operational control forces alone cannot provide asymptotic stabilization to the whole redundant manipulators. Asymptotic stabilization of the redundant system requires the use of additional dissipative joint torques.

First, let us assume that the end-effector is simply subjected to the gradient of the attractive potential

$$U_{\text{goal}} = \frac{1}{2} k_p (\mathbf{x} - \mathbf{x}_{\text{goal}})^T (\mathbf{x} - \mathbf{x}_{\text{goal}});$$

and to a dissipative operational force

$$\mathbf{F}_{dis} = -k_v \dot{\mathbf{x}};$$

where k_p and k_v are positive constants. The gravity of the manipulator is further assumed to be compensated for. In these condition, the

Lagrange equations for the controlled system are

$$\frac{d}{dt}\left(\frac{\partial T}{\partial \dot{\mathbf{q}}}\right) - \frac{\partial(T - U_{\text{goal}})}{\partial \mathbf{q}} = \mathbf{\Gamma}_{dis}; \quad (5.12)$$

where

$$\mathbf{\Gamma}_{dis} = -k_v J^T(\mathbf{q}) \dot{\mathbf{x}}.$$

Using the relationship between joint velocities and operational velocities, the dissipative torques $\mathbf{\Gamma}_{dis}$ can be written as

$$\mathbf{\Gamma}_{dis} = -k_v J^T(\mathbf{q}) J(\mathbf{q}) \dot{\mathbf{q}}.$$

Since all non-dissipative forces in this control design are conservative, the stability condition is

$$\mathbf{\Gamma}_{dis}^T \dot{\mathbf{q}} \leq 0; \quad \text{for } \dot{\mathbf{q}} \neq \mathbf{0}; \quad (5.13)$$

or

$$-\dot{\mathbf{q}}^T D(\mathbf{q}) \dot{\mathbf{q}} \leq 0; \quad \text{for } \dot{\mathbf{q}} \neq \mathbf{0};$$

where

$$D(\mathbf{q}) = k_v [J^T(\mathbf{q}) J(\mathbf{q})].$$

This condition is satisfied, since $D(\mathbf{q})$ is an $n \times n$ positive semi-definite matrix of rank m_0 . However, the redundant mechanism can still describe movements that are solutions of the equation

$$\dot{\mathbf{q}}^T D(\mathbf{q}) \dot{\mathbf{q}} = 0.$$

Asymptotic stabilization requires

$$\mathbf{\Gamma}_{dis}^T \dot{\mathbf{q}} < 0; \quad \text{for } \dot{\mathbf{q}} \neq \mathbf{0}. \quad (5.14)$$

This can be achieved by the addition of joint dissipative torques ($-k_{vq} \dot{\mathbf{q}}$). The vector of total dissipative torques becomes

$$\mathbf{\Gamma}_{dis} = -k_v J^T(\mathbf{q}) J(\mathbf{q}) \dot{\mathbf{q}} - k_{vq} \dot{\mathbf{q}}.$$

The matrix $D(\mathbf{q})$ corresponding to the new expression for the dissipative joint forces becomes

$$D(\mathbf{q}) = k_v J^T(\mathbf{q}) J(\mathbf{q}) + k_{vq} I_n;$$

where I_n is the identity matrix of order n . Now, the matrix $D(\mathbf{q})$ is positive definite and the system is asymptotically stable.

Let us now consider the case where operational space dynamic compensations are used. The operational dissipative forces are $(-k_v\Lambda(\mathbf{q})\dot{\mathbf{x}})$, and the corresponding joint torques are $(-k_vJ^T(\mathbf{q})\Lambda(\mathbf{q})J(\mathbf{q})\dot{\mathbf{q}})$. To account for the manipulator dynamics, the additional dissipative torques that are needed to asymptotically stabilize the internal motions will be weighted by the joint space kinetic energy matrix $A(\mathbf{q})$, this is $(-k_{vq}A(\mathbf{q})\dot{\mathbf{q}})$. To prevent disturbances at end-effector, these torques must be selected from the dynamically consistent null space. The total dissipative torques are

$$\mathbf{\Gamma}_{dis} = -k_vJ^T(\mathbf{q})\Lambda(\mathbf{q})J(\mathbf{q})\dot{\mathbf{q}} + [I - J^T(\mathbf{q})\bar{J}^T(\mathbf{q})][-k_{vq}A(\mathbf{q})\dot{\mathbf{q}}];$$

which can be written as

$$\mathbf{\Gamma}_{dis} = -D(\mathbf{q})\dot{\mathbf{q}};$$

with

$$D(\mathbf{q}) = [(k_v - k_{vq})J^T(\mathbf{q})\Lambda(\mathbf{q})J(\mathbf{q}) + k_{vq}A(\mathbf{q})].$$

With an appropriate selection of k_v and k_{vq} , the matrix $D(\mathbf{q})$ is positive definite and the redundant manipulator is asymptotically stable.

5.1.4 Dynamic Consistency: An Example

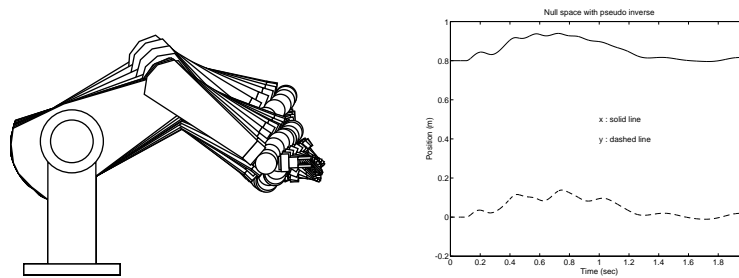


Figure 5.1: Null Space Motion with Pseudo Inverse

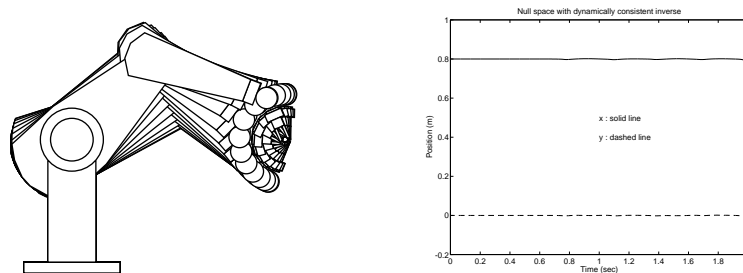


Figure 5.2: Null Space Motion with Dynamically Consistent Inverse

The impact of the dynamically consistent control decomposition is illustrated on the 3R-planar manipulator shown in Figure 5.1 and Figure 5.2. This manipulator is treated as a redundant mechanism with respect to the task of positioning the end-effector.

The goal here is to maintain the end-effector position, while letting the manipulator move in the null space. The end-effector position is controlled by operational forces, \mathbf{F} . An oscillatory motion in the null space is produced by the application, in the null space, of the gradient of an attractive potential without any dissipative forces, i.e. $\mathbf{\Gamma}_0 = -A(\mathbf{q})\nabla V_0$.

Two different generalized inverses are used to construct the projection of $\mathbf{\Gamma}_0$ onto the null space: the Moore-Penrose or pseudo inverse ($J^+ = J^T(JJ^T)^{-1}$) and the dynamically consistent inverse (\bar{J}). The simulation results are shown in Figure 5.1 and Figure 5.2.

As expected, with the dynamically consistent inverse (see Figure 5.2) the motion in the null space does not affect the end-effector position, while large coupling forces are produced at the end-effector when the pseudo inverse is used (see Figure 5.1).

5.2 Singular Configurations

A *singular configuration* is a configuration \mathbf{q} at which the end-effector mobility – defined as the rank of the Jacobian matrix – locally decreases. At a singular configuration, the end-effector locally loses the ability to move along or rotate about some direction in Cartesian space.

Singularities and mobility are characterized by the determinant of the Jacobian matrix for non-redundant manipulators; or by the determinant of the matrix product of the Jacobian and its transpose for redundant mechanisms. This determinant is a function, $s(\mathbf{q})$, that vanishes at each of the manipulator singularities. This function can be developed into a product of terms,

$$s(\mathbf{q}) = s_1(\mathbf{q}) \cdot s_2(\mathbf{q}) \cdot s_3(\mathbf{q}) \dots s_{n_s}(\mathbf{q}); \quad (5.15)$$

each of which corresponds to one of the different singularities associated with the mechanism. Here, n_s is the number of different singularities. A singular configuration always has a corresponding *singular direction*. It is in or about this direction that the end-effector presents infinite effective mass or effective inertia. The end-effector movements remain free in the subspace orthogonal to this direction. In reality, the difficulty with singularities extends to some neighborhood around the singular configuration, as illustrated in Figure (5.3). The neighborhood of the i^{th} singularity, \mathcal{D}_{s_i} , can be defined as

$$\mathcal{D}_{s_i} = \{\mathbf{q} \mid |s_i(\mathbf{q})| \leq \eta_i\}; \quad (5.16)$$

where η_i is positive.

5.2.1 Control Strategy

The basic concept in our approach to end-effector control at kinematic singularities is described as follows: In the neighborhood \mathcal{D}_{s_i} of a singular configuration \mathbf{q} , the manipulator is treated as a redundant system in the subspace¹ orthogonal to the singular direction. End-effector

¹a subspace of the end-effector operational space.

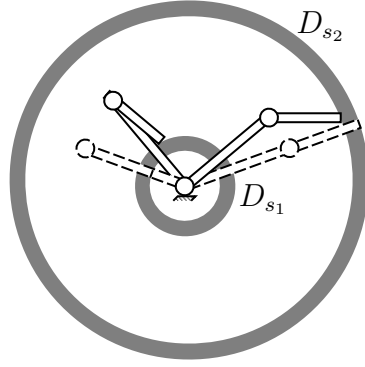


Figure 5.3: Kinematic Singularities

motions in that subspace are controlled using the operational space redundant manipulator control, while null space joint torques are used to deal with the control in the singular direction according to the type of singularity. The use of the dynamically consistent force/torque relationship guarantees decoupled behavior between end-effector control and null space control.

In the neighborhood of singular configurations, singular directions and the associated singular frames are identified. A *singular frame* is a frame in which one of the axes is aligned with the singular direction. Next, the Jacobian matrix is rotated into the singular frame and the rows corresponding to singular directions are eliminated. This redundant Jacobian corresponds to the redundant mechanism with respect to end-effector motion in the subspace orthogonal to the singular directions. The null space generated by the dynamically consistent inverse of this redundant Jacobian matrix is used to control motions in the null space.

An additional task to be carried out using the null space can be realized by constructing a potential function, $V_0(\mathbf{q})$, whose minimum corresponds to the desired task. This is accomplished by selecting

$$\mathbf{\Gamma}_{\text{null-space}} = [I - J^T(\mathbf{q})\bar{J}^T(\mathbf{q})] \mathbf{\Gamma}_0; \quad (5.17)$$

with

$$\mathbf{\Gamma}_0 = -A(\mathbf{q})[\nabla V_0 + k_{vq}\dot{\mathbf{q}}]. \quad (5.18)$$

$-A(\mathbf{q})k_{vq}\dot{\mathbf{q}}$ corresponds to the dissipative torques needed to provide asymptotic stabilization of the mechanism. The interference of $\mathbf{\Gamma}_0$ on the end-effector is eliminated by projecting this vector in the dynamically consistent null space.

The strategy for the control of a manipulator at a singularity depends on the type of singularity.

5.2.2 Types of Singularities

In previous work, singularities have been characterized in terms of the internal freedom of motion a manipulator has at a singular configuration while its end-effector remains fixed.

However, for control purposes, we separate singularities into two groups based on the control characteristics of their null spaces. Type 1 singularities are those at which the end-effector can be controlled in the singular directions using null space torques. Type 2 singularities arise when null space torques affect only the internal joint motions.

A projection of joint torques into the null space associated with a Type 1 singularity results only in a finite end-effector motion in the singular direction. A projection into the null space associated with a Type 2 singularity results only in a finite change of the singular direction through finite internal joint motions.

Singularity Type 1: The end-effector motion in the singular direction can be controlled directly through the associated null space by selecting a potential function whose minimum corresponds to the desired configuration. The resulting torques from Equation 5.18 affect the end-effector motion only along the singular direction.

Singularity Type 2: The configuration of the manipulator itself is controlled to change the singular direction until the singular direction is orthogonal to the operational force vector. By constructing a potential function such that its minimum corresponds

to the configuration where the singular direction is orthogonal to the operational force vector, the singular direction can be changed in the null space. The resulting torques from Equation 5.18 affect only the change of the singular direction via internal joint motions while maintaining the position and orientation of the end-effector.

Since a small end-effector motion in the singular direction can cause a large internal joint motion in the null space, following a time-dependent trajectory can be difficult. A solution to this difficulty is to use a simple path planning algorithm which keeps the singular direction orthogonal to the end-effector motion in the neighborhood of singularities. Paths generated in this way will avoid the time delay caused by finite internal joint motions of the manipulator. Another practical approach, which eliminates the need for this type of path planning, is to use time-independent trajectories such as the goal position method.

5.2.3 Example: The PUMA 560

The above strategy is applied here to the control a PUMA 560 with the goal position method. Figure 5.4 shows the three basic singularities in a PUMA 560: elbow lock, wrist lock, and head lock from left to right. Elbow lock is Type 1 and the other two are Type 2. Since these basic singularities can occur at the same time, the rank of the Jacobian matrix can vary from 3 to 6. The minimum rank of the Jacobian corresponds to the configuration at which the end-effector reaches the highest point directly above the base.

In Figure 5.5, the end-effector of a PUMA 560 is simultaneously moving out of two singularities, elbow lock (Type 1) and wrist lock (Type 2). The goal is to translate along the singular direction, x , while maintaining all other positions and orientations. Since internal joint motions are not needed, the end-effector motion is fully controlled as shown in the plot in Figure 5.5.

In Figure 5.6, the end-effector of a PUMA 560 is moving out of the singular configuration of wrist lock (Type 2) along the singular direction, x , while maintaining all other positions and orientations. The

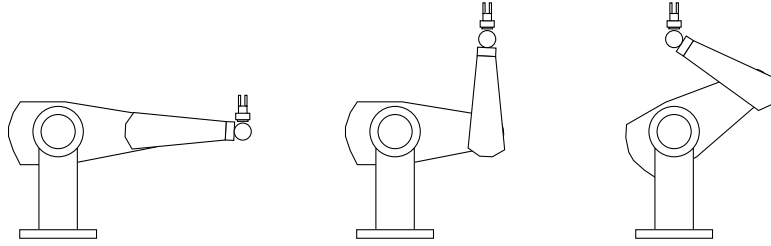


Figure 5.4: Three Basic Singular Configurations in PUMA 560

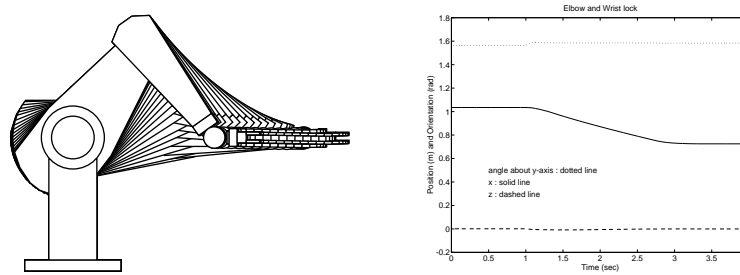


Figure 5.5: Compound Singular Configuration

initial configuration is shown in Figure 5.6 and the goal is to rotate 45° about x -axis. The motion of joint 4 and 6 is the finite internal joint motion and the motion of joint 5 accounts for the end-effector motion. The symmetric motion of joint 4 and 6 ensures the decoupled behavior. The end-effector motion remains smooth (solid line), even though there is a sharp velocity change in joint 4 and 6 at the boundary of the singular configuration.

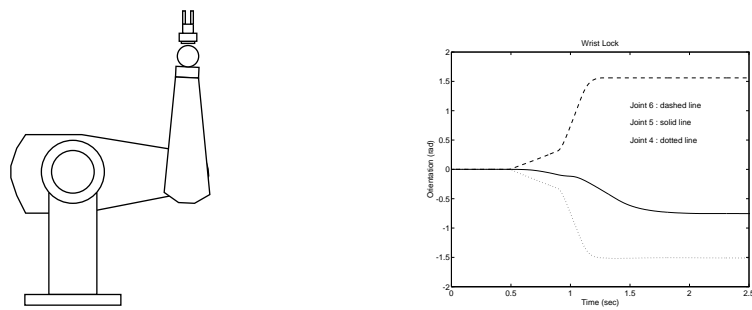


Figure 5.6: Wrist Lock

Chapter 6

Inertial Properties

The inertial properties of a manipulator are generally expressed with respect to its motion in joint space. For an n degree-of-freedom manipulator, the joint space inertial properties are described by the kinetic energy matrix, $A(\mathbf{q})$. When the dynamic response or impact force at some point at the end-effector or manipulated object are of interest, the inertial properties involved are those evaluated at the *operational point*. The operational space kinetic energy matrix $\Lambda(\mathbf{x})$ provides a description of the inertial properties of the manipulator at the operational point.

The analysis of the end-effector inertial properties relies on study of the matrix

$$\Lambda_0(\mathbf{q}) = \left(J_0(\mathbf{q}) A^{-1}(\mathbf{q}) J_0^T(\mathbf{q}) \right)^{-1};$$

where $J_0(\mathbf{q})$ is the basic Jacobian associated with the end-effector linear and angular velocities. Using this matrix, Asada (1983) proposed the generalized inertia ellipsoid as a geometric representation for the inertial properties of a manipulator. An alternative to the ellipsoid of inertia is the ellipsoid of gyration suggested by Hogan (1984). This ellipsoid is based on analysis of the matrix, $\Lambda_0^{-1}(\mathbf{q})$, whose existence is always guaranteed. The eigenvalues and eigenvectors of the matrix $\Lambda_0(\mathbf{q})$

were used in combination with the hyper-parallelepiped of acceleration in the design of manipulators aimed at achieving the smallest, most isotropic, and most uniform inertial characteristics; and the largest, most isotropic, and most uniform bounds on the magnitude of end-effector acceleration (Khatib and Burdick 1985, Khatib and Agrawal 1989).

The eigenvalues associated with the matrix $\Lambda_0(\mathbf{q})$ or its inverse $\Lambda_0^{-1}(\mathbf{q})$ provide a useful characterization of the bounds on the magnitude of the inertial properties. However, these eigenvalues correspond to eigenvectors in a six-dimensional space that combines translational and rotational motions and are difficult to interpret.

6.1 Inertial Properties and Task Redundancy

When analyzing the inertial properties of manipulators, two distinct types of tasks are examined: end-effector translational tasks and end-effector rotational tasks. Given the redundancy of the manipulator with respect to each of these tasks, the dynamic behavior at the end-effector can be described by a system of equations similar to (5.7).

First, let us consider the task of positioning the end effector. The Jacobian in this case is the matrix, $J_v(\mathbf{q})$, associated with the linear velocity at the operational point. The pseudo kinetic energy matrix is:

$$\Lambda_v^{-1}(\mathbf{q}) = J_v(\mathbf{q})A^{-1}(\mathbf{q})J_v^T(\mathbf{q}). \quad (6.1)$$

The matrix $\Lambda_v^{-1}(\mathbf{q})$ provides a description of the end-effector translational response to a force. Consider, for instance, the task of positioning the end effector along the y-axis, as illustrated in Figure 6.1-a. The Jacobian associated with this task reduces to the row matrix $J_{v_y}(\mathbf{q})$. The pseudo kinetic energy matrix in this case is a scalar, m_y , representing the mass perceived at the end effector in response to the application of a force f_y along the y axis:

$$\frac{1}{m_y} = J_{v_y}(\mathbf{q})A^{-1}(\mathbf{q})J_{v_y}^T(\mathbf{q}).$$

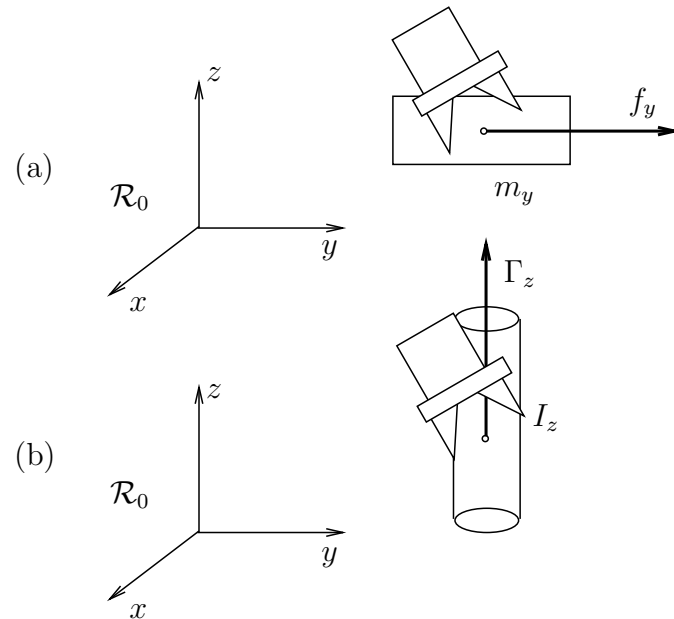


Figure 6.1: Effective Mass (a) and Effective Inertia (b)

With \mathbf{y}_0 representing the unit vector along the y -axis, the matrix $J_{v_y}(\mathbf{q})$ can be written as

$$J_{v_y}(\mathbf{q}) = \mathbf{y}_0^T J_v(\mathbf{q});$$

and

$$\frac{1}{m_y} = \mathbf{y}_0^T \Lambda_v^{-1} \mathbf{y}_0.$$

For rotational tasks, the Jacobian involved is the matrix $J_\omega(\mathbf{q})$ associated with the angular velocity measured about the different axes of the operational frame. The pseudo kinetic energy matrix is:

$$\Lambda_\omega^{-1}(\mathbf{q}) = J_\omega(\mathbf{q}) A^{-1}(\mathbf{q}) J_\omega^T(\mathbf{q}). \quad (6.2)$$

The matrix $\Lambda_\omega^{-1}(\mathbf{q})$ provides a description of the end-effector rotational response to a moment. Consider now the task of rotating the end

effector about the z axis, as illustrated in Figure 6.1-b. The Jacobian associated with this task is the row matrix

$$J_{\omega_z}(\mathbf{q}) = \mathbf{z}_0^T J_{\omega}(\mathbf{q});$$

\mathbf{z}_0 is the unit vector along the z -axis. The pseudo kinetic energy matrix in this case is a scalar, I_z , representing the inertia perceived at the end effector in response to a moment Γ_z applied about the z -axis:

$$\frac{1}{I_z} = \mathbf{z}_0^T \Lambda_{\omega}^{-1}(\mathbf{q}) \mathbf{z}_0.$$

6.2 Effective Mass/Inertia

The above analysis can be easily extended for translational and rotational motions along or about an arbitrary direction. If \mathbf{u} is the unit vector describing this direction, the inertial properties can be analyzed by considering the two matrices $J_{v_u}(\mathbf{q})$ and $J_{\omega_u}(\mathbf{q})$. These matrices are given by

$$J_{v_u}(\mathbf{q}) = \mathbf{u}^T J_v(\mathbf{q}); \quad \text{and} \quad J_{\omega_u}(\mathbf{q}) = \mathbf{u}^T J_\omega(\mathbf{q}).$$

The *effective mass*, $m_{\mathbf{u}}(\Lambda_v)$, perceived at the operational point along a direction \mathbf{u} is given by

$$\frac{1}{m_{\mathbf{u}}(\Lambda_v)} = \mathbf{u}^T \Lambda_v^{-1}(\mathbf{q}) \mathbf{u}. \quad (6.3)$$

Starting from rest, the inverse of magnitude of the effective mass is equal to the component of the linear acceleration along the direction \mathbf{u} that results in response to a unit force applied along \mathbf{u} .

The *effective inertia*, $I_{\mathbf{u}}(\Lambda_\omega)$, perceived at the operational point about a direction \mathbf{u} is given by

$$\frac{1}{I_{\mathbf{u}}(\Lambda_\omega)} = \mathbf{u}^T \Lambda_\omega^{-1}(\mathbf{q}) \mathbf{u}. \quad (6.4)$$

Starting from rest, the inverse of magnitude of the effective inertia is equal to the component of the angular acceleration about the direction \mathbf{u} that results in response to a unit moment applied about \mathbf{u} .

The above characterization can be extended to describe the overall effective inertial properties of a manipulator in a direction represented by a unit vector \mathbf{w} in the m -dimensional space. The *effective inertial properties* in a direction \mathbf{w} is described by the scalar

$$\sigma_{\mathbf{w}}(\Lambda_0) = \frac{1}{(\mathbf{w}^T \Lambda_0^{-1} \mathbf{w})}. \quad (6.5)$$

Although difficult to physically interpret, $\sigma_{\mathbf{w}}(\Lambda_0)$ provides a useful measure of the magnitude of the overall inertial properties.

6.3 Structure of Λ_0^{-1}

We have seen that the end-effector translational response to a force and its rotational response to a moment can be characterized by the matrices $\Lambda_v^{-1}(\mathbf{q})$ and $\Lambda_\omega^{-1}(\mathbf{q})$, respectively. These two matrices have been established separately by considering pure translational motion tasks and pure rotational motion tasks.

Consider again, the matrix $(J_0(\mathbf{q})A^{-1}(\mathbf{q})J_0^T(\mathbf{q}))$ expressed in terms of the matrix $A^{-1}(\mathbf{q})$ and the basic Jacobian $J_0(\mathbf{q})$. The basic Jacobian matrix can be written as

$$J_0(\mathbf{q}) = \begin{bmatrix} J_v(\mathbf{q}) \\ J_\omega(\mathbf{q}) \end{bmatrix}; \quad (6.6)$$

where $J_v(\mathbf{q})$ and $J_\omega(\mathbf{q})$ are the two block matrices associated with the end-effector linear and angular velocities, respectively. Using this decomposition, the matrix $\Lambda_0^{-1}(\mathbf{q})$ can be written in the form

$$\Lambda_0^{-1}(\mathbf{q}) = \begin{bmatrix} \Lambda_v^{-1}(\mathbf{q}) & \bar{\Lambda}_{v\omega}(\mathbf{q}) \\ \bar{\Lambda}_{v\omega}^T(\mathbf{q}) & \Lambda_\omega^{-1}(\mathbf{q}) \end{bmatrix}; \quad (6.7)$$

where $\Lambda_v(\mathbf{q})$ is the matrix given in equation (6.1) and $\Lambda_\omega(\mathbf{q})$ is the matrix given in equation (6.2). The matrix $\bar{\Lambda}_{v\omega}(\mathbf{q})$ is given by

$$\bar{\Lambda}_{v\omega}(\mathbf{q}) = J_v(\mathbf{q})A^{-1}(\mathbf{q})J_\omega^T(\mathbf{q}).$$

The matrix $\Lambda_v(\mathbf{q})$, which describes the end-effector translational response to a force, is homogeneous to a mass matrix, while $\Lambda_\omega(\mathbf{q})$, which describes the end-effector rotational response to a moment, is homogeneous to an inertia matrix. The matrix $\bar{\Lambda}_{v\omega}(\mathbf{q})$ provides a description of the coupling between translational and rotational motions.

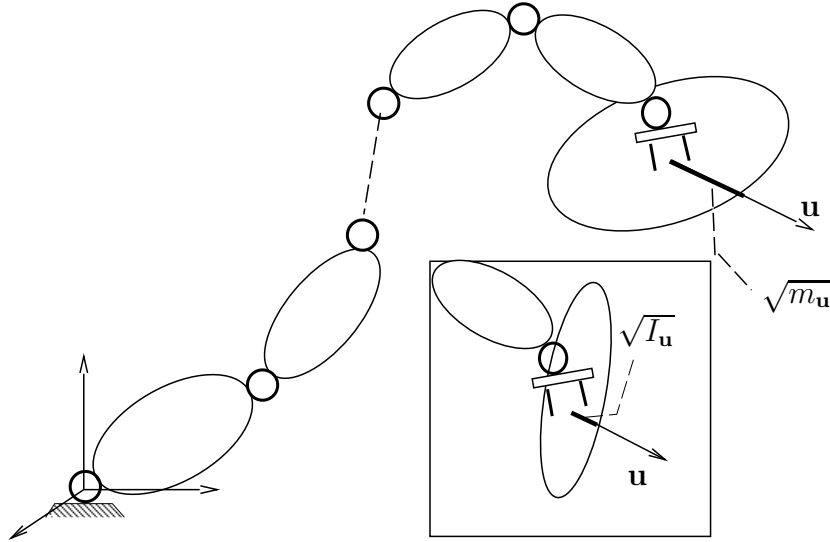


Figure 6.2: Effective Mass/Inertia (Ellipsoid Representation)

6.4 Belted Ellipsoid

As illustrated in Figure 6.2, one possible representation of the mass/inertia properties associated with the two matrices $\Lambda_v^{-1}(\mathbf{q})$ and $\Lambda_\omega^{-1}(\mathbf{q})$ is to use the two ellipsoids:

$$\mathbf{v}^T \Lambda_v^{-1}(\mathbf{q}) \mathbf{v} = 1; \quad \text{and} \quad \mathbf{v}^T \Lambda_\omega^{-1}(\mathbf{q}) \mathbf{v} = 1.$$

However, ellipsoid representations only provide a description of the square roots of effective mass (inertia) in (about) a direction.

We propose a geometric representation that characterizes the actual magnitude of these properties. This representation is based on what we have termed the *belted ellipsoid*. A belted ellipsoid is obtained by a polar transformation of an ellipsoid. A point on the ellipsoid surface is transformed to a point located along the same polar line at a distance equal to the square of the initial point distance. This construction is illustrated in Figure 6.3.

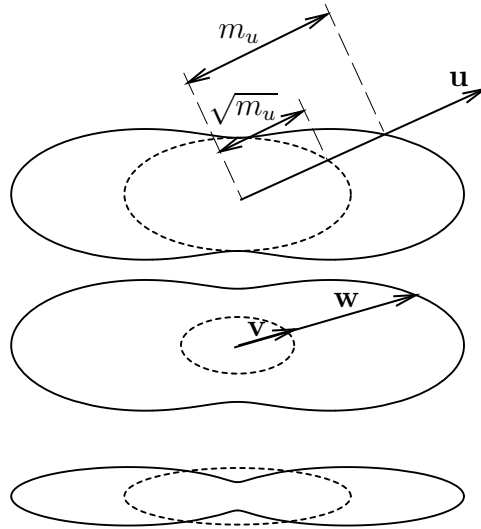


Figure 6.3: Construction of Belted Ellipsoids from Ellipsoids

A point on the ellipsoid represented by a vector \mathbf{v} is transformed into a point on the belted ellipsoid represented by a vector \mathbf{w} . The vector \mathbf{w} is collinear to \mathbf{v} and is of a magnitude equal to $\mathbf{v}^T \mathbf{v}$. That is

$$\mathbf{w} = \|\mathbf{v}\|\mathbf{v}.$$

The equation of a belted ellipsoid, therefore, can be obtained from the equation of an ellipsoid by replacing the vector \mathbf{v} by the vector $\frac{\mathbf{v}}{\sqrt{\mathbf{v}^T \mathbf{v}}}$.

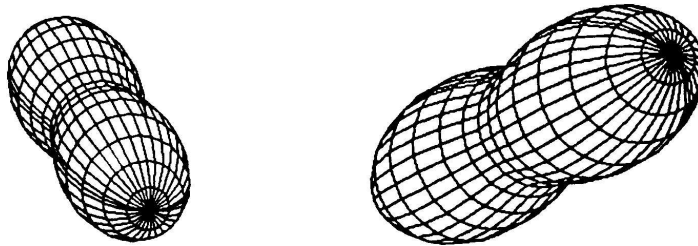


Figure 6.4: Examples of Belted Ellipsoids

The equations for the two belted ellipsoids corresponding to the two matrices $\Lambda_v^{-1}(\mathbf{q})$ and $\Lambda_\omega^{-1}(\mathbf{q})$ are

$$\frac{\mathbf{v}^T \Lambda_v^{-1}(\mathbf{q}) \mathbf{v}}{\sqrt{\mathbf{v}^T \mathbf{v}}} = 1; \quad \text{and} \quad \frac{\mathbf{v}^T \Lambda_\omega^{-1}(\mathbf{q}) \mathbf{v}}{\sqrt{\mathbf{v}^T \mathbf{v}}} = 1. \quad (6.8)$$

For instance, the ellipsoid

$$\frac{x^2}{a^2} + \frac{y^2}{b^2} + \frac{z^2}{c^2} = 1;$$

becomes

$$\frac{x^2}{a^2 \sqrt{x^2 + y^2 + z^2}} + \frac{y^2}{b^2 \sqrt{x^2 + y^2 + z^2}} + \frac{z^2}{c^2 \sqrt{x^2 + y^2 + z^2}} = 1.$$

Two examples of belted ellipsoids are shown in Figure 6.4. For a redun-

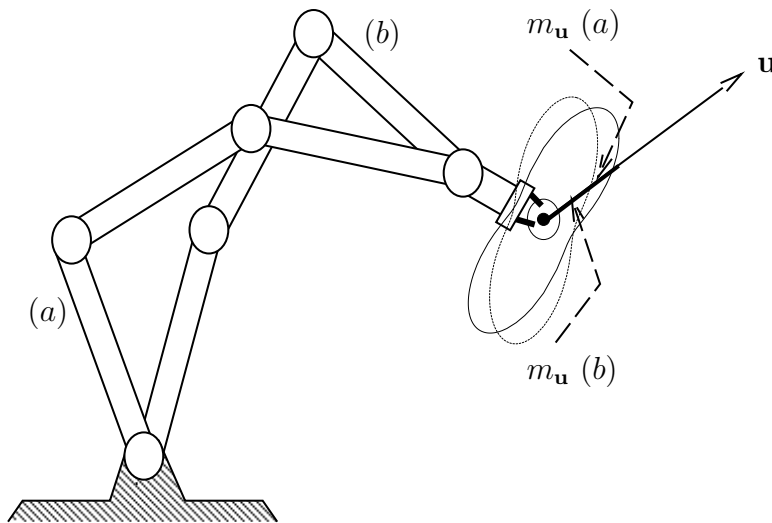


Figure 6.5: Effective Mass of a Redundant Manipulator

dant manipulator, the inertial properties perceived at a given position and orientation of the end effector vary with the manipulator configuration. This is illustrated for the effective mass in Figure 6.5 using belted ellipsoids.

Chapter 7

Macro-/Mini-Manipulators

We now consider the case of systems resulting from the serial combination of two manipulators. The manipulator connected to the ground will be referred to as the *macro-manipulator*. It has n_M degrees of freedom and its configuration is described by the system of n_M generalized joint coordinates \mathbf{q}_M . The second manipulator, referred to as the *mini-manipulator*, has n_m degrees of freedom and its configuration is described by the generalized coordinates \mathbf{q}_m . The resulting structure is an n -degree-of-freedom manipulator with $n = n_M + n_m$. Its configuration is described by the system of generalized joint coordinates $\mathbf{q} = [\mathbf{q}_M^T \mathbf{q}_m^T]^T$. If m represents the number of effector degrees of freedom of the combined structure, n_M and n_m are assumed to obey

$$n_M \geq 1 \text{ and } n_m = m. \quad (7.1)$$

This assumption says that the mini-manipulator must have the full freedom to move in the operational space. The macro-manipulator must have at least one degree of freedom.

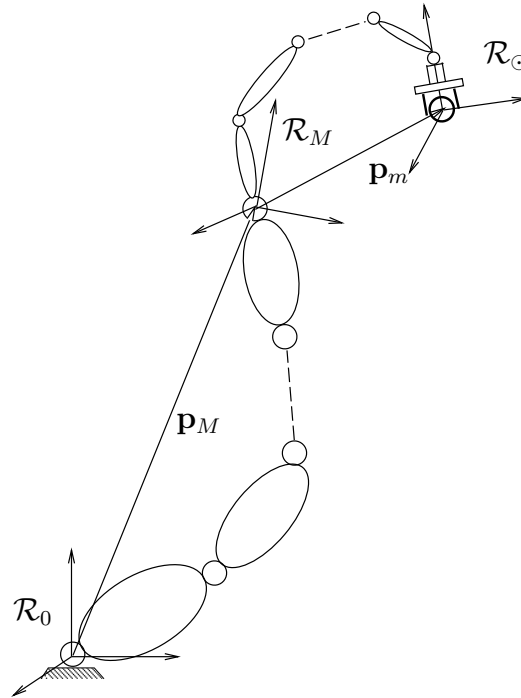


Figure 7.1: Kinematics of a Macro-/Mini-Manipulator System

7.1 Kinematics of Macro/Mini Structures

The configuration of the macro-manipulator is described with respect to a reference frame \mathcal{R}_0 and the configuration of the mini-manipulator structure is described with respect to a frame \mathcal{R}_M attached to the last link of the macro-manipulator, as illustrated in Figure 7.1. The coordinate frame associated with the operational point, is denoted by \mathcal{R}_{\ominus} . Let $S_M(\mathbf{q}_M)$ be the transformation matrix describing the rotation between the frames \mathcal{R}_M and \mathcal{R}_0 .

Let \mathbf{p}_M be the vector connecting the origins of frames \mathcal{R}_0 and \mathcal{R}_M , and \mathbf{p}_m the vector connecting those of \mathcal{R}_M and \mathcal{R}_{\ominus} . The position of the

operational point, with respect to \mathcal{R}_0 , is described by the vector

$$\mathbf{p} = \mathbf{p}_M + \mathbf{p}_m.$$

If \mathbf{v}_M and ω_M represent the linear and angular velocities at the origin of frame \mathcal{R}_M attached to the last link of the macro-manipulator, the linear velocity at the operational point is

$$\mathbf{v} = \mathbf{v}_M + \mathbf{v}_m + \omega_M \times \mathbf{p}_m;$$

where \mathbf{v}_m represents the linear velocity at the operational point resulting from the motion of the mini-manipulator. The angular velocity at the end effector is

$$\omega = \omega_M + \omega_m.$$

Thus, the linear and angular velocities at the operational point expressed with respect to the reference frame \mathcal{R}_0 are

$$\begin{bmatrix} \mathbf{v} \\ \omega \end{bmatrix}_{(\mathcal{R}_0)} = \begin{bmatrix} I & -\hat{\mathbf{p}}_{m(0)} \\ 0 & I \end{bmatrix} \begin{bmatrix} \mathbf{v}_M \\ \omega_M \end{bmatrix}_{(\mathcal{R}_0)} + \begin{bmatrix} S_M & 0 \\ 0 & S_M \end{bmatrix} \begin{bmatrix} \mathbf{v}_m \\ \omega_m \end{bmatrix}_{(\mathcal{R}_M)}; \quad (7.2)$$

where $\hat{\mathbf{p}}_{m(0)}$ is the cross product operator associated with the position vector $\mathbf{p}_{m(0)}$ and expressed in \mathcal{R}_0 . If $J_{M(0)}(\mathbf{q}_M)$ and $J_{m(0)}(\mathbf{q}_m)$ are the basic Jacobian matrices associated with two individual manipulators, the basic Jacobian matrix associated with the serial combination can be expressed as

$$J_0 = [VJ_{M(0)} \quad J_{m(0)}]; \quad (7.3)$$

where

$$V = \begin{bmatrix} I & -\hat{\mathbf{p}}_{m(0)} \\ 0 & I \end{bmatrix}. \quad (7.4)$$

7.2 Dynamics of Macro/Mini Structures

The kinetic energy matrix, $A(\mathbf{q})$, of the combined system can be decomposed in block matrices corresponding to the dimensions of the two manipulators' individual kinetic energy matrices

$$A(\mathbf{q}) = \begin{bmatrix} A_{11} & A_{12} \\ A_{12}^T & A_{22} \end{bmatrix}. \quad (7.5)$$

Lemma 1:

The $n_m \times n_m$ joint-space kinetic energy matrix, A_m , of the mini-manipulator considered alone is identical to the matrix A_{22} of (7.5).

Proof: The kinetic energy of the combined macro-/mini-manipulator is

$$T(\mathbf{q}, \dot{\mathbf{q}}) = \frac{1}{2} \dot{\mathbf{q}}^T A \dot{\mathbf{q}}.$$

The kinetic energy associated with the mini-manipulator considered alone is

$$T_m = \frac{1}{2} \dot{\mathbf{q}}_m^T A_m \dot{\mathbf{q}}_m.$$

T_m must be identical to $T(\mathbf{q}, \dot{\mathbf{q}})|_{\dot{\mathbf{q}}_M=0}$,

$$T(\mathbf{q}, \dot{\mathbf{q}})|_{\dot{\mathbf{q}}_M=0} = \frac{1}{2} \begin{bmatrix} 0 & \dot{\mathbf{q}}_m^T \end{bmatrix} \begin{bmatrix} A_{11} & A_{12} \\ A_{12}^T & A_{22} \end{bmatrix} \begin{bmatrix} 0 \\ \dot{\mathbf{q}}_m \end{bmatrix} = \frac{1}{2} \dot{\mathbf{q}}_m^T A_{22} \dot{\mathbf{q}}_m; \quad (7.6)$$

which implies the identity between A_m and A_{22} . \square

The operational space *pseudo kinetic energy matrix* Λ_0 associated with the linear and angular velocities is defined by $(J_0 A^{-1} J_0^T)^{-1}$.

Lemma 2:

The operational space pseudo kinetic energy matrix Λ_0 associated with the macro-/mini-manipulator and the operational space kinetic energy matrix $\Lambda_{m(0)}$ associated with the mini-manipulator are related by

$$\Lambda_0^{-1} = \Lambda_{m(0)}^{-1} + \bar{\Lambda}_C; \quad (7.7)$$

where

$$\bar{\Lambda}_C = \begin{matrix} (VJ_{M(0)} - J_{m(0)}A_{22}^{-1}A_{21}) & (A_{11} - A_{21}^T A_{22}^{-1} A_{21})^{-1} \\ (VJ_{M(0)} - J_{m(0)}A_{22}^{-1}A_{21})^T & \end{matrix}. \quad (7.8)$$

Proof: The proof is based on a special matrix decomposition of the kinetic energy matrix A . A is a symmetric positive definite matrix. The sub-matrix A_{22} is nonsingular. Therefore, the matrix A can be decomposed (Golub and Van Loan 1983) as

$$A = \begin{bmatrix} I & A_{21}^T A_{22}^{-1} \\ 0 & I \end{bmatrix} \begin{bmatrix} \bar{A}_{11}^{-1} & 0 \\ 0 & A_{22} \end{bmatrix} \begin{bmatrix} I & 0 \\ A_{22}^{-1} A_{21} & I \end{bmatrix}; \quad (7.9)$$

where

$$\bar{A}_{11} = (A_{11} - A_{21}^T A_{22}^{-1} A_{21})^{-1}. \quad (7.10)$$

The matrix Λ_0^{-1} is

$$\Lambda_0^{-1} = \begin{bmatrix} VJ_{M(0)} & J_{m(0)} \end{bmatrix} \begin{bmatrix} I & 0 \\ -A_{22}^{-1} A_{21} & I \end{bmatrix} \begin{bmatrix} \bar{A}_{11} & 0 \\ 0 & A_{22}^{-1} \end{bmatrix} \begin{bmatrix} I & -A_{21}^T A_{22}^{-1} \\ 0 & I \end{bmatrix} \begin{bmatrix} J_{M(0)}^T V^T \\ J_{m(0)}^T \end{bmatrix}. \quad (7.11)$$

Substituting A_m for A_{22} in the above expression yields equations (7.7) and (7.8). \square

The inertial properties of the macro-/mini-manipulator are represented by the $m \times m$ matrix, Λ_0 . The magnitude of these properties in a

direction represented by a unit vector \mathbf{w} in the m -dimensional space can be described by the scalar

$$\sigma_{\mathbf{w}}(\Lambda_0) = \frac{1}{(\mathbf{w}^T \Lambda_0^{-1} \mathbf{w})},$$

which represents the effective inertial properties in the direction \mathbf{w} .

Theorem 2: (*Reduced Inertial Properties*).

The operational space pseudo kinetic energy matrices Λ_0 (combined mechanism), and $\Lambda_{m(0)}$ (mini-manipulator) satisfy

$$\sigma_{\mathbf{w}}(\Lambda_0) \leq \sigma_{\mathbf{w}}(\Lambda_{m(0)}), \quad (7.12)$$

in any direction \mathbf{w} .

The magnitudes of the inertial properties of the macro-/mini-manipulator system shown in Figure 7.2, at any configuration and in any direction, are smaller than or equal to the magnitudes of the inertial properties associated with the mini-manipulator.

Proof: The proof of this theorem involves the following two steps:

Step 1: (*Relationship*) Equation (7.7) yields,

$$\mathbf{w}^T \Lambda_0^{-1} \mathbf{w} = \mathbf{w}^T \Lambda_{m(0)}^{-1} \mathbf{w} + \mathbf{w}^T \bar{\Lambda}_C \mathbf{w}.$$

This relation can be written as

$$\frac{1}{\sigma_{\mathbf{w}}(\Lambda_0)} = \frac{1}{\sigma_{\mathbf{w}}(\Lambda_{m(0)})} + \alpha,$$

where

$$\alpha = \mathbf{w}^T \bar{\Lambda}_C \mathbf{w}. \quad (7.13)$$

Completion of the proof requires to show that $\alpha \geq 0$, that is to show that $\bar{\Lambda}_C$ is a non-negative definite matrix.

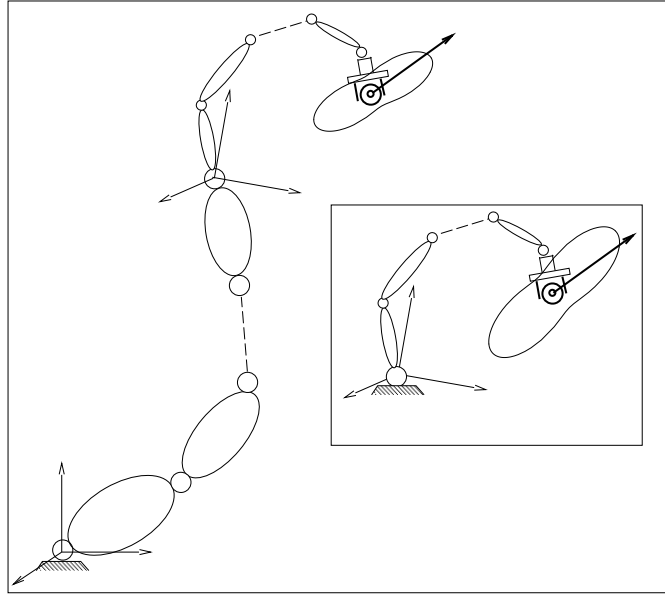


Figure 7.2: Inertial Properties of a Macro-/Mini-Manipulator

Step 2. *Non-negative Definition of $\bar{\Lambda}_C$.* Examination of equation (7.11) shows $\bar{A}_{11} = (A_{11} - A_{21}^T A_{22}^{-1} A_{21})^{-1}$ to be the upper diagonal block matrix in the inverse of A . $(A_{11} - A_{21}^T A_{22}^{-1} A_{21})^{-1}$ is thus a positive definite matrix, which can be written as BB^T . Using this form in the expression of $\bar{\Lambda}_C$ in equation (7.8) shows that the matrix $\bar{\Lambda}_C$ itself can be written as CC^T . This implies that $\bar{\Lambda}_C$ is a non-negative definite matrix. Substituting this result in equation (7.13) completes the proof of the theorem. \square

The reduced effective inertia result obtained for the matrix Λ_0 also applies to the matrices Λ_v and Λ_ω . The matrix Λ_v can be obtained from Λ_0 by replacing the Jacobian J_0 by the matrix

$$J_v = [I \quad 0] J_0. \quad (7.14)$$

Using equations (7.14), the decomposition of equation (7.7) takes the form

$$\Lambda_v^{-1} = \Lambda_{m(v)}^{-1} + \bar{\Lambda}_{C(v)}; \quad (7.15)$$

where

$$\bar{\Lambda}_{C(v)} = (I \ 0) \bar{\Lambda}_C \begin{pmatrix} I \\ 0 \end{pmatrix}. \quad (7.16)$$

This shows that, like $\bar{\Lambda}_C$, the matrix $\bar{\Lambda}_{C(v)}$ is a non-negative definite matrix. The same procedure can be applied to Λ_ω using

$$J_\omega = [0 \ I] J_0. \quad (7.17)$$

Corollary 2.1: (*Reduced Effective Inertia*).

The effective mass (inertia) in (about) any direction \mathbf{u} of a macro/mini-manipulator system is smaller than or equal to the effective mass (inertia) associated with the mini-manipulator in (about) that direction:

$$m_u(\Lambda_v) \leq m_u(\Lambda_{m(v)}) \quad \text{and} \quad I_u(\Lambda_\omega) \leq I_u(\Lambda_{m(\omega)}); \quad (7.18)$$

as defined in Section 6.2.

Example: (*A Three-Degree-of-Freedom Manipulator*) Let us consider the three-degree-of-freedom manipulator shown in Figure 7.3. This manipulator is redundant with respect to the task of positioning the end effector. In this example, the mini-manipulator portion involves two degrees of freedom, $n_m = 2$, and the macro-manipulator portion has only one degree of freedom, $n_M = 1$.

With respect to frame \mathcal{R}_1 , the Jacobian associated with the end-effector position takes the simple form

$$J_{0(1)} = \begin{bmatrix} -q_3 & 1 & 0 \\ q_2 & 0 & 1 \end{bmatrix}.$$

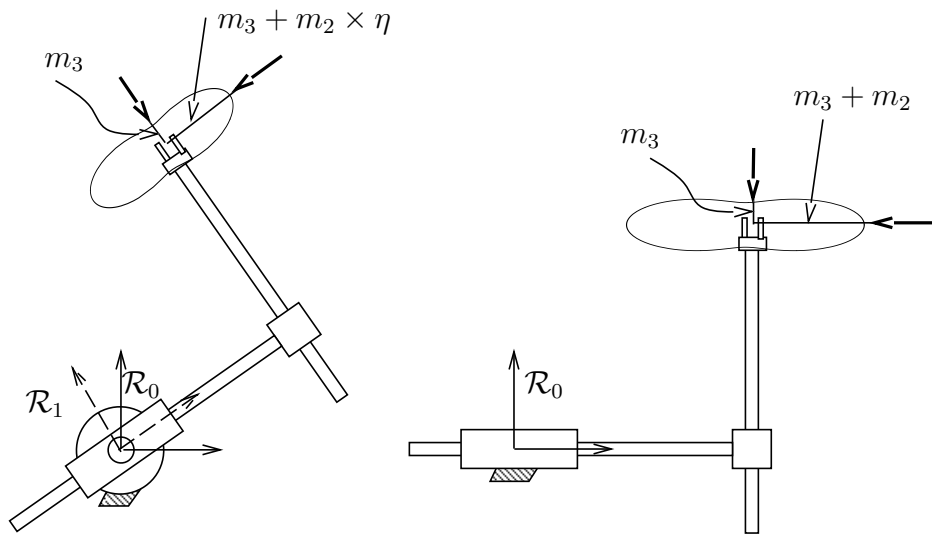


Figure 7.3: A 3 DOF Manipulator with a 2 DOF Mini-Manipulator

The joint-space kinetic energy matrix is

$$A(\mathbf{q}) = \begin{bmatrix} I_1 + m_2 q_2^2 + m_3 (q_2^2 + q_3^2) & -m_3 q_3 & m_3 q_2 \\ -m_3 q_3 & m_2 + m_3 & 0 \\ m_3 q_2 & 0 & m_3 \end{bmatrix};$$

where I_1 is the inertia of link 1 about joint axis 1 and where m_2 and m_3 are the masses of link 2 and link 3. For simplicity we have assumed that the center of mass of link 2 is located at joint axis 3 and the center of mass of link 3 is located at the end-effector. The kinetic energy matrix, $\Lambda_{m(0)}$, associated with the two-degree-of-freedom mini-manipulator is

$$\Lambda_{m(0)} = \begin{bmatrix} m_2 + m_3 & 0 \\ 0 & m_3 \end{bmatrix}.$$

In frame \mathcal{R}_1 , the kinetic energy matrix, $\Lambda_{0(1)}$, associated with the three-degree-of-freedom macro-/mini-manipulator is

$$\Lambda_{0(1)} = \begin{bmatrix} m_2 + m_3 \times \eta & 0 \\ 0 & m_3 \end{bmatrix};$$

where

$$\eta = \frac{I_1 + m_2 q_2^2}{I_1 + m_2 (q_2^2 + q_3^2)} \leq 1.$$

The inertial properties of the macro-/mini-manipulator and the mini-manipulator are illustrated in Figure 7.3. The belted ellipsoids shown in this figure correspond to the eigenvalues and eigenvectors associated with the matrices $\Lambda_{0(1)}$ and $\Lambda_{m(0)}$.

With respect to frame \mathcal{R}_0 , the kinetic energy matrix, Λ_0 is

$$\Lambda_0 = \Omega \Lambda_{0(1)} \Omega^T;$$

where

$$\Omega = \begin{bmatrix} \cos(q_1) & -\sin(q_1) \\ \sin(q_1) & \cos(q_1) \end{bmatrix}.$$

A more general statement of Theorem 2 is that *the inertial properties of a redundant manipulator are bounded above by the inertial properties of the structure formed by the smallest distal set of degrees of freedom that span the operational space.* The equality of the inertial properties in Theorem 2 is obtained for mechanisms that involve only prismatic joints (Khatib 1990).

7.3 Dextrous Dynamic Coordination

The dynamic performance of a macro-/mini-manipulator system can be made comparable to (and, in some cases, better than) that of the lightweight mini-manipulator. The basic idea behind the approach for the coordination of macro and mini structures is to treat them together as a single redundant system. High dynamic performance for the end-effector task (motion and contact forces) can be achieved with an operational space control system based on equation (5.7). Minimizing the instantaneous kinetic energy, such a controller will attempt to carry out the entire task using essentially the fast dynamic response of the mini structure. However, given the mechanical limits on the mini structure's joint motions, this would rapidly lead to joint saturation of the mini-manipulator degrees of freedom.

The *dextrous dynamic coordination* we propose is based on combining the operational space control with a minimization of deviation from the midrange joint positions of the mini-manipulator. This minimization must be implemented with joint torque control vectors selected from the dynamically consistent null space of equation (5.11). This will eliminate any effect of the additional control torques on the end-effector task.

Let \bar{q}_i and \underline{q}_i be the upper and lower bounds on the i^{th} joint position q_i . We construct the potential function

$$V_{\text{Dextrous}}(\mathbf{q}) = k_d \sum_{i=n_M+1}^n \left(q_i - \frac{\bar{q}_i + \underline{q}_i}{2} \right)^2; \quad (7.19)$$

where k_d is a constant gain. The gradient of this function

$$\mathbf{\Gamma}_{\text{Dextrous}} = -\nabla V_{\text{Dextrous}}; \quad (7.20)$$

provides the required attraction (Khatib 1986) to the mid-range joint positions of the mini-manipulator. The interference of these additional torques with the end-effector dynamics is avoided by projecting them into the null space of $J^T(\mathbf{q})$. This is

$$\mathbf{\Gamma}_{nd} = [I_n - J^T(\mathbf{q})\bar{J}^T(\mathbf{q})] \mathbf{\Gamma}_{\text{Dextrous}}. \quad (7.21)$$

In addition, joint limit avoidance can be achieved using an “artificial potential field” function (Khatib 1986). It is essential that the range of motion of the joints associated with the mini-manipulator accommodate the relatively slower dynamic response of the arm. A sufficient margin of motion is required to achieve dextrous dynamic coordination.

This approach has been implemented for the coordination and control of a free-flying robotic systems (Russakow and Khatib 1992). In the context of this system, several other internal motion behaviors have been proposed for the coordination of the free-flying base, treated as a macro structure, and the manipulator, considered as the relatively lightweight mini structure.

Chapter 8

Multi-Effector/Object System

We now consider the problem of object manipulation in a parallel system of N manipulators. The effectors are assumed to be rigidly connected to the manipulated object. The number of degrees of freedom of the parallel system will be denoted by n_s .

First, we will consider the case of a system of N non-redundant manipulators that all have the same number of degrees of freedom, n . The end effectors are also assumed to have the same number of degrees of freedom, m ($m = n$). Under these assumptions, the number of degrees of freedom of the parallel system in the planar case ($n = m = 3$) is $n_s = 3$. In the spatial case ($n = m = 6$), this number is $n_s = 6$.

8.1 Augmented Object Model

To analyze the dynamics of this multi-effector system, we start by selecting the operational point as a fixed point on the manipulated object.

Because of the rigid grasp assumption, this point is also fixed with respect to the end effectors. The number of operational coordinates, m , is equal to the number of degrees of freedom, n_s , of the system. Therefore, these coordinates form a set of generalized coordinates for the system in any domain of the workspace that excludes kinematic singularities. Thus the kinetic energy of the system is a quadratic form of the generalized operational velocities, $\frac{1}{2} \dot{\mathbf{x}}^T \Lambda_{\oplus}(\mathbf{x}) \dot{\mathbf{x}}$. The $m \times m$ kinetic energy matrix $\Lambda_{\oplus}(\mathbf{x})$ describes the combined inertial properties of the object and the N manipulators at the operational point. $\Lambda_{\oplus}(\mathbf{x})$ can be viewed as the kinetic energy matrix of an *augmented object* representing the total mass/inertia at the operational point.

Now, let $\Lambda_{\mathcal{L}}(\mathbf{x})$ be the kinetic energy matrix associated with the object itself. We will analyze the effect of this load on the inertial properties of a single manipulator, and generalize this result to the N -manipulator system to find $\Lambda_{\oplus}(\mathbf{x})$.

Effect of a Load

The kinetic energy matrix $\Lambda(\mathbf{x})$ associated with the operational coordinates \mathbf{x} describes the inertial properties of the manipulator as perceived at the operational point. When the end effector carries a load (see Figure 8.1) the system's inertial properties are modified. The addition of a load results in an increase in the total kinetic energy. If we let $m_{\mathcal{L}}$ be the mass of the load and $\mathcal{I}_{\mathcal{L}(C)}$ be the load inertia matrix evaluated with respect to its center of mass \mathbf{p}_C , the additional kinetic energy due to the load is

$$T_{\mathcal{L}} = \frac{1}{2} \left(m_{\mathcal{L}} \mathbf{v}_C^T \mathbf{v}_C + \omega^T \mathcal{I}_{\mathcal{L}(C)} \omega \right); \quad (8.1)$$

where \mathbf{v}_C and ω_C are the linear and angular velocities measured at the center of mass with respect to the fixed reference frame. The kinetic energy matrix associated with these velocities is

$$\Lambda_{\mathcal{L}(C)} = \begin{bmatrix} m_{\mathcal{L}} I & \mathbf{0} \\ \mathbf{0} & \mathcal{I}_{\mathcal{L}} \end{bmatrix}; \quad (8.2)$$

where I and 0 are the identity and zero matrices of appropriate dimensions.

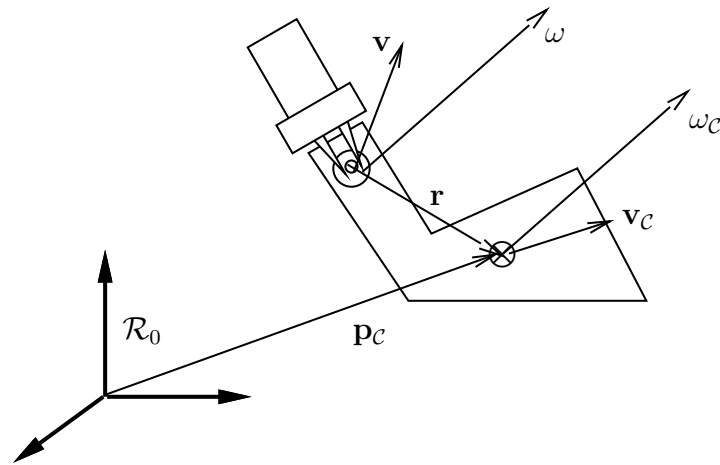


Figure 8.1: Center-of-Mass/Operational-Point Velocities

To compute the kinetic energy matrix with respect to the operational point, we define \mathbf{r} as the vector connecting the operational point to the object's center of mass \mathbf{p}_c . The linear and angular velocities, \mathbf{v} and ω , at the operational point are related to the linear and angular velocities at the center of mass by

$$\begin{bmatrix} \mathbf{v} \\ \omega \end{bmatrix} = \begin{bmatrix} I & \hat{\mathbf{r}} \\ \mathbf{0} & I \end{bmatrix} \begin{bmatrix} \mathbf{v}_c \\ \omega_c \end{bmatrix}; \quad (8.3)$$

where $\hat{\mathbf{r}}$ is the cross product operator associated the vector \mathbf{r} . Using the inverse of this relationship, the kinetic energy matrix associated with the load and expressed with respect to the velocities at the operational point can be written as

$$\Lambda_{\mathcal{L}(0)} = \begin{bmatrix} m_{\mathcal{L}}I & -m_{\mathcal{L}}\hat{\mathbf{r}} \\ -m_{\mathcal{L}}\hat{\mathbf{r}}^T & \mathcal{I}_{\mathcal{L}} + m_{\mathcal{L}}\hat{\mathbf{r}}^T\hat{\mathbf{r}} \end{bmatrix}. \quad (8.4)$$

The generalized operational velocities $\dot{\mathbf{x}}$ are related to the linear and angular velocities by a matrix $E(\mathbf{x})$. Expressed in terms of operational velocities, the kinetic energy due to the load is

$$T_{\mathcal{L}} = \frac{1}{2} \dot{\mathbf{x}}^T \Lambda_{\mathcal{L}}(\mathbf{x}) \dot{\mathbf{x}}; \quad (8.5)$$

where

$$\Lambda_{\mathcal{L}}(\mathbf{x}) = E^{-T}(\mathbf{x})\Lambda_{\mathcal{L}(0)}E^{-1}(\mathbf{x}). \quad (8.6)$$

Lemma 3

The operational space kinetic energy matrix of the effector and load system is the matrix

$$\Lambda_{\text{effector+load}}(\mathbf{x}) = \Lambda_{\text{effector}}(\mathbf{x}) + \Lambda_{\mathcal{L}}(\mathbf{x}). \quad (8.7)$$

This is a straightforward implication of evaluation of the total kinetic energy of the system with respect to the operational coordinates.

To extend this result to an N -manipulator system, let $\Lambda_i(\mathbf{x})$ be the kinetic energy matrix associated with the i^{th} unconnected end effector expressed with respect to the operational point.

Theorem 3: (*Augmented Object*)

The kinetic energy matrix of the augmented object is

$$\Lambda_{\oplus}(\mathbf{x}) = \Lambda_{\mathcal{L}}(\mathbf{x}) + \sum_{i=1}^N \Lambda_i(\mathbf{x}). \quad (8.8)$$

This results from the evaluation of the total kinetic energy of the N effectors and object system expressed with respect to the operational velocities,

$$T = \frac{1}{2}\dot{\mathbf{x}}^T \Lambda_{\mathcal{L}}(\mathbf{x})\dot{\mathbf{x}} + \sum_{i=1}^N \frac{1}{2}\dot{\mathbf{x}}^T \Lambda_i(\mathbf{x})\dot{\mathbf{x}}$$

The use of the additive property of the augmented object's kinetic energy matrix of Theorem 3 allows us to obtain the system equations

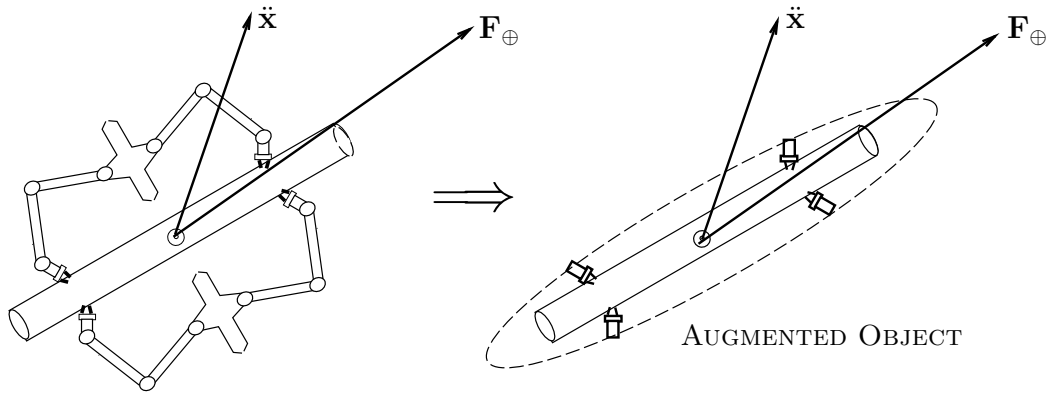


Figure 8.2: A Multi-Arm Robot System

of motion from the equations of motion of the individual manipulators. As illustrated in Figure 8.2, the dynamic behavior of a multi-effector/object system is described by the augmented object model

$$\Lambda_\oplus(\mathbf{x})\ddot{\mathbf{x}} + \mu_\oplus(\mathbf{x}, \dot{\mathbf{x}}) + \mathbf{p}_\oplus(\mathbf{x}) = \mathbf{F}_\oplus. \quad (8.9)$$

The vector, $\mu_\oplus(\mathbf{x}, \dot{\mathbf{x}})$, of centrifugal and Coriolis forces also has the additive property

$$\mu_\oplus(\mathbf{x}, \dot{\mathbf{x}}) = \mu_{\mathcal{L}}(\mathbf{x}, \dot{\mathbf{x}}) + \sum_{i=1}^N \mu_i(\mathbf{x}, \dot{\mathbf{x}}); \quad (8.10)$$

where $\mu_{\mathcal{L}}(\mathbf{x}, \dot{\mathbf{x}})$ and $\mu_i(\mathbf{x}, \dot{\mathbf{x}})$ are the vectors of centrifugal and Coriolis forces associated with the object and the i^{th} effector, respectively. Similarly, the gravity vector is

$$\mathbf{p}_\oplus(\mathbf{x}) = \mathbf{p}_{\mathcal{L}}(\mathbf{x}) + \sum_{i=1}^N \mathbf{p}_i(\mathbf{x}), \quad (8.11)$$

where $\mathbf{p}_{\mathcal{L}}(\mathbf{x})$ and $\mathbf{p}_i(\mathbf{x})$ are the gravity vectors associated with the object and the i^{th} effector. The generalized operational forces \mathbf{F}_\oplus are the resultants of the forces produced by each of the N effectors at the

operational point.

$$\mathbf{F}_\oplus = \sum_{i=1}^N \mathbf{F}_i. \quad (8.12)$$

The effector's operational forces \mathbf{F}_i are generated by the corresponding manipulator actuators. The generalized joint torque vector $\mathbf{\Gamma}_i$ corresponding to \mathbf{F}_i is given by

$$\mathbf{\Gamma}_i = J_i^T(\mathbf{q}_i) \mathbf{F}_i;$$

where \mathbf{q}_i is the vector of joint coordinates associated with the i^{th} manipulator and $J_i^T(\mathbf{q}_i)$ is the Jacobian matrix of the i^{th} manipulator computed with respect to the operational point. The dynamic decoupling and motion control of the augmented object in operational space is achieved by selecting a control structure similar to that of a single manipulator (Khatib 1987),

$$\mathbf{F}_\oplus = \widehat{\Lambda}_\oplus(\mathbf{x})\mathbf{F}^* + \widehat{\mu}_\oplus(\mathbf{x}, \dot{\mathbf{x}}) + \widehat{\mathbf{p}}_\oplus(\mathbf{x}); \quad (8.13)$$

where, $\widehat{\Lambda}_\oplus(\mathbf{x})$, $\widehat{\mu}_\oplus(\mathbf{x}, \dot{\mathbf{x}})$, and $\widehat{\mathbf{p}}_\oplus(\mathbf{x})$ represent the estimates of $\Lambda_\oplus(\mathbf{x})$, $\mu_\oplus(\mathbf{x}, \dot{\mathbf{x}})$, and $\mathbf{p}_\oplus(\mathbf{x})$. With a perfect nonlinear dynamic decoupling, the augmented object (8.9) under the command (8.13) becomes equivalent to a *unit mass, unit inertia object*, I_m , moving in the m -dimensional space,

$$I_m \ddot{\mathbf{x}} = \mathbf{F}^*. \quad (8.14)$$

Here, \mathbf{F}^* is the input to the decoupled system. The control structure for constrained motion and active force control operations is similar to that of a single manipulator.

The control structure (8.13) provides the net force \mathbf{F}_\oplus to be applied to the augmented object at the operational point for a given control input, \mathbf{F}^* . Due to the actuator redundancy of multi-effector systems, there is an infinity of joint-torque vectors that correspond to this force.

In tasks involving large and heavy objects, a useful criterion for force distribution is minimization of total actuator activities (Khatib 1988). In contrast, dextrous manipulation requires accurate control of internal forces. This problem has received wide attention and algorithms for

internal force minimization (Nakamura 1988) and grasp stability (Kumar and Waldron 1988) have been developed. Addressing the problem of internal force in manipulation, we have proposed a physical model, the *virtual linkage* (Williams and Khatib 1993), for the description and control of internal forces and moments in multi-grasp tasks. This approach has been used in the manipulation of objects with three PUMA 560 manipulators.

8.2 Redundancy in Multi-Arm Systems

When redundant structures are involved in multi-arm manipulation, the number of degrees of freedom of the entire system might increase. When this happens, the configuration of the whole system cannot be uniquely described by the set of parameters that specify only the object position and orientation. Therefore, the dynamic behavior of the entire system cannot be described by a dynamic model in operational coordinates. As in the single redundant manipulator case, however, the dynamic behavior of the augmented object itself can still be described, and its equations of motion in operational space can still be established.

The number of *degrees of redundancy* of the multi-arm system can be defined by $n_s - m$, where m is the number of degrees of freedom of the augmented object. Obviously, the freedom of the object is restricted by the freedom of the effectors. If m_i is the number of degrees of freedom for the i^{th} effector before connection to the object, the number, m , of degrees of freedom the connected object has will satisfy

$$m \leq \min_i \{m_i\}. \quad (8.15)$$

The inequality in (8.15) reflects the fact that additional constraints can be introduced by the connection of effectors.

When the multi-manipulator system is redundant, (i.e. $n_s > m$), this implies that one or more manipulators must be redundant. In this case, the redundancy of the system can either be localized in one manipulator or distributed between several manipulators. If n_i represents the number of degrees of freedom for the i^{th} manipulator, *the number of degrees of redundancy of the i^{th} manipulator is given by $n_i - m$* . Only one of the two manipulators in Figure 8.3-a is redundant (one degree of redundancy) and both manipulators in Figure 8.3-b are redundant (one degree of redundancy each).

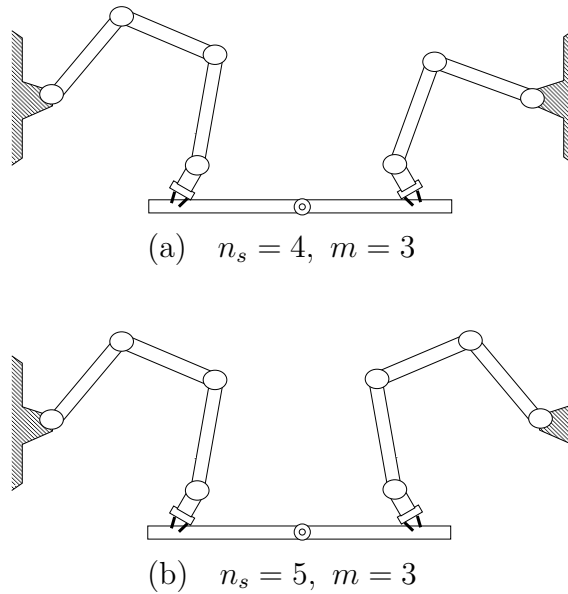


Figure 8.3: Redundancy in Multi-Arm Systems

8.3 Augmented Object in a Redundant System

To establish the augmented object dynamic model for redundant manipulators, we first determine the number of degrees of freedom of the object, m ($m \leq \min_i \{m_i\}$). The dynamic behavior of the augmented object is then obtained by summing the dynamic properties of the individual manipulators in this m -dimensional operational space. The dynamics of each manipulator will be “projected” into the m -dimensional operational space following the same procedure described for a single redundant manipulator. At this point, the dynamic behavior of each of the effectors will be described by an equation of the form (4.6). The dynamic behavior of the augmented object system will be given by an equation similar to equation (8.9), which was established for the non-redundant multi-arm system. In this case however, the inertial properties of the augmented object are dependent on the full configuration of

the system, which is described by

$$\mathbf{q} = (\mathbf{q}_1^T \quad \mathbf{q}_2^T \quad \dots \quad \mathbf{q}_N^T)^T.$$

In this equation, \mathbf{q}_i is the vector of generalized joint coordinates for the i^{th} manipulator. The pseudo kinetic energy matrix of the redundant multi-arm system is

$$\Lambda_{\oplus}(\mathbf{q}) = \Lambda_{\mathcal{L}}(\mathbf{x}) + \sum_{i=1}^N \Lambda_i(\mathbf{q}_i). \quad (8.16)$$

Dynamic decoupling and control of the multi-effector/object system can be achieved by selecting the same control structure (8.13) used in the non-redundant case. However, as in the case of a single redundant manipulator, dynamics in the null spaces associated with the redundant manipulators must be calculated and controlled. This requires the identification of dynamically consistent relationships between joint torque vectors and end-effector operational forces.

8.4 Dynamic Consistency in Multi-Arm Systems

In the case of a single redundant manipulator, we have seen that the general relationship between joint torques and end-effector forces is based on the use of a dynamically consistent generalized inverse of the Jacobian transpose. For a single manipulator, this inverse is given (see equation 5.6) by

$$\bar{J}(\mathbf{q}) = A^{-1}(\mathbf{q})J^T(\mathbf{q})\Lambda(\mathbf{q}).$$

The extension of this relationship to redundant multi-arm systems is complicated by the fact that the dynamically consistent generalized inverse is dependent on the joint-space kinetic energy matrix $A(\mathbf{q})$. The joint-space kinetic energy matrix of a redundant manipulator in a multi-arm system is not simply the matrix associated with the unconnected manipulator considered alone. Connection of the manipulator to an object results in increased loading on the effector of this manipulator. This load, which is due to the object and all the other manipulators connected to it, affects the kinetic energy matrix of this manipulator.

To analyze this, we will first examine how the joint-space kinetic energy matrix in the case of a single manipulator is affected by the addition of a simple load.

Effect of a Load on a Single Manipulator

The addition of a load to the effector of a single manipulator will result in an increase in the kinetic energy of the system. Let $\Lambda_{\text{load}}(\mathbf{x})$ be the kinetic energy matrix associated with the load and expressed with respect to the operational point.

Lemma 4:

The joint-space kinetic energy matrix of a manipulator with load is the matrix

$$A_{\text{arm+load}}(\mathbf{q}) = A_{\text{arm}}(\mathbf{q}) + [J^T(\mathbf{q})\Lambda_{\text{load}}(\mathbf{x})J(\mathbf{q})]. \quad (8.17)$$

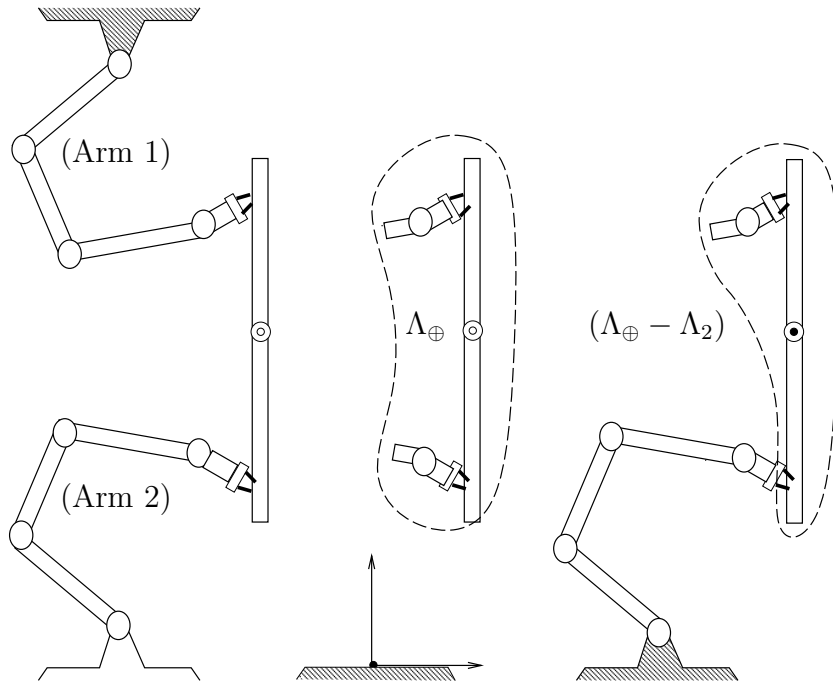


Figure 8.4: Reflected Load

This result is derived by expressing the total kinetic energy of the combined arm/load system in joint space:

$$\begin{aligned}
 T &= \frac{1}{2} \left[\dot{\mathbf{q}}^T A(\mathbf{q}) \dot{\mathbf{q}} + \dot{\mathbf{x}}^T \Lambda_{\text{load}}(\mathbf{x}) \dot{\mathbf{x}} \right]; \\
 &= \frac{1}{2} \dot{\mathbf{q}}^T \left[A(\mathbf{q}) + J^T(\mathbf{q}) \Lambda_{\text{load}}(\mathbf{x}) J(\mathbf{q}) \right] \dot{\mathbf{q}}. \quad (8.18)
 \end{aligned}$$

Reflected Load

The pseudo kinetic energy matrix $\Lambda_{\oplus}(\mathbf{q})$ describes the inertial characteristics of the N -effector/object system as reflected at the operational point. Viewed from a given manipulator, the object and the other effectors can be seen as a load attached to its effector. The additional

load perceived by the i^{th} manipulator is $\Lambda_{\oplus}(\mathbf{q}) - \Lambda_i(\mathbf{q}_i)$, as illustrated in Figure 8.4. Following Lemma 4, the kinetic energy matrix of the manipulator resulting from this additional load is

$$A_{+i}(\mathbf{q}) = A_i(\mathbf{q}_i) + J_i^T(\mathbf{q}_i) [\Lambda_{\oplus}(\mathbf{q}) - \Lambda_i(\mathbf{q}_i)] J_i(\mathbf{q}_i). \quad (8.19)$$

Theorem 4: (*dynamic consistency in multi-arm system*)

The generalized inverse associated with the i^{th} manipulator and consistent with the dynamic behavior of the multi-effector/object system is

$$\bar{J}_i(\mathbf{q}) = A_{+i}^{-1}(\mathbf{q}) J_i^T(\mathbf{q}_i) \left[J_i(\mathbf{q}_i) A_{+i}^{-1}(\mathbf{q}) J_i^T(\mathbf{q}_i) \right]^{-1}. \quad (8.20)$$

Finally, the joint torque end-effector force relationship for the i^{th} manipulator is

$$\mathbf{\Gamma}_i = J_i^T(\mathbf{q}_i) \mathbf{F}_i + \left[I_n - J_i^T(\mathbf{q}_i) \bar{J}_i^T(\mathbf{q}) \right] \mathbf{\Gamma}_{i_0}; \quad (8.21)$$

where $\mathbf{\Gamma}_{i_0}$ is an arbitrary joint-torque vector. Asymptotic stabilization (Khatib 1987), dextrous dynamic coordination, link collision avoidance (Khatib, 1986), and control of manipulator postures can all be integrated in the vector $\mathbf{\Gamma}_{i_0}$ which causes no acceleration at the operational point.